FIELD-BASED STRAIN THRESHOLDS FOR FLEXIBLE

PERPETUAL PAVEMENT DESIGN

Except where reference is made to the work of others, the work described in this dissertation is my own or was done in collaboration with my advisory committee. This dissertation does not include proprietary or classified information.

_____
James Richard Willis

Certificate of Approval:

_____   _____
Rod E. Turochy   David H. Timm, Chair
Associate Professor   Associate Professor
Civil Engineering   Civil Engineering

_____   _____
Randy C. West   John P. Fulton
Director   Assistant Professor
National Center for Asphalt Technology   Biosystems Engineering

_____
George T. Flowers
Dean
Graduate School

FIELD-BASED STRAIN THRESHOLDS FOR FLEXIBLE

PERPETUAL PAVEMENT DESIGN

James Richard Willis

A Dissertation

Submitted to

the Graduate Faculty of

Auburn University

in Partial Fulfillment of the

Requirements for the

Degree of

Doctor of Philosophy

Auburn, Alabama
May 9, 2009

FIELD-BASED STRAIN THRESHOLDS FOR FLEXIBLE

PERPETUAL PAVEMENT DESIGN

James Richard Willis

_____

Signature of Author

_____

Date of Graduation

VITA

James Richard Willis, son of David Weldon and Dwina Louise (Whittle) Willis, was born on November 27, 1980 in San Antonio, Texas. He graduated from Chester County High School as Salutatorian in 1999. He attended Freed-Hardeman University in Henderson, Tennessee, for three years and then enrolled in Auburn University in August, 2002. In 2003, he graduated *summa cum laude* and with University Honors with a Bachelor of Science degree in Physical Science from Freed-Hardeman University. In 2004, he graduated *summa cum laude* from Auburn University with a Bachelor of Civil Engineering. He immediately entered into Graduate School at Auburn University in August, 2004, where he worked under the supervision of the Auburn University Highway Research Center. In December 2005, he received his Master of Science from Auburn University. He continued in Graduate School at Auburn University in January, 2006, where he worked with the National Center for Asphalt Technology Test Track.

DISSERTATION ABSTRACT

FIELD-BASED STRAIN THRESHOLDS FOR FLEXIBLE

PERPETUAL PAVEMENT DESIGN

James Richard Willis

Doctor of Philosophy, May 9, 2009
(Master of Science, December 16, 2005)
(B.C.E., Auburn University, 2004)
(B.S., Freed-Hardeman University, 2003)

209 Pages Typed

Directed by David H. Timm

In the recent years, there has been a push towards designing roadways which will

sustain 50 years of trafficking without having any structural fatigue damage. These

"perpetual pavements" are designed using mechanistic-empirical design methodologies

which limit the strain imposed on the pavement at the bottom of the bituminous layer of

a pavement structure to a specific value which negates bottom-up fatigue damage.

Previously, only laboratory data had been developed to identify this strain threshold, and

it has proven difficult to make correlations between laboratory and field data in the area

of fatigue cracking. Therefore, the objectives of this research included developing field-

based strain thresholds for perpetual pavement design and establishing a relationship between laboratory fatigue thresholds and field-measured strain. Accomplishing these objectives would ultimately lead to more efficient perpetual pavement design.

To accomplish these objectives, strain distributions were developed for twenty-one test sections at the National Center for Asphalt Technology (NCAT) Pavement Test Track. The sections represented three cycles of research and trafficking using both theoretical and measured strains. A unique method of characterizing the entire cumulative probability distribution of strains experienced by each test section was developed.

Strain distributions of those sections that experienced fatigue cracking were compared with the distributions of those that did not experience cracking. Interestingly, it was found that sections with bottom-up fatigue cracking experienced higher strain levels above the 55th percentile compared to those that did not crack. New strain criteria, in the form of a recommended maximum strain distribution, for flexible perpetual pavements design were developed using an average of the four sections which experienced the most traffic without fatigue cracking. This strain distribution can be used provisionally for the design of perpetual pavements to prevent fatigue cracking.

Laboratory fatigue thresholds were related to strain distributions through the concept of a fatigue ratio. The fatigue ratio accurately quantified the entire distribution of strain by comparing it to the laboratory-developed 95th percentile lower bound of the confidence interval fatigue threshold. Attempts to compare the laboratory fatigue thresholds to one point on the cumulative strain distribution proved difficult for relationship development.

Though this study developed a provisional recommendation for both a strain distribution and fatigue ratio, it is recommended that more investigations take place to validate this work. Materials representing a wider range of fatigue thresholds should be field-tested to validate these concepts.

ACKNOWLEDGEMENTS

Style maunal used: <u>MLA Handbook for Writers of Research Papers (5th Edition)</u>

Computer software used: Microsoft Word, Microsoft Excel, Microsoft Access, Total Access Statistics, and PerRoad 3.3.

TABLE OF CONTENTS

LIST OF TABLES

LIST OF FIGURES

CHAPTER ONE

INTRODUCTION

BACKGROUND

Pavement engineers have been producing long-lasting hot-mix asphalt (HMA) pavements since the 1960s. Research has shown that well-constructed and adequately designed flexible pavements can perform well for extended periods of time (Mahoney, 2001). Many of these pavements in the past forty years were the products of full-depth or deep strength asphalt pavement designs, and both have design philosophies that have been shown to provide adequate strength over extended life cycles (Asphalt Pavement Alliance (APA), 2002).

Full-depth pavements are constructed by placing HMA on modified or unmodified soil or subgrade material. Deep strength pavements consist of HMA layers on top of a thin granular base. Both of these design scenarios allow pavement engineers to design thinner pavements than if a thick granular base were used. By reducing the potential for fatigue cracking and containing cracking to the upper removable/replaceable layers, many of these pavements have far exceeded their design life of 20 years with minimal rehabilitation; therefore, they are considered to be superior pavements (APA, 2002).

1

Inferior pavements are pavements that exhibit structural distresses, such as fatigue cracking and rutting (Mahoney, 2001), before their design life is achieved. The successes seen in the full-depth and deep strength pavements are the results of designing and constructing pavements that resist these detriments to the pavement's structure. In recent years, pavement engineers have begun to introduce a methodology of designing pavements to resist the two main pavement distresses seen on roadways, and with this change in thinking has come the idea of perpetual pavements or long-lasting pavements.

The APA has defined a perpetual pavement as "an asphalt pavement designed and built to last longer than 50 years without requiring major structural rehabilitation or reconstruction, and needing only periodic surface renewal in response to distresses confined to the top of the pavement" (APA, 2002). Most pavement engineers in the US approach the idea of perpetual pavements with a 50 year structural design life in mind (APA, 2002). However, while the structural integrity of the pavement should be in-tact during the entirety of the pavement's life, periodic resurfacing often needs to occur after 20 years to improve friction, reduce noise, and mitigate surface cracking (Newcomb et al., 2001). While it is important to realize the importance of proper design for a long-lasting pavement, one must also understand that design life is a function of the design requirements, material characteristics, layer thicknesses, maintenance activities, and the failure criterion. In many cases, engineers consider pavement failure either 10% fatigue cracking in the wheelpath or 0.5 inches of rutting (Von Quintus, 2001).

Though the APA defined a perpetual pavement through its design life, Ferne (2006) expanded upon this idea by saying a "long-life pavement is a well-designed and constructed pavement that could last indefinitely without deterioration in the structural

elements provided it is not overlooked and the appropriate maintenance is carried out."

Pavement performance is more than a function of design. Trafficking, climate, subgrade and pavement parameters (such as modulus), pavement materials, construction, and maintenance levels all contribute to how a pavement will perform over the course of its life (Von Quintus, 2001; Walubita et al., 2008).

Assuming that pavements will be constructed adequately, engineers approach designing perpetual pavements using the following philosophy (Merrill et al., 2006; Walubita et al., 2008):

1. Perpetual pavements must have enough structural integrity and thickness to preclude distresses such as fatigue cracking, permanent deformation, and structural rutting.

2. Perpetual pavements must be durable enough to resist damage from traffic (such as abrasion) and the environment.

While one might think pavements designed to last longer would incur more costs than pavement with shorter life-cycles, research has shown that perpetual pavements have the following benefits (Timm and Newcomb, 2006):

1. Perpetual pavements eliminate reconstruction costs at the end of a pavement's structural capacity.

2. Perpetual pavements lower rehabilitation-induced user delay costs.

3. Perpetual pavements reduce use of non-renewable resources like aggregates and asphalt.

4. Perpetual pavements diminish energy costs while the pavement is in service.

5. Perpetual pavements reduce the life-cycle costs of the pavement network.

FATIGUE CRACKING

Fatigue cracking is one of the three major modes of distresses in flexible pavements with rutting and thermal cracking comprising the others. While fatigue cracking occurs in the HMA, it soon affects all the layers of the pavement structure allowing water to change the material properties of the unbound material layers. This phenomenon results in accelerated surface deterioration, pumping, and rutting.

Fatigue cracking typically begins due to high repeated strains at the bottom of an HMA layer from heavy loads (Huang, 1993). Research has shown that limiting the horizontal strains at the bottom of the HMA can help control fatigue cracking (Shook et al., 1982; Asphalt Institute, 1982). A schematic of the fatigue cracking mechanism driven by tensile strain at the base of the HMA is shown in Figure 1-1. Figure 1-2 provides a visual of extensive fatigue cracking on a roadway.

Repeated tensile loads at the base of the HMA fatigue the pavement
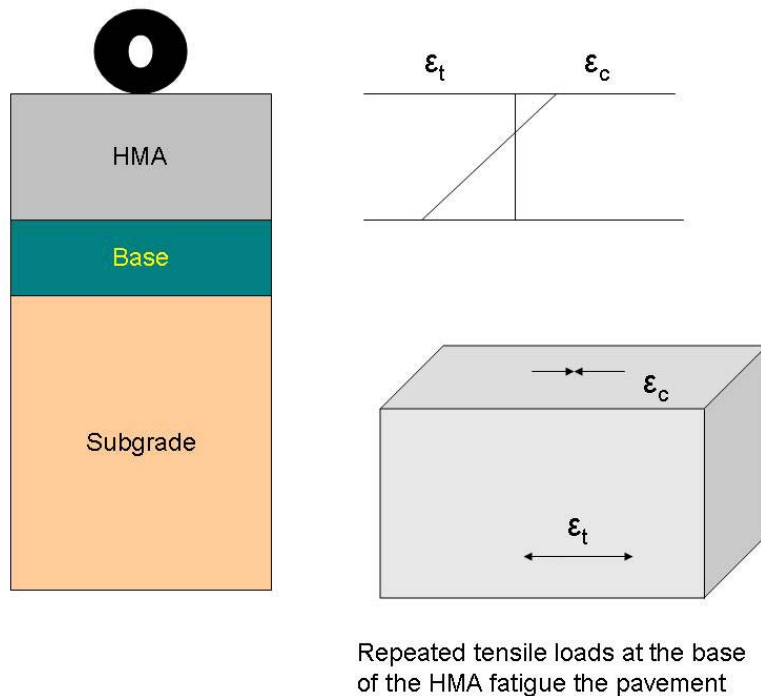
Figure 1-1. Fatigue Cracking Schematic.

Figure 1-2. Fatigue Cracking on a Roadway (Priest and Timm, 2006).

STRUCTURAL DESIGN

One way to decrease the probability of bottom-up fatigue cracking is to increase the thickness of the pavement structure. Thick pavements have been shown to limit cracking to the surface of pavements by reducing the maximum strain at the bottom of the HMA (APA, 2002; Romanoschi et al., 2008; Al-Qadi et al., 2008; Merrill et al., 2006).

When the tensile strain at the bottom of the HMA is reduced, most engineers believe that the critical location for strains in pavements is relocated from the base of the HMA to the surface of the structure where tire interaction and binder aging contribute to

hardened and weaker wearing courses that are prone to top-down cracking (Mahoney, 2001; Rolt, 2001). At this point, since the distresses in the pavement are kept in the wearing course, it is possible to avoid deep structural maintenance and focus on functional maintenance such as skid resistance and ride quality (Ferne, 2006). To eradicate the surface cracks, a "mill and fill" maintenance plan is appropriate for extending the pavement's life (Mahoney, 2001).

While mitigating fatigue cracking is important in creating a perpetual pavement, one cannot sacrifice rutting protection for fatigue life. Studies on thick pavements at the National Center for Asphalt Technology (NCAT) Pavement Test Track (Brown et al., 2002) and by Rolt (2001) have shown that thick pavement structures tend to prevent structural rutting in the subgrade and limit rutting to the surface layers of the pavement structure. This being the case, additional structural life would not be necessary to keep the pavement in-use. Surface treatments would be adequate for keeping the roadway in-service (Mahoney, 2001; Brown et al., 2002).

MIX DESIGN AND MATERIALS

Increasing the thickness of a pavement is not a guarantee that the pavement will have a long service life. Washington State's study of long-lasting pavements showed that in many cases pavements with shorter life-cycles in Washington were thicker than its superior pavements (Mahoney, 2001). Other studies have shown that while increasing the thickness of a pavement will decrease the tensile strain at the bottom of the HMA layer, the magnitude by which this reduction occurs is mix dependant (Romanoschi et al., 2008).

Engineers have compiled knowledge and research to create a composite pavement structure which can be utilized to increase the chances of a flexible pavement achieving long life. This pavement structure (Figure 1-3) includes a rut and wear resistant impermeable upper layer of HMA. In many cases, a stone matrix asphalt (SMA), an open-graded friction course (OGFC), or a dense Superpave design is used for this lift. Below the wearing course, engineers design a rut resistant and durable intermediate layer. Finally, the base layer of the HMA needs to be a fatigue resistant, durable layer. This final lift is designed many times at an increased asphalt content and reduced air voids (Newcomb et al., 2001).

OGFC or SMA Surface

4" to 6" — Zone Of High Compression

High Modulus Rut Resistant Material (Varies As Needed)

Max Tensile Strain

Flexible Fatigue Resistant Material 3 - 4"

Pavement Foundation
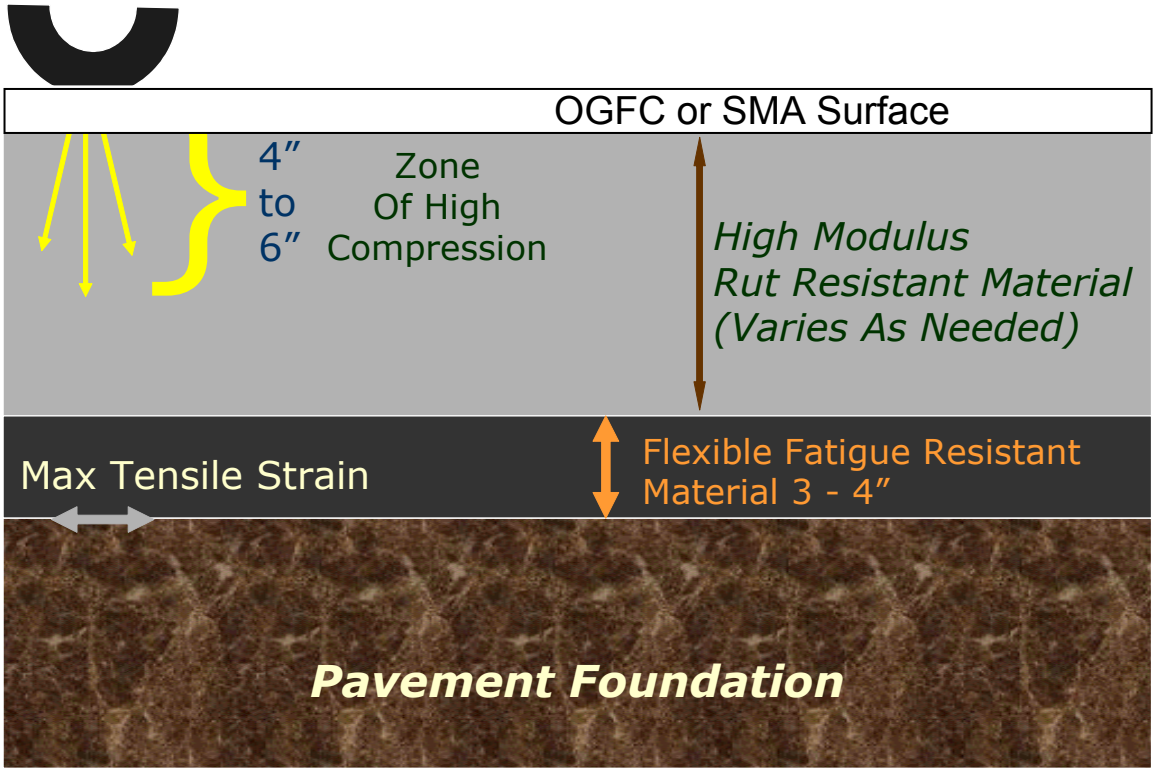
Figure 1-3. Perpetual Pavement Design Concept (Newcomb et al., 2001).

MECHANISTIC-EMPIRICAL DESIGN AND PERFORMANCE THRESHOLDS

Mechanistic-empirical (M-E) pavement design and analysis, though not a new concept, has recently made great advances toward widespread implementation throughout the United States. Currently, there are existing M-E pavement design methodologies (Monismith, 1992; Kentucky Transportation Cabinet, 2007; Timm et al., 1998; Asphalt Institute, 1982), but as the new M-E Pavement Design Guide (MEPDG) is being completed and implemented, more attention is being spent on proper material and pavement response characterization (Timm and Priest, 2006). Material properties are needed in this design framework to determine theoretical load-induced responses in pavement structures. These responses are then used in transfer functions to predict the life of the pavement through Miner's Hypothesis (Miner, 1959). Transfer functions rely on theoretical strains and pressures to estimate the design life of pavement structures. If these values are accurately estimated, the transfer functions will provide the engineer with a pavement of optimized thickness.

Since perpetual pavement design relies upon maintaining pavement responses below some critical thresholds, it is well suited to M-E pavement design. To capture the fatigue and rut lives of pavements, engineers can estimate pavement responses so the pavement will have sufficient life. In perpetual pavement design, two mechanistic pavement responses are typically studied and limited. The first limiting response is the vertical compressive strain at the top of the subgrade. This pavement response has been linked to subgrade or structural rutting. In order to minimize this distress, engineers typically design for a maximum of 200 $\mu\varepsilon$ at this location (St. Martin et al., 2001; Walubita et al., 2008).

A second limiting pavement response is the tensile strain at the bottom of the HMA. As discussed above, this mechanistic response is limited to mitigate the possibility for bottom-up fatigue cracking (Newcomb et al., 2001; St. Martin et al., 2001). The longitudinal strain at this pavement location has proven to be critical in thinner pavements, and in a fully-bonded pavement, it is always the location of highest tensile strain (Al-Qadi et al., 2008). In a 2006 survey of accelerated pavement testing (APT) facilities in the United States, 85.7% of the responding facilities measured horizontal strain at the base of the HMA layer to study fatigue life (Willis, 2008). Other projects, such as the I-5 in Oregon and the Marquette Interchange in Wisconsin, have also incorporated measuring strain at the base of the HMA into their research (Estes, 2005; Hornyak et al., 2007). In protecting a perpetual pavement against fatigue cracking, engineers typically attempted to keep the tensile strain at the base of the HMA below 70 $\mu\varepsilon$ (Walubita et al., 2008). However, other engineers propose that one should limit the strain anywhere from 60 to 100 $\mu\varepsilon$ based upon laboratory testing (Romanaschi et al., 2008). A recent experimental pavement project in China allowed perpetual pavement design to reach the seemingly unconservative value of 125 $\mu\varepsilon$ (Yang et al., 2005).

It is important for engineers to determine an appropriate and reliable value to use as a strain threshold in M-E perpetual pavement design. While many engineers currently use a 70 $\mu\varepsilon$ fatigue threshold, these values come from laboratory testing at one temperature. It is difficult, if not impossible, to relate these values and correlate them to field testing. If the field design threshold could be raised, based on sound research and engineering, state agencies would be able to build thinner pavements. A perpetual

pavement experiment in China was able to reduce its pavement thickness from 20 to 15 inches when changing its fatigue threshold limit from 70 to 125 $\mu\varepsilon$ (Yang et al., 2005). This would reduce the construction and material costs for state agencies at a time where funding is extremely limited. This would also cut back on the enormous amount of natural resources being consumed. In the end, the pavement system as a whole would be more efficient.

While laboratory work has been conducted to establish fatigue thresholds for perpetual pavements, little has been published to relate these laboratory values to what is experienced in the field. Are there pavement structures that have shown superior performance while undergoing strains greater than the proposed laboratory-based limits? Have field pavements exhibited pavement responses smaller than the proposed strain limit and failed prematurely? Currently, field thresholds for fatigue cracking are only conservative estimates based upon laboratory work. It is possible the field thresholds for fatigue cracking will be higher than those seen in laboratory work. If this is the case, engineers are overdesigning their pavements.

OBJECTIVES

Since there is a great disconnect between laboratory fatigue threshold testing and what is experienced under highway trafficking, this research was designed to help bridge that disconnect by reaching the following objectives.

1. Recommend strain criteria for fatigue cracking in flexible perpetual pavement design.

2. Determine if a relationship exists between laboratory fatigue thresholds and measured field strains.

SCOPE

The aforementioned objectives were completed by correlating simulated and measured strains at the bottom of the HMA layer to field performance over three cycles of the NCAT Pavement Test Track. For the 2000 experiment, strain distributions were estimated for six sections along the north and south tangents using PerRoad, a mechanistic modeling software package. Direct strain measurements from the base of the HMA were used to develop strain profiles for seven structural sections from the 2003 Test Track and eight sections from the 2006 Test Track.

The secondary objective was completed by using the newly developed strain profiles and comparing them to laboratory fatigue thresholds from two of the base mixes in the 2003 Test Track. The laboratory fatigue tests were conducted in association with National Cooperative Highway Research Program (NCHRP) Project 9-38.

ORGANIZATION OF DISSERTATION

This dissertation contains a literature review of the design and performance of perpetual pavements. Included is an in-depth look at the requirements for the three-layer perpetual pavement design and prior research conducted on strain thresholds. Following the literature review is a basic overview of the test facility, the NCAT Test Track, used to conduct this research.

Chapters 4, 5, and 6 describe the methodology for developing strain distributions for the analyzed test sections. Chapter 4 provides the methodology and strain profiles for six sections from the 2000 Test Track sections while Chapters 5 and 6 provide the methodologies and strain profiles for seven test sections from the 2003 and eight sections from the 2006 Test Tracks, respectively.

Chapter 7 discusses the results of two different analyses. The first analysis compared estimated laboratory fatigue thresholds to the strain distributions developed in the previous chapters. The second analysis compared the cumulative distributions from all three Test Track experiments to validate the theory that strain distributions could be distinguished based upon field performance. The final conclusions and recommendations for future work are discussed in the last chapter.

CHAPTER TWO

LITERATURE REVIEW

INTRODUCTION

Perpetual pavements were in existence long before M-E pavement design was developed. Full depth and deep strength pavements, such as Southern Cross Drive in Australia (Bushmeyer, 2002), have been in existence since the 1960s with very little maintenance (Newcomb et al., 2001). Successes, such as this one, have prompted agencies to delve into the concept of perpetual pavement design. States like California, Washington, and Ohio have all begun perpetual pavement projects (Monismith, 1992; Hornyak et al., 2007; Ursich, 2005). By 2005, Texas had even completed eight perpetual pavement projects (Scullion, 2006), and in 2003, the NCAT Pavement Test Track began experimenting with perpetual design concepts in its structural study (Willis and Timm, 2007).

When Washington State was studying long-lasting pavements, it developed very specific goals which would define a pavement as perpetual. These goals, along with basic perpetual pavement concepts, give engineers four design qualifications for these pavements (Mahoney, 2001; Newcomb et al., 2001).

1. Perpetual pavements should have a wearing course life of 20 years.

2. Perpetual pavements should have a structural design life of 40 to 50 years.

3. Perpetual pavements use a mill and fill as their primary surface rehabilitation.

   Perpetual pavements contain their distresses to the top few centimeters of the

   surface.

DESIGN THICKNESS

The needed thickness for a perpetual pavement has been a much debated and

researched topic since the conception of designing long-life pavements began. In 1997,

Nunn et al. began to propose the idea of a thickness limit for asphalt pavements. In

other words, there was a certain thickness where no more material was useful for

prolonging the structural life of a pavement (APA, 2002). Some states propose

perpetual pavements 20 inches thick (Gierhart, 2008) while others have seen distresses

limited to surface cracking in pavements as thin as 6.3 inches. When Texas was

designing pavements through the Asphalt Institute (AI) M-E design method, typical

pavements were 20.5 inches thick. Perpetual pavement designs allowed for Texas to

reduce their designs by seven inches of HMA (Walubita and Scullion, 2007).

Nunn et al. were among the first researchers to conduct studies on pavement

thickness and fatigue cracking in Europe. From their research, upper and lower limits

for pavement thicknesses were proposed. Using the existing design charts for the

United Kingdom, after 15.35 inches (390 mm) of asphalt had been placed, no additional

material was needed for increased fatigue life. This structure would perform

perpetually. However, pavements thinner than 7.87 inches (200 mm) were found to be

substandard for lightly trafficked roads (i.e. the road would not last 40 years). Structural

deformation and rapidly propagating surface cracking occurred in the thinner sections that led to a premature pavement failure (Nunn and Ferne, 2001).

Study continued on pavement thickness in Europe and how it affected cracking by Merrill et al. (2006) in the Netherlands. Ultra-thin pavements less than 3.15 inches (80 mm) showed evidence of full-depth cracking. When the pavement thickness progressed beyond 11 inches (280 mm), only 28% of the pavements even exhibited signs of cracking. Those that did show cracking between the thicknesses of 7.48 and 16.64 inches (190 and 410 mm) only showed signs of cracking in the upper wearing course layers. A distinct difference in crack development and propagation was found between the thicknesses of 6.69 and 7.87 inches (170 and 200 mm). At this point, the formation of cracks changed from full-depth or fatigue cracking to top-down surface cracking (Merrill et al., 2006).

Rolt (2001) found similar results in his study on pavement thickness and effective pavement structure. His research found that 10.7 inches (270 mm) of properly constructed and designed asphalt could provide a structure with enough strength to resist fatigue cracking, and 7.1 inches (180 mm) would accumulate little deformation over time. These thicknesses excluded any portion of the HMA that exhibited signs of cracking. Therefore, if surface cracking were to be expected, perpetual pavements should be greater than 11.81 inches (300 mm) for long life pavements containing some surface cracking (Rolt, 2001).

In the United States, research has not been as extensive on the relationship between pavement thickness and performance; however, research by Al-Qadi et al. has shown that pavements 13.58 inches (345 mm) thick have exhibited strains well below

any proposed fatigue threshold limit. In fact, a significant increase in strain occurs when a pavement's thickness is reduced beyond 10 inches (254 mm). This could contribute to the early failure of thinner pavements (Al-Qadi et al., 2008).

In-service roadways in the United States, such as the Kansas Turnpike, have shown little to no fatigue cracking over the course of their 40 year service lives having a pavement structure thinner than 13 inches (Wu and Hossain, 2002). Minnesota's Mn/ROAD and Washington State have experiences where pavements greater than 6.3 inches (160 mm) only exhibit surface cracking (Mahoney, 2001).

Fee simplifies most of the research by saying perpetual pavements can typically be designed between 12 and 14 inches but never less than 8 (Fee, 2001). One must remember in the case of each study that different climates and mixes were tested. Strain and fatigue life are highly dependant upon the type of mix being used and at what temperatures the testing is being conducted.

MIX DESIGN AND MATERIALS SELECTION

While the thickness of a perpetual pavement is important, much of the success should be attributed to the materials and mix designs selected for the pavement structure. A common theme is found among perpetual pavements to reduce the probability of fatigue cracking and rutting. This theme contains four specific parts (Harm, 2001; Newcomb et al., 2001; Gierhart, 2008):

1. A solid foundation

2. A flexible, fatigue-resistant HMA base layer

3. A durable, rut-resistant intermediate HMA layer

16

4. A rut-resistant, renewable surface layer.

This relatively simple design scenario has been interpreted on an agency-to-agency basis as needs see fit. Figure 2-1 shows the basic APA perpetual pavement design concept. The first designed perpetual pavement in the United States was designed very similar to this philosophy. I-710 in California was built with a 3 inch rich-bottom layer as its fatigue resistant layer. Six inches of standard HMA was placed on the rich-bottom base (i.e. additional asphalt was added above optimum), and the top four inches of HMA was a 1 inch open-graded friction course (OGFC) layer over three inches of modified asphalt to resist high-temperature rutting (Bushmeyer, 2001).
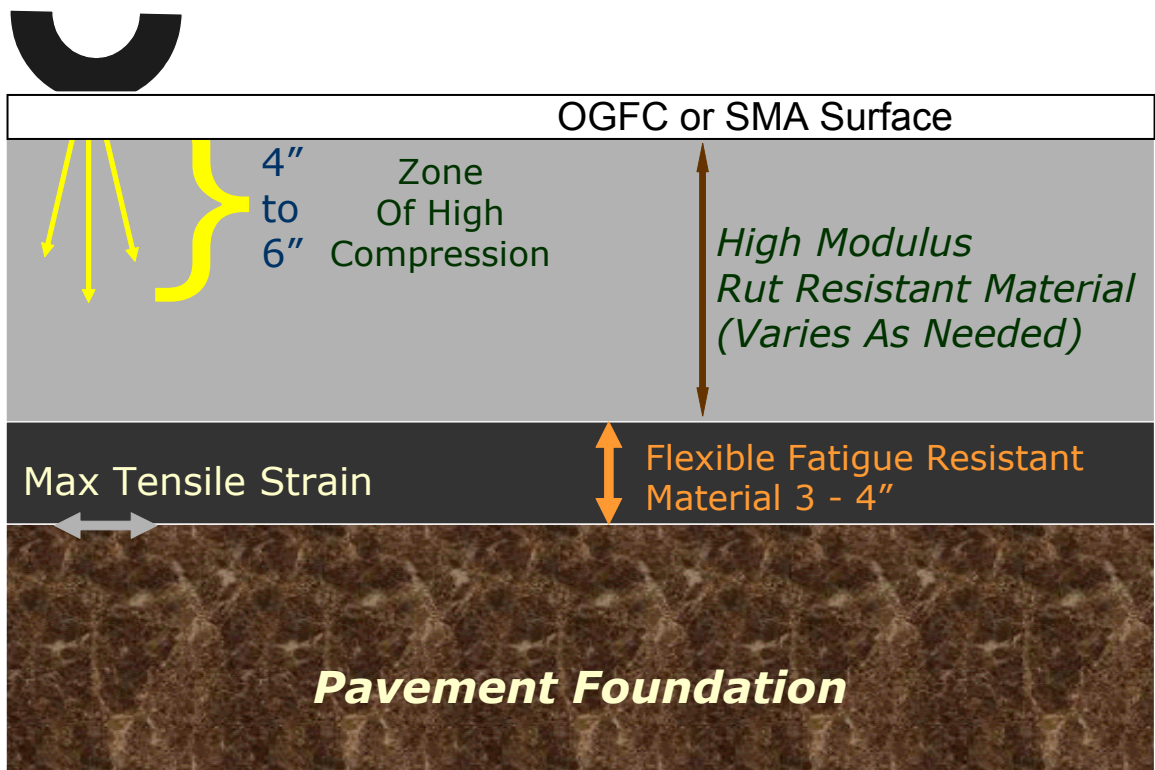
Figure 2-1. Perpetual Pavement Design Concept (Newcomb et al., 2001).

Texas has taken the APA concept and proposed a design (Figure 2-2) that consists of 2 to 3 inches of SMA over a 2 to 3 inch transitional HMA layer. The next 8 plus inches are a rut resistant HMA layer placed on a 2 to 4 inch fatigue resistant layer.

An optional porous friction course (PFC) 1 to 1.5 inches thick can be placed over the SMA to reduce noise and surface damage. This asphalt design is compacted on a 6 inch lime-stabilized granular base layer which is supported by a natural well-compacted subgrade. Texas proposes this design should allow it to achieve 30 million equivalent single axle loads (ESALs) of design life (Walubita et al., 2008; Scullion, 2006).

	1-1.5" Optional PFC
	2-3" SMA
	2-3" Transitional HMA Layer
	8+" Rut Resistant HMA Layer
	2-4" Fatigue Resistant HMA Layer
	6" Lime-Stabilized Base
	Natural Subgrade
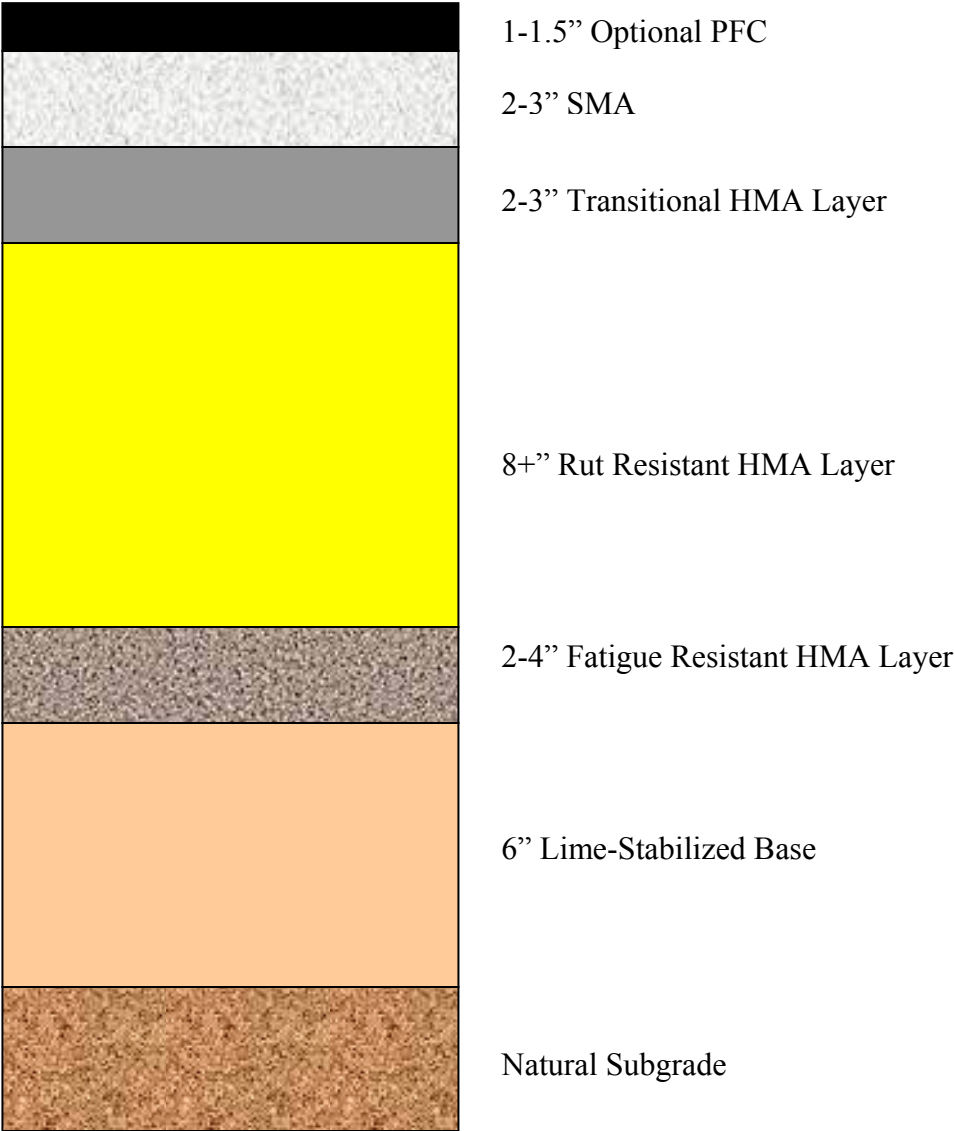
Figure 2-2. Texas Perpetual Pavement.

Designs of perpetual pavements will vary from agency to agency and from location to location; however, a more detailed look should be taken at the four specific components of creating a perpetual pavement: the foundation, base HMA layer, intermediate layer, and wearing course.

Perpetual Foundation

A solid foundation of well-compacted subgrade, chemically stabilized subgrade or granular materials, or unstabilized granular materials is vital to the success of a perpetual HMA pavement. Foundations provide four essential components to the life of a pavement structure (APA, 2002).

1. Foundations act as working platforms for dump trucks and other pavement placing equipment.

2. Foundations resist deformation and deflections during pavement compaction.

3. Foundations support the traffic loads of flexible pavements.

4. Foundations can reduce seasonal variability.

For a foundation to achieve these four goals, a minimum stiffness is required to provide adequate strengths, drainage should be provided if it is needed, and the material should be stabilized if warranted (APA, 2002).

If granular bases are chosen for use in the pavement design, a minimum of 6 inches should be incorporated into the design. This material should be free of highly plastic fines which can be a detriment to stiffness and strength of the base (Muench et al., 2007; APA, 2002). If a granular base is less than 6 inches thick, strength is not added to the structure, little frost heave protection is noticed, fines can inhibit drainage

of the layers, the base material can be difficult to compact, and it is difficult to create a smooth layer of granular material (Muench et al., 2007).

It is vital that granular base layers be stiff enough to protect the subgrade below. This can be done through stabilizing the soil with a lime-treatment or proper compaction. In Texas, during the construction of a perpetual pavement, a paver caused structural damage to the soil because the foundation was not strong enough to be a stable working platform. An unsatisfactorily stabilized or strengthened base can also increase the probability for surface roughness (Scullion, 2006).

Seasonal variability must be characterized for both the subgrade and the unbound materials used in a pavement foundation. The changes of moduli in these layers largely affect the mechanistic responses of the pavement, and for one to design a conservative pavement, the worst-case scenario should be considered (APA, 2002).

One area besides the foundation modulus where seasonal variability should be considered is frost protection. A properly designed pavement should prevent volume changes in the subgrade and base materials from both wet/dry and freeze/thaw cycles. Frost protection, like soil stabilization, improves the ride quality of the pavement by reducing the potential for frost heave (Newcomb et al., 2001; APA, 2002). In dealing with freeze/thaw problems, the pavement thickness should also be considered. APA recommends that in Northern states the minimum pavement structure should be 50% of the frost depth. In some cases, up to 70% of the frost depth may be required to protect the pavement (APA, 2002).

To ensure a quality foundation is placed, in-situ testing of density by a nuclear gauge is recommended. Surface stiffness can also be used as a substitute test for the nuclear gauge if necessary (APA, 2002).

Fatigue-Resistant Base Layer

The fatigue resistant base HMA layer is one of the most important pavement components for increasing the pavement's resistance to fatigue cracking. Before designing the mixes, it is important to understand the end-goal of the mix design. If the engineer is designing a stiff structure, the tensile strain at the base of the HMA will be reduced. A thicker pavement structure might provide similar results. If a pavement is designed thick enough or stiff enough where the tensile strains at the base of the HMA are insignificant, a fatigue-resistant base layer is not necessary, and the mix used for the intermediate layer can be used for the base HMA layer (APA, 2002; Newcomb et al., 2001). As is the case for most pavement structures, however, the tensile strains at the base of the HMA are critical in the design process. Therefore, one must design a fatigue-resistant mix to protect the perpetual pavement (Al-Qadi et al., 2008).

Two basic principles for improving the fatigue life of this base layer have been proposed in research. They are as follows (Epps and Monismith, 1972; APA, 2002; Romanoschi et al., 2008):

1. Use a softer binder

2. Use a higher binder content.

While softer binders allow mixes to stretch without cracking, the most common method for increasing the fatigue life of a pavement is incorporating a higher asphalt

content in the mix design (Romanoschi et al., 2008; APA, 2002; Newcomb et al., 2001; Epps and Monismith, 1972).

Layers which incorporate the use of excess asphalt above the optimum have become known as "rich-bottom" layers, and they have been used extensively to reduce fatigue cracking in pavements by California, Illinois, Oklahoma, Texas, China, and NCAT (APA, 2002; Gierhart, 2008; Scullion, 2006; Yang et al., 2005; Willis and Timm, 2007; Harm, 2001).

Additional asphalt has been known to have the following benefits on pavement structures (APA, 2002; Harm, 2001; St. Martin et al., 2001; Newcomb et al., 2001):

1. Additional asphalt allows for greater compaction

2. Additional asphalt improves fatigue resistance (Figure 2-3)

3. Additional asphalt at the bottom of a pavement does not affect rutting

4. Additional asphalt reduces moisture susceptibility.

Fatigue Resistant Asphalt Base

Figure 5a

High Asphalt Content

log ε

Low Asphalt Content

log N
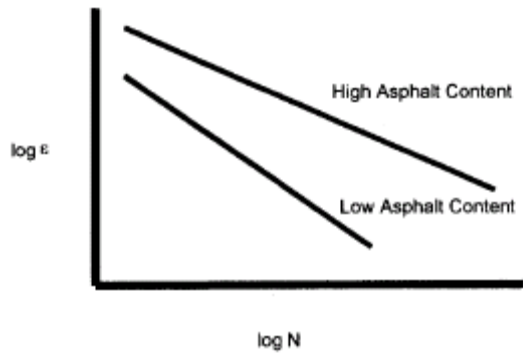
Improve Fatigue Resistence with High Asphalt Content Mixes

Figure 5b

log ε

log N

Compression

Compression

Tension

Tension
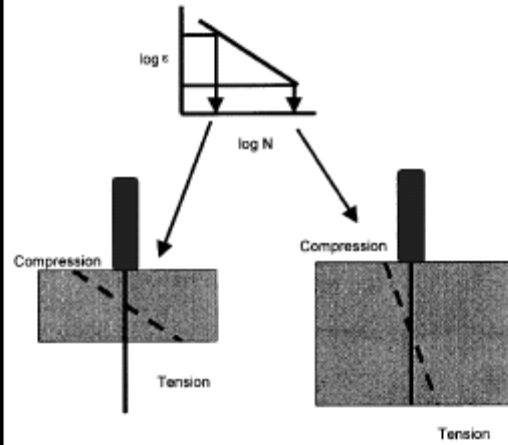
Minimize Tensile Strain with Pavement Thickness

Figure 2-3. Fatigue Resistant Asphalt Base (APA, 2002).

In-place air voids in the field are typically near 7.0% on most projects; however, the additional asphalt in rich-bottom mixes allows in-place air voids to be reduced to less than 6% in many cases (Harm, 2001). This increased asphalt content and density in the mix design is critical in providing the pavement with durability and flexibility by increasing the voids filled with asphalt (VFA). The increased flexibility allows the pavement to stretch and inhibits fatigue cracks (Monismith et al., 1985; APA, 2002) as seen in Figure 2-4.
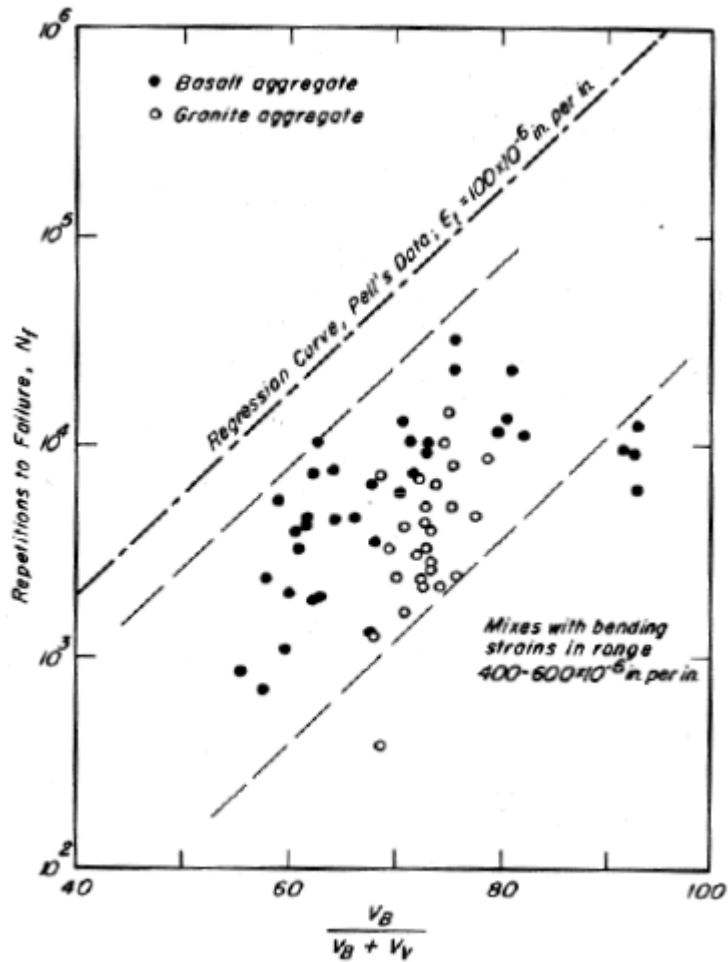
Figure 2-4. Effects of VFB on Fatigue Life (Monismith et al., 1985).

Laboratory tests have been conducted showing the relationship asphalt content and air voids have on fatigue resistance. The air void content has been shown to have a greater affect than asphalt content. Figure 2-5 shows that lower air contents correspond to longer fatigue lives. It also shows very minor positive effects due to the increased asphalt content. However, one must remember that compactability is improved with additional asphalt (Harvey et al., 2004).
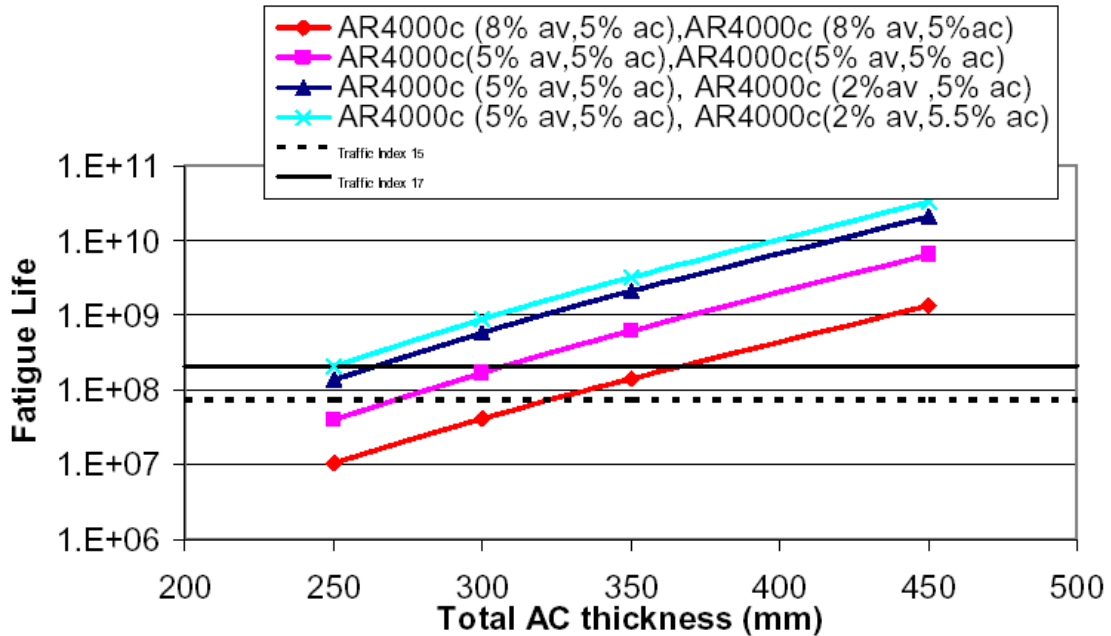
Figure 2-5. Air Voids and Fatigue Life (Harvey et al., 2004).

Research has been conducted in the past few years to determine the needs and

limitations of pavement structures including rich-bottoms. Owners would still like to

have the pavements as thin as possible to help reduce initial costs, so research has been

conducted to determine the most appropriate location and thickness of the rich-bottom

layer. Today, it is recommended that rich-bottom pavements be built with about an

0.5% increase in asphalt in the bottom lift that is between 2 to 3 inches in thickness.

Thickness beyond three inches proved to have insignificant benefits to the fatigue life of

the structure. This layer should be at least 6 inches below the surface to protect it from

possible damage due to its lack of shear resistance (Harvey et al., 2004).

While most pavement design engineers will agree that increasing the asphalt

content in the mix design is the most appropriate way to provide additional fatigue life

to a pavement, different agencies design their rich-bottom layers using varying design

methodologies. On the I-710 project in California, an additional 0.5% asphalt was

25

added beyond optimum in a 3 inch lift to increase the fatigue life of the layer (St. Martin et al., 2001). A perpetual pavement project in China increased the optimal asphalt content by 0.6% to achieve a rich-bottom structure (Yang et al., 2005).

While increasing the asphalt content is a viable option for increasing fatigue life, some engineers feel that just "bumping" the optimum asphalt content may not provide realistic definitions of the mix characteristics (Harm, 2001). To correct for this, many states design their rich-bottom layers for a reduced air void content. States like Texas, Oregon, and Ohio design for 3% air voids in the laboratory. The recently placed perpetual sections at the NCAT Test Track were designed by the Oklahoma DOT for 2% air voids. This translates into 5 to 7% air voids in the field. While there is a different design process, the end results are much the same. The needed reduction in air voids typically requires about an additional 0.5% asphalt content (Walubita and Scullion, 2007; Estes, 2005; Ursich, 2005).

In choosing a binder grade to use in this layer, the high temperature should be chosen by performance grade specifications for that depth. The low temperature grade should be that of the intermediate layers. The additional binder will help resist fatigue cracking while the high binder grade will provide additional rut resistance (Newcomb et al., 2001; APA, 2002).

A minimum of two tests should be run on the base layer of the HMA. The first and most critical test is a fatigue/stiffness characterization test. APA recommends testing fatigue by four point bending. This test will allow the designer to fully characterize the fatigue resistance properties of the mix. The second test for mixes at the base of the HMA is moisture susceptibility. This is the layer that will come into

contact with the most moisture over the life of the pavement. While the additional asphalt does help prevent moisture damage, it is still possible for stripping and debonding to occur because of moisture damage to these layers. Properly testing the mix in both fatigue and moisture susceptibility for this layer should help inhibit possible pitfalls in the fatigue-resistant bottom layer (APA, 2002).

Intermediate Layer

The intermediate layer of a perpetual pavement should be designed using Superpave design methodologies at the optimum asphalt content. While the base layer of the HMA structure should be fatigue-resistant, the qualities needed in the intermediate layers are stability and durability (APA, 2002).

Much of the stability of this layer comes from the stone skeleton of the structure. Crushed stone with a large nominal maximum size adds internal friction to the intermediate layer mix. This stone-on-stone contact in the coarse aggregate gives stability to the mix. The Bailey Method is a methodology that tests the interlock of a mix in question and can be used to enhance the design of intermediate layers for perpetual pavements. This method focuses on the packing properties of the aggregate structure. The test characterizes the skeletal structure's relationship to volumetrics, segregation, and compaction (APA, 2002; Gierhart, 2008).

Durability is added to the mix design by choosing an appropriate high temperature grade for the asphalt binder (Newcomb et al., 2001). When choosing the grade of the asphalt binder, the high temperature grade of the intermediate layer should be that of surface to mitigate structural rutting the pavement. Since the temperature

27

gradient is not as steep in the interior of the pavement, the low temperature can be

relaxed one grade since it will not experience the severe surface temperatures (APA,

2002; Newcomb et al., 2001).

While the intermediate layers sometimes compose the thickest layers of the

pavement structure, they are also the simplest to design and test. Its proximity to the

base of the HMA increases the need for moisture susceptibility testing to be

incorporated into the testing regimen to prevent stripping of the binder (APA, 2002;

Newcomb et al., 2001).

Rut-Resistant Wearing Course

The surface layer or wearing course of a perpetual pavement is required to resist

rutting, mitigate surface cracking, provide adequate friction, minimize splash and spray,

and reduce tire noise. Some have classified this simply as a rut-resistant, wear resistant

layer (Newcomb et al., 2001, APA, 2002). Like the rich-bottom layer, the wearing

surface of a pavement will depend on many factors such as trafficking, environmental

conditions, local experience, and economics (APA, 2002).

Three options are given by APA as to appropriate choices for wearing courses on

perpetual pavements: dense-graded Superpave, SMA, and OGFC. While dense-graded

Superpave is a viable option, SMA and OGFC have had better long-term results (Harm,

2001).

Stone Matrix Asphalt (SMA) has been chosen as one option for perpetual

wearing courses because its ability to resist ruts and durable nature (Harm, 2001).

While both these characteristics are vital for the surface layers, SMAs also resist wear.

SMAs have been highly successful in urban and high traffic environments because of its

ability to carry the traffic load in its coarse stone skeleton. The matrix adds ruggedness

and stiffness to the mix through the addition of polymers, fibers, and mineral fillers; the

added fibers have been shown to be beneficial in precluding draindown in these mixes

(APA, 2002).

Texas requires a 2 to 3 inch SMA under an optional porous friction course;

however, research from Illinois suggests that SMA thicknesses should be dependant

upon trafficking (Table 2-1). The additional thickness would add structural integrity to

resist the high shear stresses which would occur in high trafficking situations (Harm,

2001).

Table 2-1. Required SMA Thicknesses in Illinois (Harm, 2001).

Traffic Level	Minimum Thickness (in)
Low	2
Medium	4
High (>25 million ESAL)	6

Open-Graded friction courses (OGFC) have been used as renewable wearing

courses for perpetual pavements (Newcomb et al., 2001). Unlike the SMA, OGFC is a

porous mix that is combined with polymer-modified binder or asphalt rubber binder to

produce a wearing course that reduces tire splash, spray, noise, hydroplaning, and aging

(St. Martin et al., 2001). The ability for water to move rapidly through this mix stems

from its void structure. OGFC's typically are designed for above 20% air voids as

compared to 4% in a typical Superpave design. This allows water to move through large

void spaces and flow out of the pavement before it can become a safety hazard to

drivers. Some research has shown that increasing the void spaces of OGFC from 15%

to an 18-22% range can even improve the long-term performance of the pavement (APA, 2002).

It is important when choosing the binder grade for a wearing course to remember this is the layer that will experience surface cracking and rutting. Harm suggests modifying the top 6 inches of any perpetual pavement to help resist surface cracking (Harm, 2001). APA recommends using a performance grade one temperature higher than is typically used for the area. The low temperature should be within a 95-99% reliability for the area (APA, 2002).

Rutting is the only test recommended by APA; however, other engineers suggest possibly adding a shear analysis using the Strategic Highway Research Program Superpave Shear Tester on the top 4 inches of the pavement to determine rutting and cracking potential (Harm, 2001; APA, 2002; Newcomb et al., 2001).

M-E DESIGN

One of the most important road tests, the AASHO Road Test, was conducted in Ottawa, Illinois from 1958 until 1960. The results of this test were later an integral part in the creation of the methodology for the AASHTO Design Guide for Pavement Structures (AASHTO, 1993). This design guide is currently the practice for many agencies in the United States; however, it is hindered by the conditions at the test road such as "one environmental condition, a limited number of axle weights, tire pressures and axle configurations, and only 1.1 million axle load repetitions" (Timm et al., 2004). Furthermore, the empirical layer coefficients in the AASHTO Design Guide represent

the overall behavior of the material and relate it to the serviceability of the 1963 test (Newcomb et al*.,* 2001, Timm et al., 2004).

A painful downfall to this type of design is the inability to separate the layers of the structure to understand each layer's contribution to the pavement's life (APA, 2002). While this is the case with the AASHTO Design Guide, CBR design and many other thickness design methodologies lack the functionality to consider each layer's role in mitigating distresses (APA, 2002).

As research has continued and test roads have become more advanced, a shift has begun to occur from purely empirical design to mechanistic-empirical (M-E) design. Even in the 1960s, some engineers began using mechanics to calculate stresses in pavements (APA, 2002); however, a complete M-E design methodology was still years away.

The 1980s brought states closer to instituting M-E design principles when states such as Washington, Kentucky, Illinois, and Minnesota began experimenting with M-E design methodologies. These methods used basic mechanical principles to estimate a pavement's reaction to specified loads as seen in Figure 2-6 (APA, 2002). In 1989, Illinois implemented its mechanistic pavement design procedure. At this point, pavement engineers were limiting the maximum tensile strain in the bottom lift of the pavement to 60 $\mu\varepsilon$. Engineers were also limiting the subgrade stresses to protect the base material (Harm, 2001).
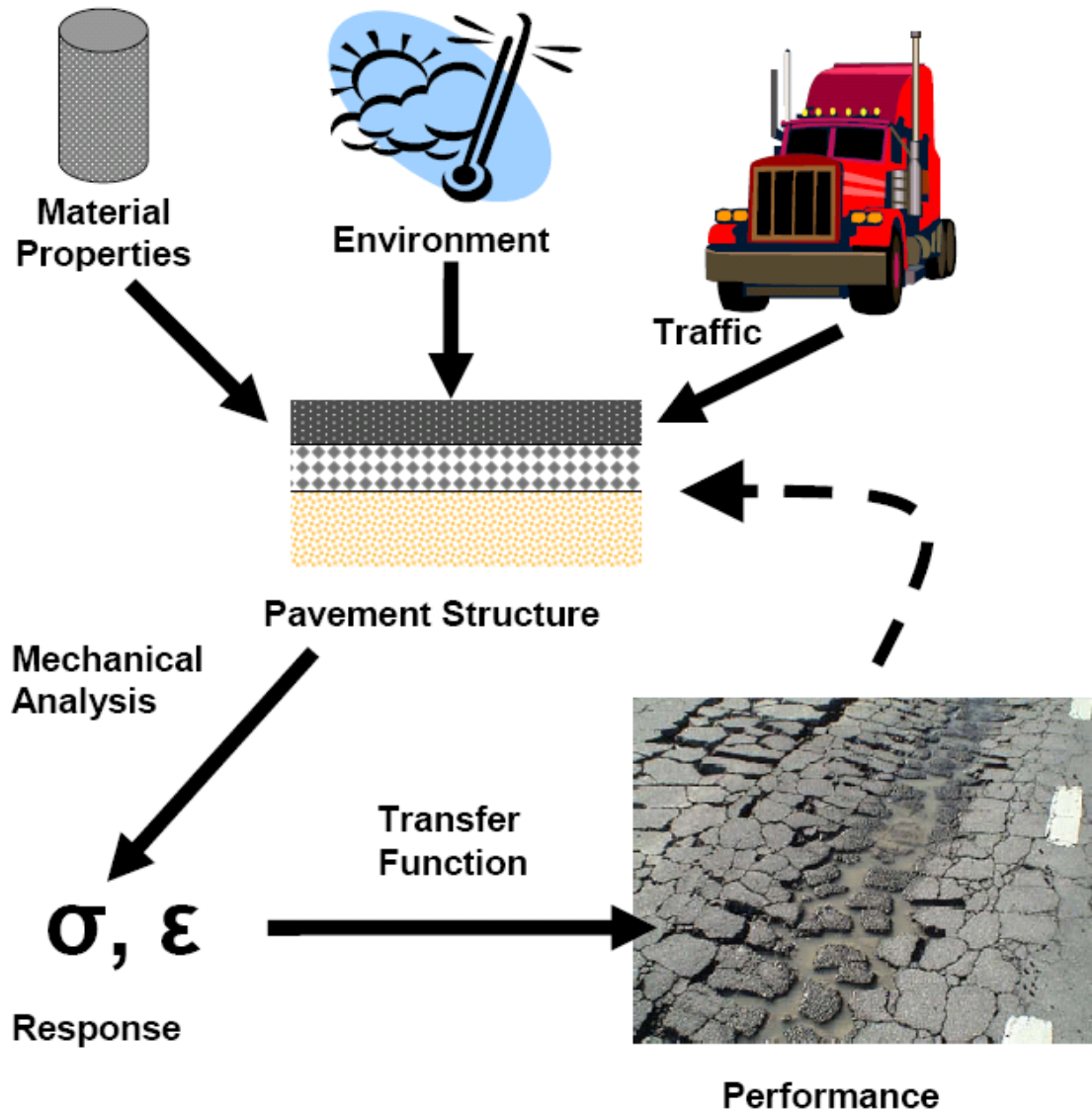
Figure 2-6. M-E Design Schematic (Priest and Timm, 2006).

Currently, there are M-E pavement design methodologies in place, such as the Asphalt Institute (1982). AASHTO is also in the process of completing and implementing its own M-E design procedure (AASHTO, 2008) because these design scenarios can provide the following advantages that previous design guides could not (Timm and Newcomb, 2006):

1. M-E design can model and accommodate various tire loads, axle configurations, tire pressures, and other load characteristics.

2. M-E design can incorporate new advances in material design.

3. M-E design accounts for material variability and seasonal changes through the use of Monte Carlo simulations.

4. M-E design produces reliability that is sensitive to its input variables.

5. M-E design uses transfer functions coupled with Miner's Hypothesis (Miner) to predict distresses and pavement life.

Computer programs such as WESLEA, IlliPave, and PerRoad have all been incorporated into the design process to relate tensile strength and vertical strain to field performance (APA, 2002).

The basic design framework (Figure 2-7) requires using the mechanical properties of the pavement, with the traffic, climate, and predicted performance to design a pavement of adequate thickness (APA, 2002; Timm and Newcomb, 2006).
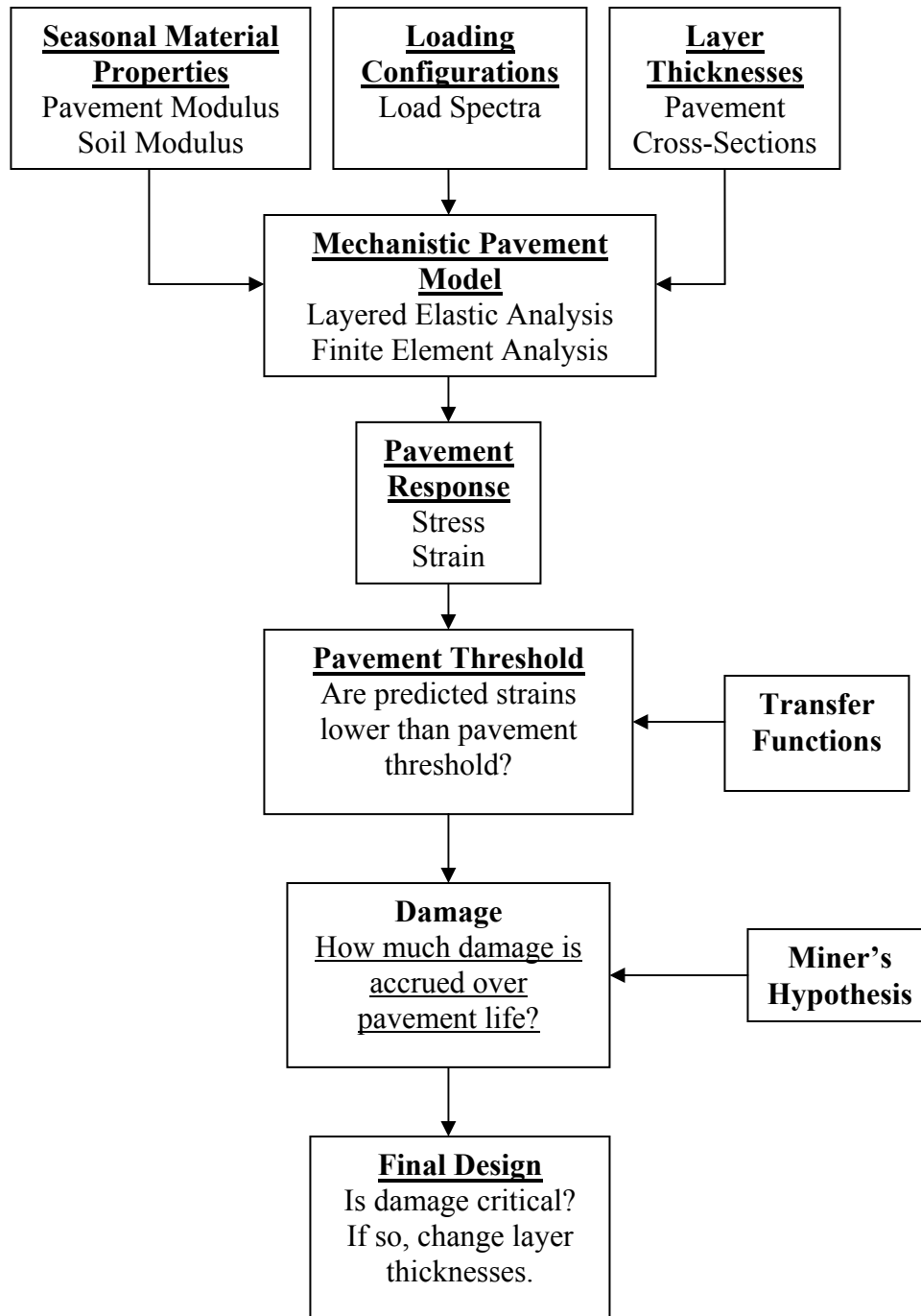
Figure 2-7. Perpetual Pavement Design Framework (Timm and Newcomb, 2006).

Three groups of parameters are characterized in the completion of an M-E

design: seasonal material properties, loading configurations, and layer thicknesses. The

seasonal material properties encompass the stiffness and strength of the pavement

structure and how each reacts to changes in climate. During warmer seasons, HMA becomes softer which causes strains to be higher. When properly characterized, adequate pavement response predictions can be made.

Loading configurations must also be characterized in M-E design. In the 1993 AASHTO Design Guide, loads were defined as equivalent single axle loads (ESALs). Using this principle, a loading configuration could be normalized to an 18 kip single axle. M-E pavement design hinges its loading configurations on the idea of load spectra. This principle creates a distribution of axle types and weights to predict pavement response. Each grouping will impose certain stresses and strains on the pavement structure and accurately quantifies traffic variety instead of normalizing it to an ESAL value.

The final parameter of the pavement structure that needs to be characterized is layer thickness. This parameter consists of accurately creating a cross-section of the desired pavement structure. Each individual layer contributes to the overall performance of the pavement as a whole. In other words, each layer has a role it must play for it to become a long-lasting pavement.

When the seasonal material properties, load configurations, and layer thicknesses are accurately quantified, a mechanistic pavement model is used to estimate the potential pavement response. These models can vary from the simple Boussinesq and Westergaard equations to highly complex finite element analysis procedures. While the model is typically program dependant, the final result of the model is an estimated stress or strain.

These stresses and strains are compared to threshold values established from laboratory testing to determine if the pavement has the potential to become perpetual. Typically, Miner's Hypothesis is coupled with a transfer function, a relationship between pavement response and pavement performance, to determine if the cumulative damage over the design life of the pavement is going to reach a critical value. If the damage exceeds an allowable level, the M-E design process is repeated using a thicker pavement structure.

PAVEMENT DISTRESS THRESHOLDS

Since the idea for developing perpetual pavements has been proposed, the need to determine a fatigue endurance limit has sparked much debate and research. An endurance limit for a flexible pavement has been defined as "the horizontal asymptote of the relationship between the applied stress or strain and the number of load repetitions, such that a lower stress or strain will result in an infinite number of load repetitions" (Von Quintus, 2001). At this point, increasing the thickness of a pavement would provide no extra protection against fatigue cracking (Carpenter et al., 2003).

When this idea was first proposed, a 60 $\mu\varepsilon$ limit was imposed at the bottom of the HMA to prevent fatigue cracking (Newcomb et al., 2001). Since that time, this limit has fluctuated depending on researcher from 65 to 70 to 100 $\mu\varepsilon$ (Von Quintus, 2001; Timm and Newcomb, 2006).

Research was conducted in 2002 at the University of Illinois to delve deeper into the idea of validating a specific fatigue threshold for perpetual pavements. Carpenter et al. (2003) noted that most fatigue models propose a linear log-log relationship between

36

tensile strain and number of load repetitions; however, this idea is in direct contrast to the basic premise of a fatigue threshold. To validate the theory of an endurance limit, he tested asphalt beams using AASHTO T321 at different strain levels. AASHTO T321 is a beam fatigue test that loads asphalt specimens using a 10-Hz haversine load at 20°C with a constant strain. A schematic of the testing device is seen in Figure 2-8.

KEY:

1. REACTION CLAMP
2. LOAD CLAMP
3. RESTRAINER
4. SPECIMEN
5. LOADING ROD

6. STOP NUTS
7. LOAD BAR
8. PISTON ROD
9. THOMPSON BALL BUSHING
10. LVDT HOLDER
11. LVDT
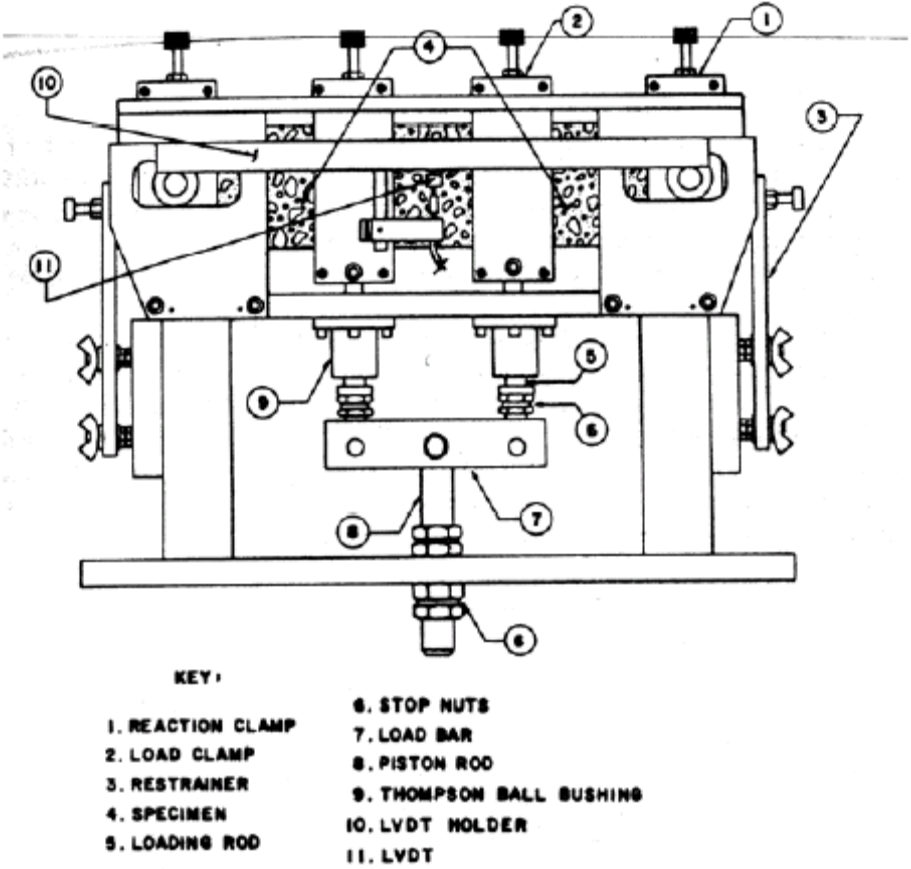
Figure 2-8. Schematic of Third Point Beam Fatigue Testing Device (Monismith et al., 1985)

Typically, samples are tested between 250 and 1000 µε until failure occurs. The horizontal strain is calculated by measuring the vertical deflection of the beam. Equation 2-1 calculates the horizontal strain based upon that measurement.

37

$$\varepsilon = \frac{12t\Delta}{3l^2 - 4a^2}$$ Equation 2-1

Where: ε = horizontal strain, microstrain

t = thickness, inches

Δ = deflection at center of beam, inches

l = length of beam, inches

a = distance between support and load, in

Failure is defined as the number of cycles required to reduce the material's initial stiffness by 50%. Flexural fatigue testing can be very time-consuming and inefficient for laboratories at low strains due to the large number of cycles it requires to fail the specimen; therefore, low strain relationships are typically extrapolated below 300 $\mu\varepsilon$. Testing was conducted at various constant strains between 250 and 1000 $\mu\varepsilon$, and the extrapolated data showed an asymptote occurred in the data at approximately 70 $\mu\varepsilon$ (Carpenter et al., 2003).

Similar testing was conducted by the Asphalt Institute using AASHTO T-321. In this case, one fatigue flexural test was conducted at the low strain value of 70 $\mu\varepsilon$ due to time constraints. This test did not reach the failure value of 50% stiffness after 4,000,000 cycles (Peterson et al., 2004).

Some researchers believe that a 50% reduction in the asphalt's stiffness might not truly indicate the remaining life in the structure. To circumvent this issue, researchers have developed the dissipated energy ratio and the reduced energy ratio as ways of characterizing fatigue damage. Both Carpenter et al. and Peterson et al. conducted fatigue threshold research using the dissipated energy model. The dissipated

energy ratio relates the rate of change in dissipated energy to fatigue failure by quantifying how damage accumulates in a fatigue test from one cycle to the next (Carpenter et al., 2003).

Dissipated energy ratios are plotted versus log load repetitions. This graphical representation looks somewhat like a "U" (Figure 2-9). The plateau value shows where damage is not increasing between cycles. This value continues until damage begins to increase between cycles. This is when the mix becomes unstable and loses its ability to carry load (Carpenter et al., 2003).
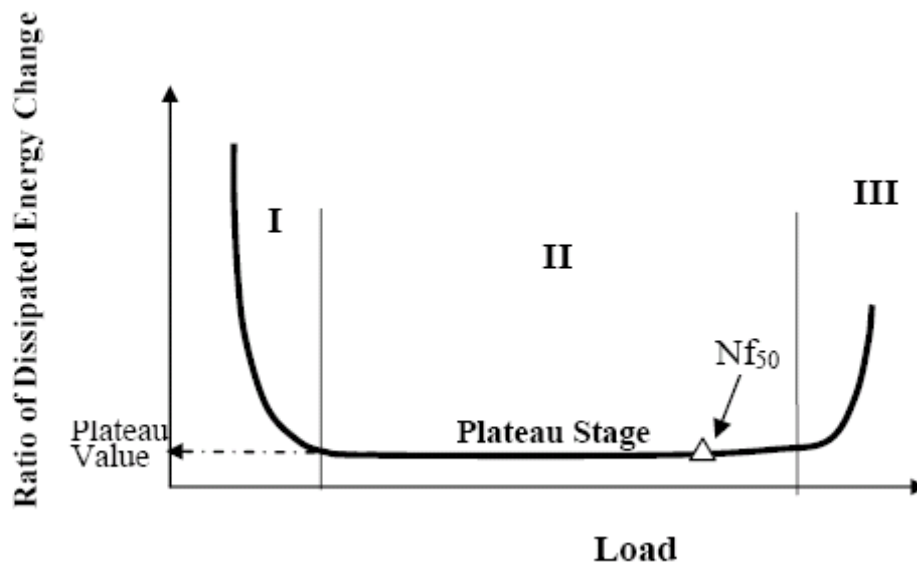
Figure 2-9 Typical Ratio of Dissipated Energy Change versus Loading Cycles Plot (Carpenter et al., 2003).

Peterson et al.'s (2004) test on one mix found an asymptote between the 70 and 100 $\mu\varepsilon$ level. When testing was conducted at 70 $\mu\varepsilon$, the plateau was never reached at 4,000,000 cycles. Carpenter et al. (2003) found similar results showing that 70 $\mu\varepsilon$

provided long fatigue life; however, the threshold depended on the mix as some mixes could withstand 100 $\mu\varepsilon$ without achieving their ultimate failure.

Reduced energy ratios use the theory of fatigue cracking involving four stages (internal heating, micro-crack formation, crack formation, and sample breakdown) to quantify the fatigue characteristics of the mix being tested. Failure, in this methodology, occurs when cracks begin to form. Cycles are multiplied by the measured modulus and plotted against cycles. The point of pavement failure occurs at the peak of this graph. This must be determined because typically initial cracking may not be visible. As the strain level is decreased, the cycles until failure increase as expected. At 70 $\mu\varepsilon$, the crack formation stage is not reached at 4,000,000 cycles. This supports the idea of an ultimate fatigue limit (Peterson et al., 2004).

While laboratory testing has been used to help predict field fatigue life, there has been great difficulty in developing correlations between the laboratory value and the actual field performance of the pavement (Harvey et al., 1995). A few reasons which might explain this discontinuity between the lab and the field are listed below (Tangella et al., 1990):

1. In the field, wheel wander affects loaded areas so the same point on the pavement is not continuously loaded.

2. The support of underlying layers might provide additional support to increase the fatigue life of the HMA.

3. Fatigue life relationships are dependant upon the type of fatigue testing, mode of loading, and test temperature.

4. Pavements in the field experience rest and healing.

5. Field performance is dependant upon thickness of the pavement structure.

Agencies have been using perpetual pavement thresholds in their designs with much success in Kansas, Ohio, and Shandong Province, China. Each of these entities instrumented roadways with strain gauges so they could measure strain at the base of the HMA layer. Kansas designed and built four perpetual pavement sessions in 2005 using the Illi-PAVE algorithm to design the structure of the pavement section. It assumes traffic loadings of 22,600 lbs at a pavement temperature between 99 and 118°F. To date, even the thinnest sections are still measuring strains below the design threshold of 70 $\mu\varepsilon$ (Romanoschi et al., 2008).

Similar results have been seen near Canton, Ohio. In 2002, a 2-mile, six-lane section of HMA perpetual pavement was constructed along I-77. The pavement structure in this case was to respond to loads 20% greater than the critical load with a 70 $\mu\varepsilon$ maximum tensile strain at the base of the HMA. The structural design consisted of 16.25 inches of HMA over 6 inches of granular base. Strain values have been consistently recorded in the 30 $\mu\varepsilon$ range for this project (Kuennen, 2004; Ursich, 2005). These strain measurements may be from an underestimation of the pavement's stiffness in the design scenario. Texas has consistently seen pavement stiffnesses higher than predicted in designs causing reduced strain values (Scullion, 2006).

China's three perpetual pavement test sections were constructed in the summer of 2005. The design philosophy was different from those in the U.S. because of the loading capacity required. In China, the average single axle weighs approximately 20 kips. A 90th percentile axle weight was chosen for design. Two fatigue threshold were evaluated, 70 and 125 $\mu\varepsilon$, which produced pavements 20 and 15 inches thick,

41

respectively. Currently, 90% of the strains have fallen below the designed thresholds (Yang et al., 2005).

CONSTRUCTION CONCERNS

Perpetual pavements have been shown to provide an economic advantage over a non-perpetual pavement (Rolt, 2001; APA, 2002; Cheneviere and Ramdas, 2006); however, this distinct advantage will become null if proper mixing and construction is not accomplished. Thick and stiff pavements should be capable of reducing stresses and strains in the pavement, but variables in the construction process can negatively influence the longevity of the pavement (Estes, 2005).

Mixes must be properly constructed and placed for pavements to achieve long lives. Since Texas has been experimenting with perpetual pavements, the modulus of the pavement has typically been greater than their design. This increase in pavement modulus leads to low pavement deflections such as those in rigid pavements (Scullion, 2007).

France used a high stiffness binder (10/20 pen) in its perpetual pavement study. With the reduced air voids and stiffer binder, a 35% increase in pavement stiffness was seen. This led to resistance in fatigue cracking and rutting. Due to France's milder climate, thermal cracking was not found to be a concern except in a few extremely cold (-10 °C) regions (Fee, 2001).

Proper stiffness is essential to the pavement because a stiff pavement will increase the fatigue life of the structure. As a mix ages, the surface of the structure will become harder than the base of the structure because of trafficking and oxidation (Fee,

42

2001). When this occurs, longitudinal cracking at the surface becomes the dominant

form of surface distress in perpetual pavements (Mahoney, 2001). The longitudinal

cracks initiate near the surface and begin to propagate downward decreasing the

effective road structure (Von Quintus, 2001; Rolt, 2001). These cracks deteriorate the

surface of the pavement allowing interconnection between the surface distresses which

weakens the entire pavement structure (Rolt, 2001; Von Quintus, 2001). When this

occurs, the perpetual pavement should receive maintenance to provide additional fatigue

life (APA, 2002).

While a proper mix design is essential to the pavement's life, quality

construction is also vital. The following suggestions have been given to increase a

mixture's durability (Harm, 2001):

1. Require a minimum lift thickness 3 to 6 times greater than the nominal maximum

   aggregate size to increase the in-place density of the mix.

2. Require positive dust control on plants for better mixture production control.

3. Tack each lift with polymer before paving to better facilitate lift bonding.

4. Reduce variability in the bottom layer of HMA by using virgin aggregate.

5. Use a material transfer vehicle (MTV) to prevent segregation.

6. Revise in-place density testing to promote more uniform material density.

7. Increase the required density for the middle layer to be less than 7% air voids.

Two of the most common construction issues are segregation and debonding.

Due to the stiff nature of many perpetual pavement surface courses, the segregation of

coarse aggregates can easily occur. Segregation is the result of improper material

handling and can be lessened by the use of MTVs. If segregation occurs in HMA, the

43

pavement could be susceptible to top-down cracking (Harmelink et al., 2008) and/or future moisture damage (Lu et al., 2007).

A second construction problem that affects all types of pavements, regardless of design philosophy, is debonding. When debonding occurs, pavements cannot transfer the traffic load to the base of the HMA structure. This creates higher strains in the upper strata of the pavement which can lead to early pavement failure (Willis and Timm, 2007).

Two perpetual pavement experiments have failed prematurely because of debonding issues. In the 2003 cycle of the NCAT Pavement Test Track, a perpetual pavement design was constructed and instrumented with strain gauges on the top and bottom of the fatigue-resistant rich-bottom layer. Another instrumented section was built with the same design except for the rich-bottom layer was not present. Over the course of testing, the perpetual structure began to show early signs of fatigue cracking. Willis and Timm (2007) performed a forensic investigation into the failure mechanism of the pavement using theoretical and measured strains to determine the cause of the premature deterioration.

Strains were measured at the base of the HMA layer and at the rich-bottom/HMA interface. Strains were also simulated using WESLEA for different scenarios where the pavement either remained fully bonded, slipped at the SMA upper layer, or debonded at both the SMA and rich-bottom layers. Strain ratios ($\frac{\varepsilon_{7"}}{\varepsilon_{5"}}$) were compared for both the measured and theoretical values. These results (Figure 7), along with a thorough crack investigation of cut trenches, supported the theory of debonding at

44

both the SMA and rich-bottom layers. The reasons for debonding in this section were

unknown (Willis and Timm, 2007).
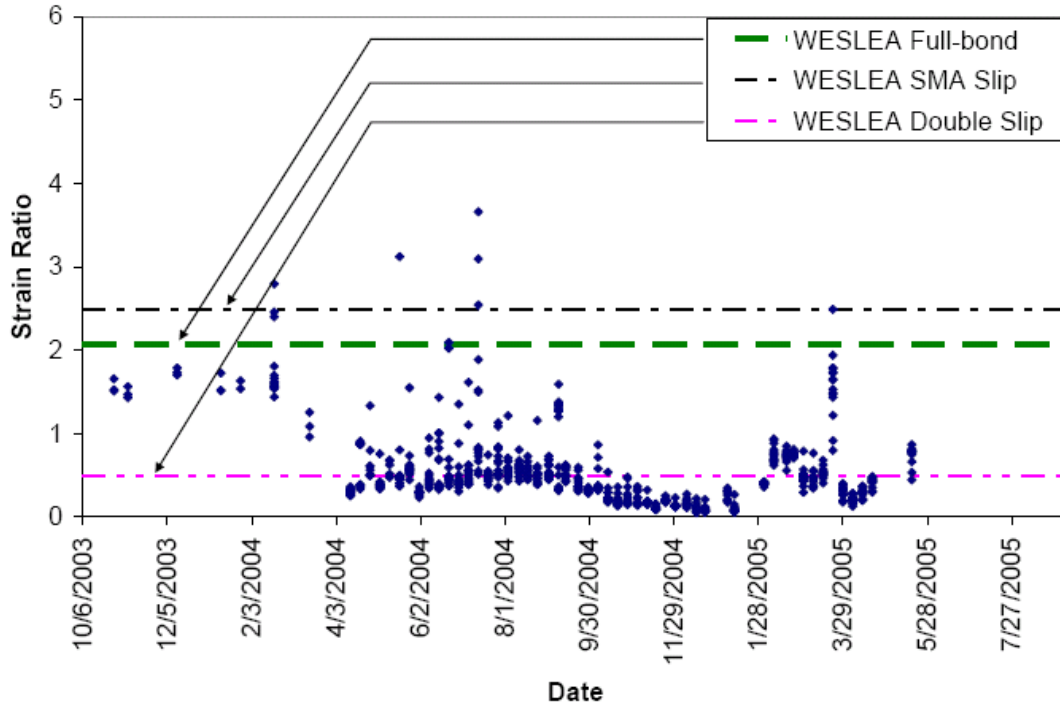
Figure 2-10 Strain Ratio Comparisons for Deteriorated Section of the NCAT Pavement Test Track (Willis and Timm, 2007).

Similar results were seen at the Texas perpetual pavement experiment.

Premature fatigue cracking occurred prompting a forensic investigation. When cores

were removed from the pavement, debonding was evident. A tack coat was not placed

between pavement layers; therefore, the researchers believed the failure to properly tack

the pavement resulted in the debonding (Scullion, 2006). Currently, it is at the state's

discretion as to whether or not a pavement should receive a tack coat. Organizations

such as CalTrans do not currently require tacking; however, for its perpetual pavements

on I-710, a tack coat was required for bonding purposes (St. Martin et al., 2001).

Pavement engineers understand the components of a pavement necessary to help it achieve a long lifespan. A rut-resistant upper layer of the pavement is going to allow the structure to withstand rutting, and the fatigue resistant base layer will help mitigate the presence of fatigue cracking. However, how are these concepts going to translate into the forthcoming M-E design?

M-E design allows engineers to design pavement structures to withstand certain strain levels (i.e. strain at the base of the HMA layer) to help delay or completely eradicate fatigue cracking so as only surface cracking needs to be rehabilitated. However, what is this strain value? Currently, laboratory experiments have resulted in a fatigue endurance limit between 70 and 100 $\mu\varepsilon$, but it is difficult at best to correlate laboratory values to field measured strains. Measured strains from the field need to be analyzed to bridge the gap between laboratory and field strains in determining a design fatigue threshold limit for perpetual pavements.

CHAPTER THREE

TEST FACILITY

ACCELERATED PAVEMENT TESTING

As M-E design progresses, the need for states to validate their findings will continue to grow. While some organizations consider doing full-scale testing on actual in-service roads, completing such research can be severely limited by the following factors: (1) testing could take many (15-20) years to complete, (2) it is often difficult and unsafe to close lanes on in-service roads for inspection, (3) Departments of Transportation tend to be reluctant to leave roads in service until failure occurs, (4) the public can be intolerant to traffic delays due to road closures and (5) changes in personnel and political climates can compromise long-term experiments (Brown et al., 2002).

Because of these difficulties, the development of a new testing system for pavements was developed. This new system began when the world was in a similar state of developing new design and analysis techniques. Much like M-E design today, these new procedures needed to be validated with performance data observed under trafficking. From this need came accelerated pavement testing (APT) facilities, also known as accelerated loading facilities. APTs were able to bridge the empirical with actual pavement performance (du Plesis et al., 2006).

An APT is defined as a "controlled application of a loading to pavement structures for the purpose of simulating the effect of long-term in-service loading conditions in a compressed period of time" (Hugo, 2004).

APTs began modestly with the United Kingdom's "Road Machine" in 1912 (Powell, 2006). After migrating to the United States in 1919, the Arlington Test Road tested newly designed concrete pavements by simply loading them with a truck. From this simplistic beginning came other such roads like the Bates experimental road, the Maryland Test Road, and the Western Association of State Highway Officials Road Test which tested the effects of loading on pavements using simulated or actual traffic (Metcalf, 1996).

APTs were brought to the forefront of the pavement research industry when the American Association of State Highway Officials (AASHO) Road Test was established to help develop a new pavement design guide. This experiment played a vital role in making road construction a "rational process" (du Plesis et al., 2006).

The 1990s brought about a surge in APT facility construction (Rollings and Rollings, 1991). In 1996, 28 APT programs were being run around the world (Metcalf, 1996). After the addition of facilities by organizations such as the Federal Aviation Administration in New Jersey, the Florida Department of Transportation, and the National Center for Asphalt Technology, 45 APT facilities were functioning world-wide by 2002. Fourteen were located within the borders of the United States of America (Saeed and Hall, 2003).

THE NCAT PAVEMENT TEST TRACK

In 2000, NCAT, in cooperation with the Alabama Department of Transportation

and Auburn University, built its APT facility in Opelika, Alabama. The NCAT

Pavement Test Track (Figure 3-1) is a 1.7 mile closed loop full-scale loading facility.

Closed loop facilities allow multiple test sections of pavement to experience similar

trafficking patterns and environmental conditions so comparisons may be made between

all the test sections (Brown et al., 2002). A unique feature of the NCAT Test Track is

that other states and organizations may sponsor test sections to meet state-specific

research needs.

Figure 3-1. The NCAT Test Track.

The NCAT Pavement Test Track is comprised of 46 experimental test sections

that are 200 feet long (Figure 3-2). Mix and structural designs are tested on a section by

section basis depending upon the desires of the section sponsor. The sections are built-

full scale using standard construction practices and quality control procedures to ensure

the sections are representative of what is seen on typical roadways (Willis and Powell,

2008).
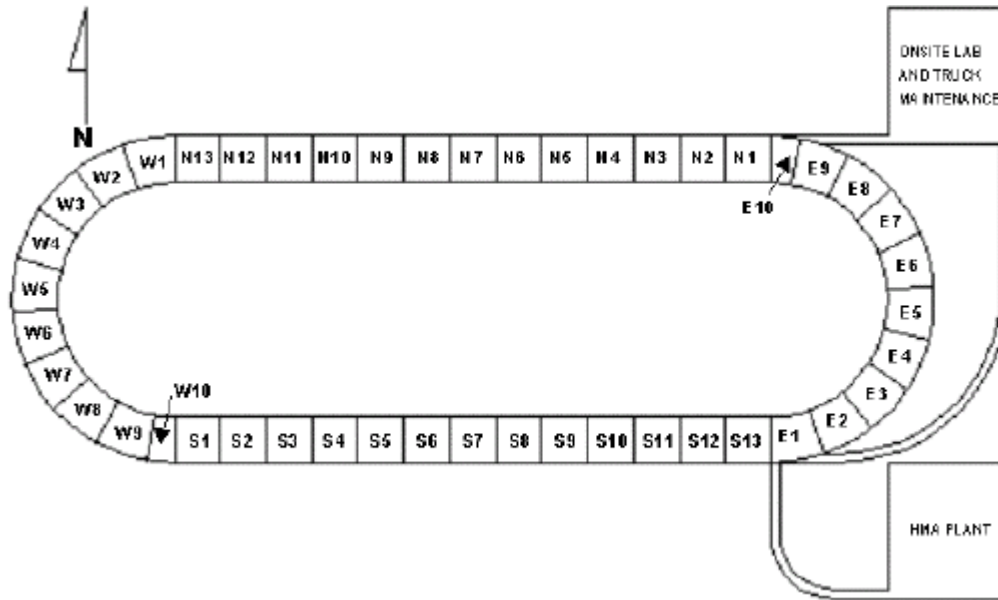
Figure 3-2. Layout of Test Track (Brown et al., 2002).

Trafficking at the Test Track is accomplished by using a fleet of trucks manned

by professional drivers. The decision to use a manned fleet of trucks was based on a

desire to realistically test the pavements through the introduction of wander. When

trucks traverse a pavement structure, wheel wander occurs as vehicles move transversely

in their lanes. Using drivers allows this variable to be considered in the performance

analysis of each section.

Over two and a half years, each test section receives approximately 10 million

ESALs of traffic. This is accomplished by running traffic from approximately 5 a.m.

until 10:45 p.m. five or six days a week. During the 2000 Test Track, traffic was run six

days a week, but that number was reduced by a day at the beginning of the 2003 Test

Track. Sunday and Monday were then used as days to repair and maintain the track

vehicles and conduct pavement performance measurements such as rut depths and crack

maps (Brown et al., 2002).

The 2000 Test Track was originally designed using thick pavement cross-

sections and experimental mixes to study the relationship between field and laboratory

rutting performance. While many of these sections proved to be rut resistant, all 46

sections proved to be highly successful in preventing fatigue cracking as well (Brown et

al., 2002).

As the Test Track continued to evolve, the 2003 experimented added a new

dimension of study by including pavement instrumentation in thinner cross-sections

along the North tangent so pavement responses could be measured. The goal of this

research was to evaluate the structural performance of differing pavement designs.

While the structural experiment was just one additional component to the 2003 Test

Track, many of the original thick test sections from the 2000 experiment were left in-

place for additional trafficking. Again, comparing mixture and materials to rutting

performance was the primary goal of the additional traffic (Timm et al., 2006).

In 2006, the scope of the Pavement Test Track once again grew to incorporate

new and timely research projects. As the implementation of the new AASHTO MEPDG

approached, the structural study grew from eight to eleven instrumented sections where

pavement responses could be measured. Due to the increasing interest in using

reclaimed asphalt pavement (RAP) as a cost saving initiative, new sections were

developed that incorporated high amounts (50%) of this recycled product into the mix

design to test its durability. One section even tested new construction techniques. In an

effort to improve smoothness and bonding, a new twin-layer paver has been developed that places two pavement lifts simultaneously (Figure 3-3). The Georgia Department of Transportation sponsored a test section using this new technology to test the integrity of a pavement placed using this new device.

Figure 3-3. Twin Layer Paver that Paved Section N13 in 2006.

Though many different experiments have been associated with the NCAT Test Track, the primary focus of this research revolved around the sections instrumented with asphalt strain gauges. These test sections were used to compare strain measurements at the bottom of the HMA to performance over time. Much more detail pertaining to each of the experimental cycles (2000, 2003 and 2006) is provided in the following chapters.

CHAPTER 4

DETERMINING A LOWER BOUND FATIGUE LIMIT

THE 2000 NCAT PAVEMENT TEST TRACK

In 2000, NCAT built and developed an accelerated loading facility experiment in Opelika, Alabama. This experiment was designed to study rutting potential in surface mixes. In completing this task, all 46 sections of the Test Track were built with a minimum thickness of 23 inches of bituminous material to help control the potential for bottom-up fatigue cracking. At the conclusion of the first experiment (10 million equivalent single axle loads (ESALs)), no fatigue cracking had been observed (Brown et al., 2002).

When the 2003 NCAT Test Track experiment began, many of the original test sections were left in-place to receive another 10 million ESALs of traffic. The additional traffic did not prove detrimental to the pavement structure in terms of fatigue cracking which was still not observed after 20 million ESALs of traffic.

The third experiment at the NCAT Test Track began trafficking the pavement on November 10, 2006. At this point in time, only eight of the original 2000 Test Track sections remained in-place. Of those sections, however, as of December 4, 2008, 30 million ESALs had been trafficked over these eight test sections and signs of fatigue cracking have yet to be witnessed.

The thick nature of these sections coupled with the lack of fatigue cracking implies that the strains seen at the bottom of the bound materials in the pavement structure were theoretically small. Not only would the thick nature of the pavements contribute to minute strains, but adequate stiffness and quality construction would help prevent alligator cracking. If it were the case that small strains were experienced at the bottom of the bound materials, it would be natural to set a minimum field-based fatigue threshold equal to the strain distributions found in these sections for perpetual pavements.

Researchers have postulated that perpetual pavements only need to be 14 inches thick (Fee, 2001) in order to successfully prevent fatigue cracking for 20 years; if a pavement is 23 inches thick or more, such as those at the Test Track, and has sustained 30 million ESALs without showing signs of fatigue cracking, it is logical to say that a pavement structure 14 inches thick with similar material properties in the bound and unbound layers would exhibit higher strains. This being the case, a lower bound for a field-fatigue threshold could be set from these thicker pavements so pavements could be built with an overall thinner design.

GENERAL METHODOLOGY

Since perpetual pavement design is based upon limiting strains at the base of the bound materials or hot-mix asphalt (HMA), the basic mechanistic-empirical (M-E) design framework was chosen to serve as the basis for the methodology of each dataset analysis. In an M-E analysis, the seasonal material properties, loading configuration, and layer thicknesses are all assembled into a pavement model which estimates or

calculates a pavement response. This, in turn, is correlated to the pavement's

performance through the use of transfer functions.

Figure 4-1 provides a model for the data analysis methods for the 2000 Test

Track data. The seasonal material properties were estimated from falling-weight

deflectometer (FWD) testing that occurred during the 2000 experiment. During the time

of the testing, temperature readings were taken at 10 inches deep in the pavement.

Using these data, the modulus of the pavement and the resilient modulus of the soil

could be correlated to the temperature measured at the time of testing.

The loading configuration and the layer thicknesses were both developed using

databases kept by the staff of the NCAT Test Track. The loading configuration database

consisted of ESALs per day, and the construction database provided individual layer

thicknesses at multiple locations within a section.
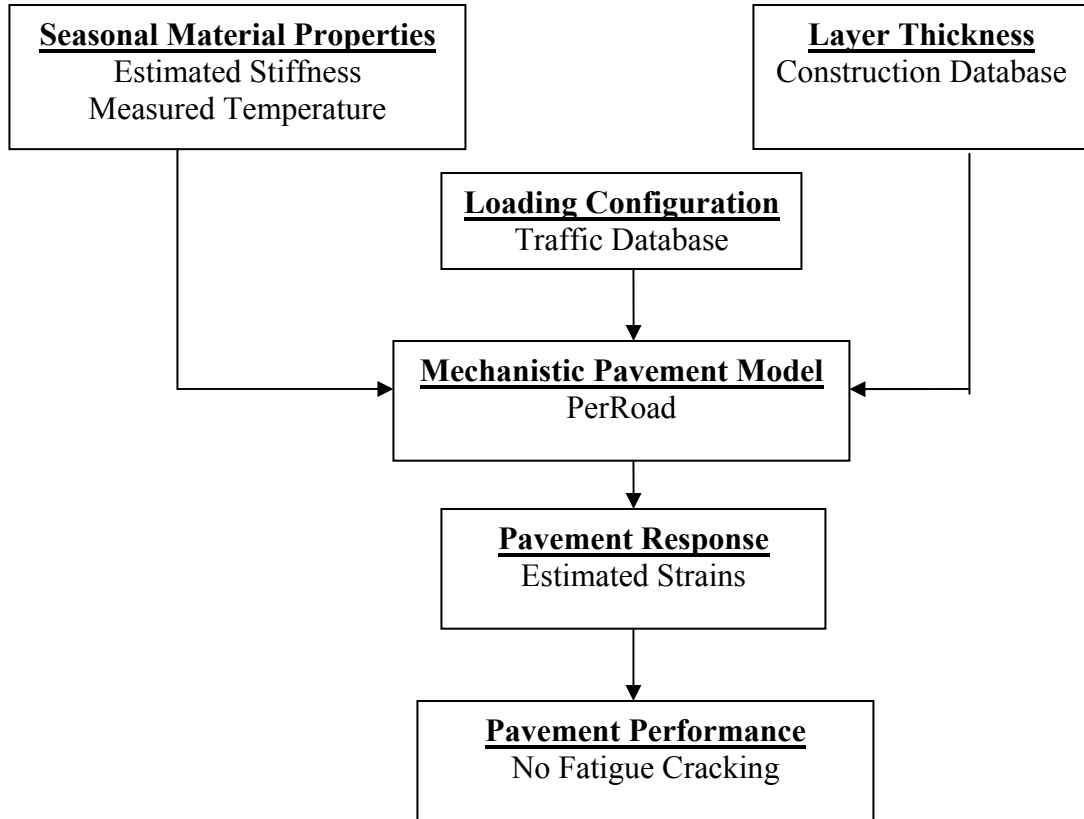
Figure 4-1. Flowchart for 2000 Test Track Analysis.

PerRoad

PerRoad, a computer analysis program used to design perpetual pavements using the M-E design philosophy, was used as the mechanistic pavement model in this data analysis. The program couples layered elastic analysis with a statistical analysis procedure (Monte Carlo simulation) to estimate stresses and strains within a pavement (Timm and Newcomb, 2006). In order to predict the strains which would prove detrimental for fatigue cracking, PerRoad requires the following inputs:

- Seasonal pavement moduli and annual coefficient of variation (COV)

- Seasonal resilient moduli of unbound materials and annual COV

- Thickness of bound materials and COV

- Thickness of unbound materials

- Load spectrum for traffic

- Location for strain analysis

Structural and Seasonal Information

For PerRoad to calculate strains in a pavement, the first inputs characterized were the material properties of the pavement structure on a seasonal basis. PerRoad has the ability for material properties to be characterized from a simple one season analysis to a more complicated five-seasonal approach. In doing such analyses, one must first determine how many layers the analysis will include. Once this is determined, the modulus and thicknesses of each layer can be inserted into the computer program as seen in Figure 4-2.

Figure 4-2. Seasonal PerRoad Inputs.

One important advantage of using Monte Carlo Simulations is the ability to quantify the variability of design features (i.e., modulus, thickness). Figure 4-3 shows the variability choices for the asphalt concrete layers of the pavement structure. This is optional, and not required; however, in any construction project, variations in both the thickness and stiffness of the pavement will occur. These functions allow the variability to come from either normal or lognormal distributions. Variability can also be incorporated into the subgrade or granular base layers by analyzing the COV of the layer thickness and resilient modulus.
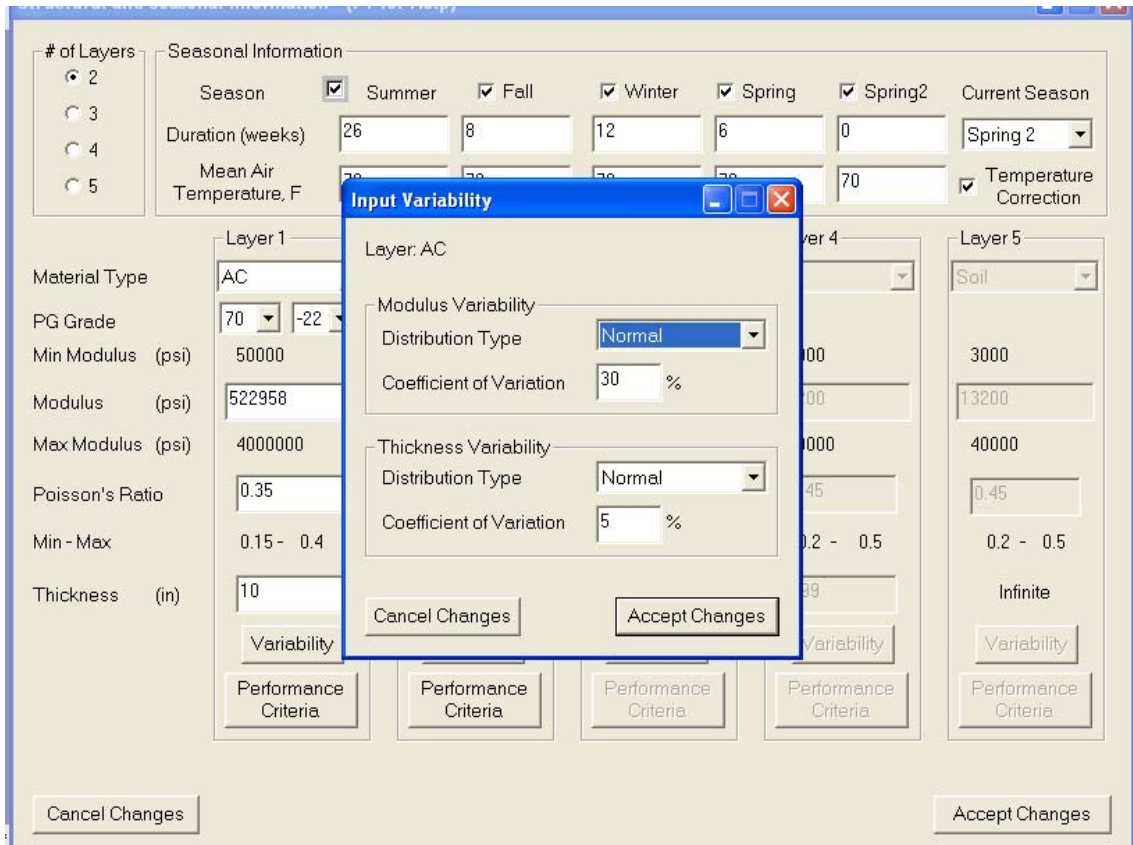
Figure 4-3. HMA Variability.

PerRoad also has the capability of calculating mechanistic responses. These responses can vary from horizontal strain to vertical deflection; however, one must choose the location where the response is to be calculated, and if desired, choose a threshold for that critical response as seen in Figure 4.4. PerRoad uses Weslea for Windows, a computer program utilizing layered elastic theory, to calculate the pavement responses.

59
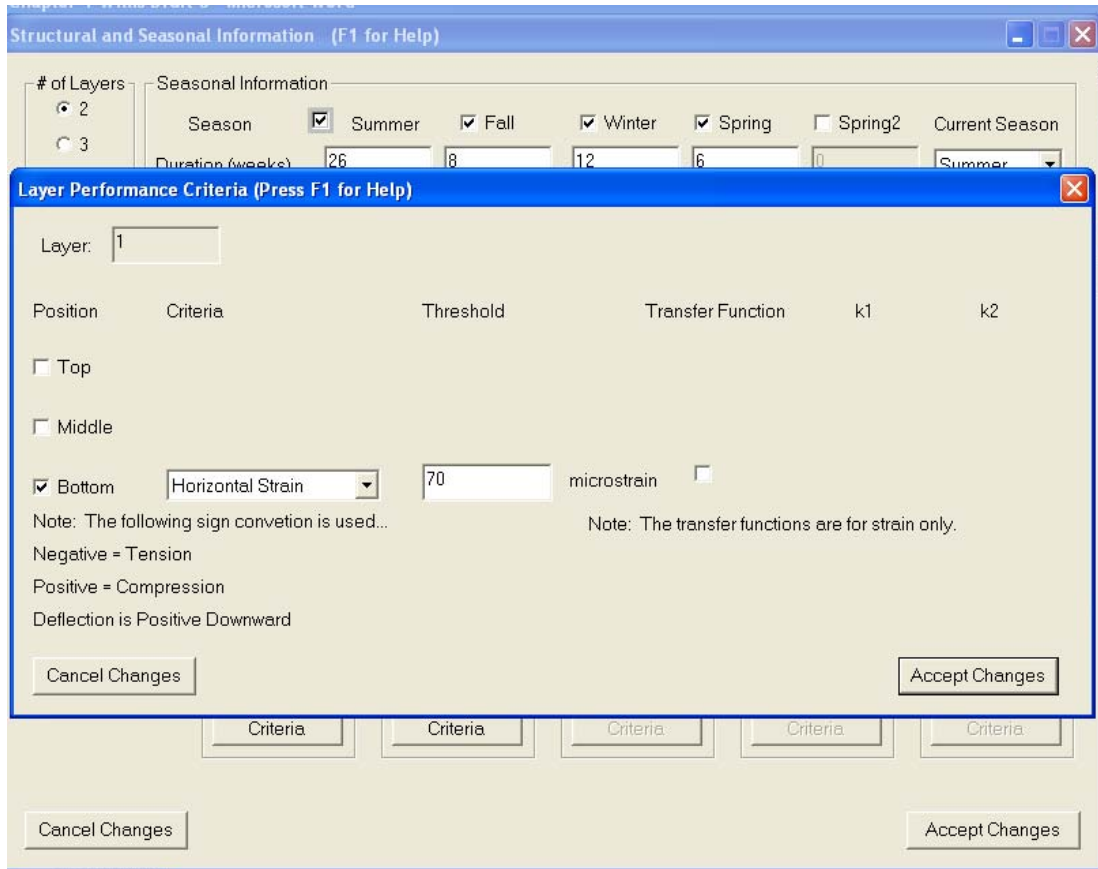
Figure 4.4 Layer Performance Criteria.

Loading Configuration

Figure 4-5 shows PerRoad's requirements for traffic inputs. The program uses the philosophy of characterizing traffic by load spectra instead of ESALs as seen in earlier design methodologies. In the case of PerRoad, traffic is separated by axle type (percent single, percent tandem, percent tridem, and percent steer). After determining the percentage each axle is of the total traffic, traffic is then subdivided into weight classes on 2 kip intervals. These percentages are based on axle type. For example, if 24 of the 200 single axles weighed 19 kips, 12% of the single axles would be placed into the 18-20 kip subdivision. The general traffic data were not used in the Test Track

analysis since the precise traffic patterns of the past five years were available and could be input directly as load spectra.

Figure 4-5. Loading Conditions.

PerRoad Outputs

Once all the desired inputs have been entered in PerRoad, an output file is produced by the program. This file includes the following information: run number, season, modulus of each layer, depth of each layer, axle type, and the user-selected mechanistic responses.

DETERMINING SEASONAL MATERIAL PROPERTIES AND LAYER

THICKNESSES

The first step in completing the M-E analysis procedure for the 2000 Test Track

was to determine the seasonal material properties and layer thicknesses of the sections

being analyzed. To accomplish this, the methodology provided in Figure 4-6 was

developed. Sections were initially chosen for analysis based on available FWD data and

pavement longevity. Once these sections were chosen, their cross-sections were built so

their material properties could be backcalculated using the AASHTO 2-layer

backcalculation methodology. Having then completed the material property analysis,

relationships between the material properties and temperature were developed so the

modulus for each season could be calculated for use in PerRoad. Specific details of

each analysis component are given in the following sub-sections.

Choose Test Sections for Analysis	→	Build Cross-Sections	→	Backcalculate Material Properties

Find Modulus for Each Season	←	Determine Seasons for Analysis	←	Determine Material Properties-Temperature Relationship
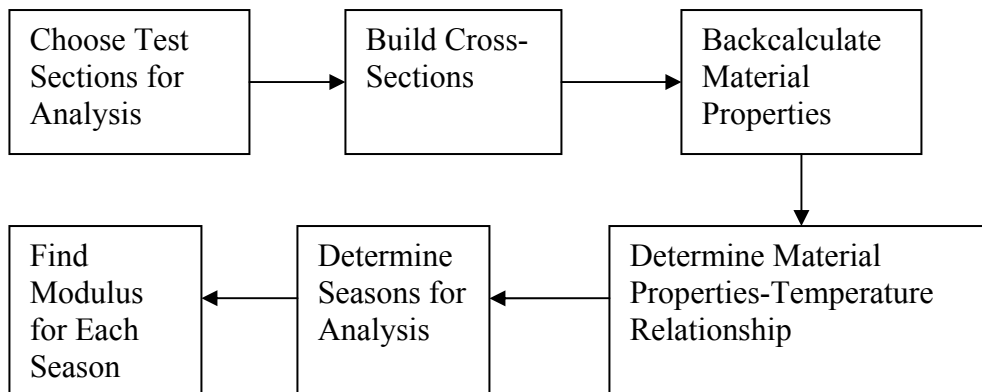
Figure 4-6. Material Properties Flowchart.

Choose Test Sections for Analysis

The first task in determining the seasonal material properties and layer

thicknesses was choosing appropriate sections for use in this analysis. In order for a test

section to be chosen for this analysis, three criteria had to be met. First, the section had to be a part of the FWD testing that was incorporated into the 2000 Test Track testing cycle. Without these data, there was no way to estimate the engineering material properties of the pavement structures. This criterion limited the scope of the analysis to sections in the North and South tangents of the Test Track. FWD testing was unable to be conducted in the East and West curves because of the steep superelevation needed in the 180° turn.

The second criterion important to this study was that no fatigue cracking could have been observed at the end of the experiment. Some pavement sections from the 2000 Test Track were left in-place for up to three cycles of testing while others were removed after one or two trafficking cycles. The criterion did not eliminate any test sections along the north or south tangents from consideration as all proved rugged towards fatigue deterioration.

Third, the sections involved in this analysis had to have been exposed to significant trafficking. As of September 2008, eight sections (W1, W7, W10, S9, S10, S13, E4, E8) had been trafficked for nearly 29 million ESALs. However, the W and E sections were a part of the experiments in the East and West curves. Due to the lack of material property data, five of these test sections could not be used in the analysis process; therefore, three more sections from the North and South tangents (N11, N12, and S2) were chosen as complimentary sections for this study. These three sections were in-place for the 2000 and 2003 experiments with no signs of fatigue cracking; therefore, they had experienced 20 million ESALs. Table 4-1 provides a complete list

of the sections analyzed from the 2000 experiment and how long each section was in-service.

Table 4-1. Sections Analyzed from the 2000 NCAT Test Track.

Section	Service Life
N11	2000-2005
N12	2000-2005
S2	2000-2005
S9	2000-present
S11	2000-present
S13	2000-present

Build Cross-Sections

Each test section at the 2000 Test Track consisted of an experimental surface mix on top of a perpetual buildup. The perpetual buildup, shown in Figure 4-7, was essentially the same for each section around the track with slight variations in constructed thickness. The subgrade for the experiment was an improved roadbed material, also documented as track soil, taken from rock formations in the West curve of the Test Track compacted to 95% of Proctor maximum density. Above the subgrade was another 12 inch lift of the improved roadbed material; however, this lift was compacted to 100% of Proctor for a higher density. A densely crushed granite base layer, often used by ALDOT, was built in a 6 inch lift above the track soil. The final layer separating the unbound materials from the bound materials was a non-woven geotextile fabric. This layer was placed above the granular materials to allow the flow of water through the layer, but not allow fines to pump to the surface or through the pavement layers.

The perpetual buildup of the 2000 Test Track included three layers of bound materials as well as the previously mentioned unbound materials. The bottom layer of the bound materials was 4 inches of permeable asphalt treated base (PATB). While four inches of material was planned as a part of the experiment, the thick spread rate made the build-up closer to 5 inches in most areas of the Track. 15 inches of Superpave mix was placed on top of the PATB layer. The bottom nine inches of the Superpave mix consisted of a mix design using a PG 67 binder. The top six inches used a PG 76 binder to increase the rutting resistance (Brown et al., 2002).

The original goal of the experiment was to compare the rutting potential of the experimental mixes above the perpetual buildup. Table 4-2 lists the experimental thicknesses of the sections used in the 2000 Test Track analysis. The coefficient of variation for the thickness of each section was also calculated from 8 surveyed thicknesses in each section using Equation 4-1.

$$COV = \frac{\sigma}{\bar{x}}$$

Equation 4-1

Where: σ = standard deviation

$\bar{x}$ = mean

6" Superpave Mix with PG 76

9" Superpave Mix with PG 67

4" PATB

6" Granite Base

12" Improved Roadbed

Improved Roadbed
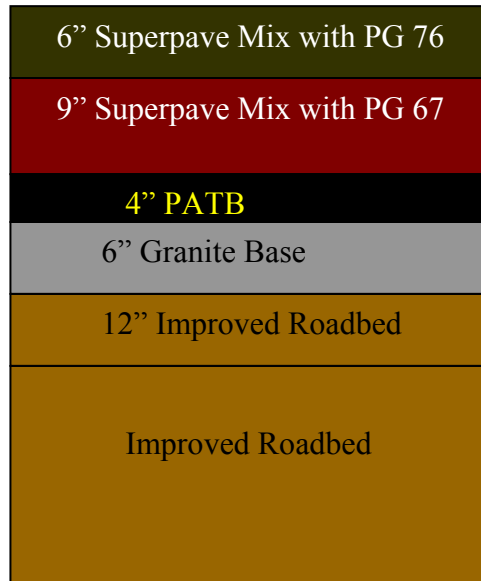
Figure 4-7. Perpetual Buildup at the 2000 Test Track.

Table 4-2. Experimental Mix Thicknesses.

Test Section	Experimental Mix Thickness (in)	Thickness COV (%)
N11	4.1	3.2
N12	3.9	3.0
S2	3.9	1.0
S9	3.0	3.9
S10	3.1	3.4
S13	4.0	3.6

Backcalculate Material Properties

During 2001, falling weight deflectometer (FWD) testing was conducted seven

times between January and September as a tool to backcalculate material properties of

the pavement structures in the North and South tangents. This testing was conducted by

dropping a load ranging between 7 and 10 kips at two different locations in each section.

As the loads were dropped, seven geophones spaced one foot on center measured the

deflection at the surface of the pavement to create a deflection basin (as seen in Figure

4-8). Using the deflection basins produced during this testing and the American Association of State Highway and Transportation Officials'(AASHTO) two-layer backcalculation methodology (AASHTO, 1993), the material properties for each section could be characterized seasonally.
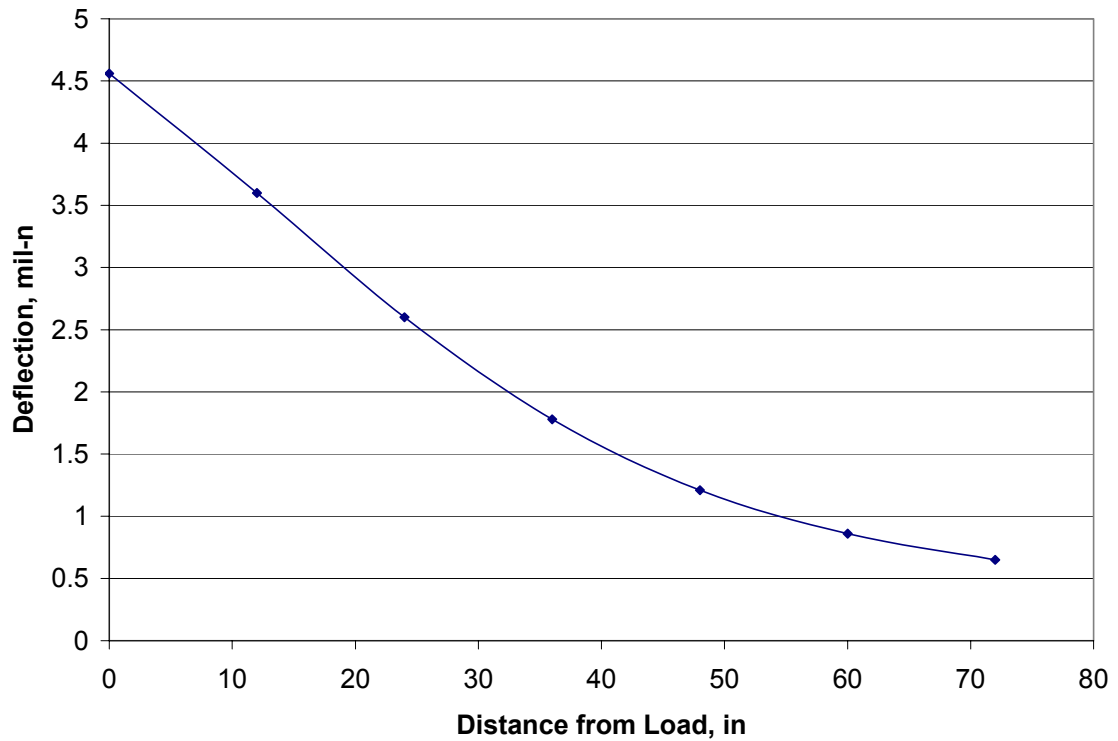
Figure 4-8. Example Deflection Basin.

The AASHTO 2-layer backcalculation methodology is found in Section L5.3 of the 1993 AASHTO Guide for Pavement Design. The methodology simplifies a complex pavement structure, such as the one shown in Figure 4-7, into two pavement layers: subgrade an everything else above this material (base material and HMA). This being done, both the resilient modulus of the soil and the elastic modulus of the pavement can be estimated. The equations developed come from the assumption that Boussinesq theory holds true and the material is homogeneous and isotropic.

67

In this analysis, the division between the two layers occurs at the geotextile or beneath the PATB. Since the subgrade is a stiff material, it was put into one layer with the 12 inches of improved roadbed and 6 inches of granite base. The HMA layer included all the bound materials. The resilient modulus of the subgrade was calculated by using the deflection at the furthest geophone, d_6, according to:

$$M_r = \frac{0.24P}{d_r r} \qquad \text{Equation 4-2}$$

Where: M_r = resilient modulus of soil, psi

P = load, lbs

d_r = deflection at radius r, in

r = distance from load, in

The elastic modulus of the pavement (E_p) was estimated using the deflection directly under the loading plate, d_0, and the computed subgrade modulus from above. This was computed using a numerical bisection technique applied to equation 4-3.

$$d_0 = 1.5p \left[\frac{1}{M_r \sqrt{1 + \left(\frac{D}{a} \sqrt[3]{\frac{M_r}{E_p}} \right)^2}} + \frac{\left(1 - \frac{1}{\sqrt{1 + \left(\frac{D}{a} \right)^2}} \right)}{E_p} \right] \qquad \text{Equation 4-3}$$

Where: d_0 = deflection measured at the center of the load plate, in

q = non-destructive testing (NDT) load plate pressure, psi

a = NDT load plate radius, in

68

M_r = subgrade resilient modulus, psi

D = total thickness of pavement layers above the subgrade, in

E_p = effective modulus of all the pavement layers above the subgrade, psi

Determine Material Properties-Temperature Relationship

During FWD testing, temperatures were recorded 10 inches deep in the pavement. With these recorded data, non-linear regression was used to develop relationships between the backcalculated material properties and temperature at the time of the testing. Figure 4-9 shows one example of the relationship developed between temperature and the modulus of the hot-mix asphalt from section S10 on a semi-log plot.
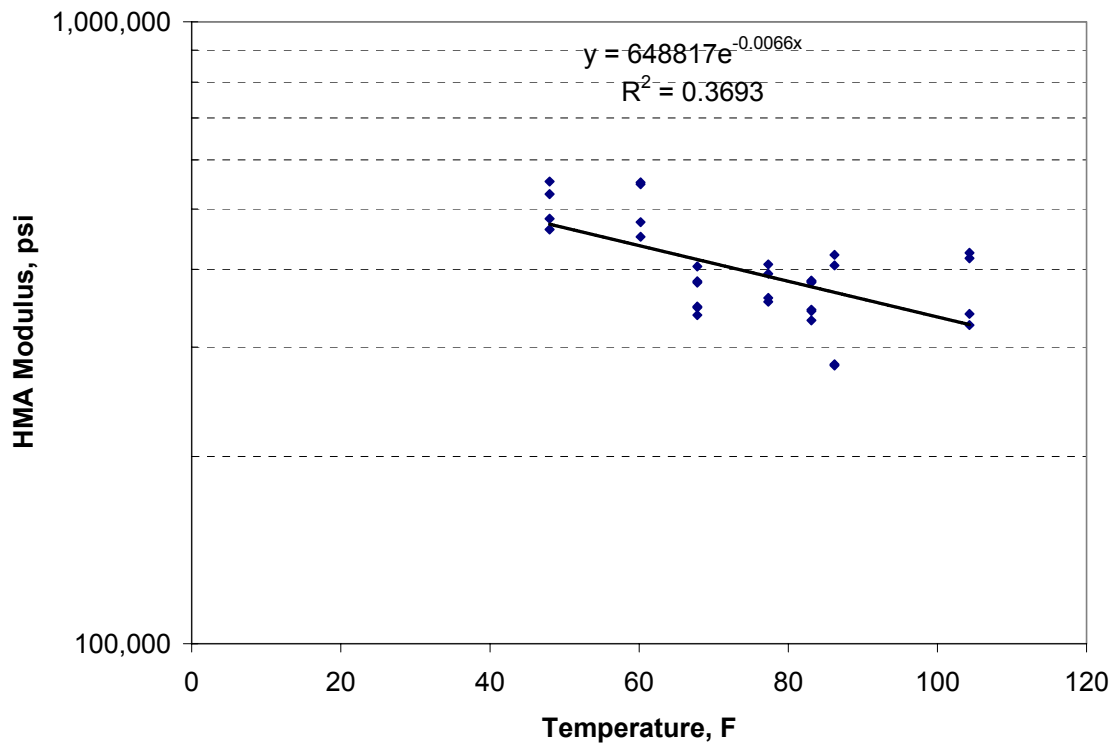
Figure 4-9. HMA and temperature relationship for S10.

When comparing power, linear, and exponential relationships, negative exponential relationships returned consistently higher R^2 values. One would expect a

negative relationship between temperature and HMA modulus because as the temperature in a pavement structure increases, the pavement should become softer and its modulus would be reduced. Therefore, the equations developed for the six experimental sections follow the format of Equation 4-4, and Table 4-3 displays each equation's constants and R^2 value.

$$E_p = k_1 e^{k_2 T}$$
<div align="right">Equation 4-4</div>

Where: E_p = HMA modulus, psi

k_1 = section specific constant

k_2 = section specific constant

T = temperature, F

Table 4-3. Constants for equation 4-4.

Section	k_1	k_2	R^2
N11	816061	-0.0087	0.73
N12	797238	-0.0091	0.47
S2	384073	0.0036	0.09
S9	605842	-0.0093	0.71
S10	648817	-0.0066	0.37
S13	747956	-0.0107	0.75

As Table 4-2 indicates, three of the sections maintained a relatively strong relationship ($R^2 > 0.7$) between temperature and the modulus of the pavement. Two of the sections were weaker with R^2 values ranging from 0.37 to 0.47. Section S2 had no relationship that could be developed between its HMA modulus and the temperature. The lack of relationship prevented a multi-seasonal analysis from being conducted on section S2.

When looking at the mix properties shown in Table 4-4, it was seen that section S2 was built with a stiffer binder than the other test sections in the analysis, and it was

also the only section to incorporate gravel as its aggregate skeleton. This partially could

account for the higher backcalculated stiffnesses. The higher binder grade would be

used to produce a stiffer mix which would help eradicate the rutting potential of the mix.

In fact, the mix was so stiff in the field that no rutting was ever seen in this test section.

Not only did S2 prove to be a stiffer mix in the field under FWD testing, but it

also exhibited similar characteristics in the laboratory. Figure 4-10 provides a

laboratory comparison of the dynamic modulus for the six test sections analyzed. The

values plotted were the average of three dynamic modulus tests completed on sample

mixes from the test sections. As can be seen, the dynamic modulus of the binder mix in

S2 was more than double that of the mixes in the other sections. These data confirm that

the FWD data were not compromised due to faulty testing or temperature

measurements; therefore, S2 was stiffer than the other five sections in this analysis.

Table 4-4. Mix Properties of 2000 Test Track Sections (Brown et al., 2002).

Section	Aggregate Blend Type	Design Method	Design Nominal Maximum Aggregate Size	Binder Grade
N11	Granite	Super	19.0	67-22
	Granite	Super	12.5	76-22
N12	Granite	Super	19.0	67-22
	Granite	SMA	12.5	76-22
S2	Gravel	Super	19.0	76-22
	Gravel	Super	9.5	76-22
S9	Granite	Super	12.5	67-22
S10	Granite	Super	12.5	67-22
S13	Granite	Super	12.5	70-28

*Two entries for one section indicate the use of two mixes. The first mix listed was a
binder mix. The second mix was a surface mix.
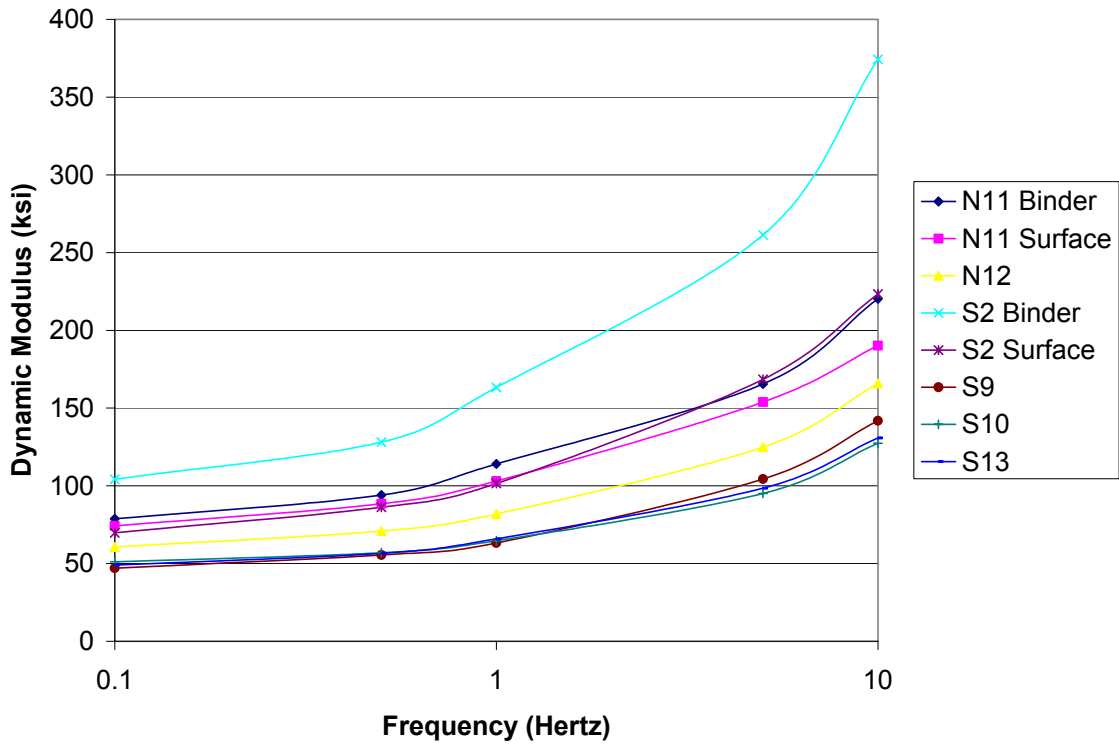
Figure 4-10. Dynamic Modulus Testing for 2000 Test Sections.

Figure 4-11 shows the results of comparing S10's resilient modulus of the soil to the pavement temperature during the FWD testing. As can be seen, there is no real trend upwards or downwards with temperature for the soil's material properties. This was the case for each of the six sections analyzed from the 2000 Test Track. Since no relationship could be developed, the average modulus from the FWD testing was used along with the COV of the backcalculated data.
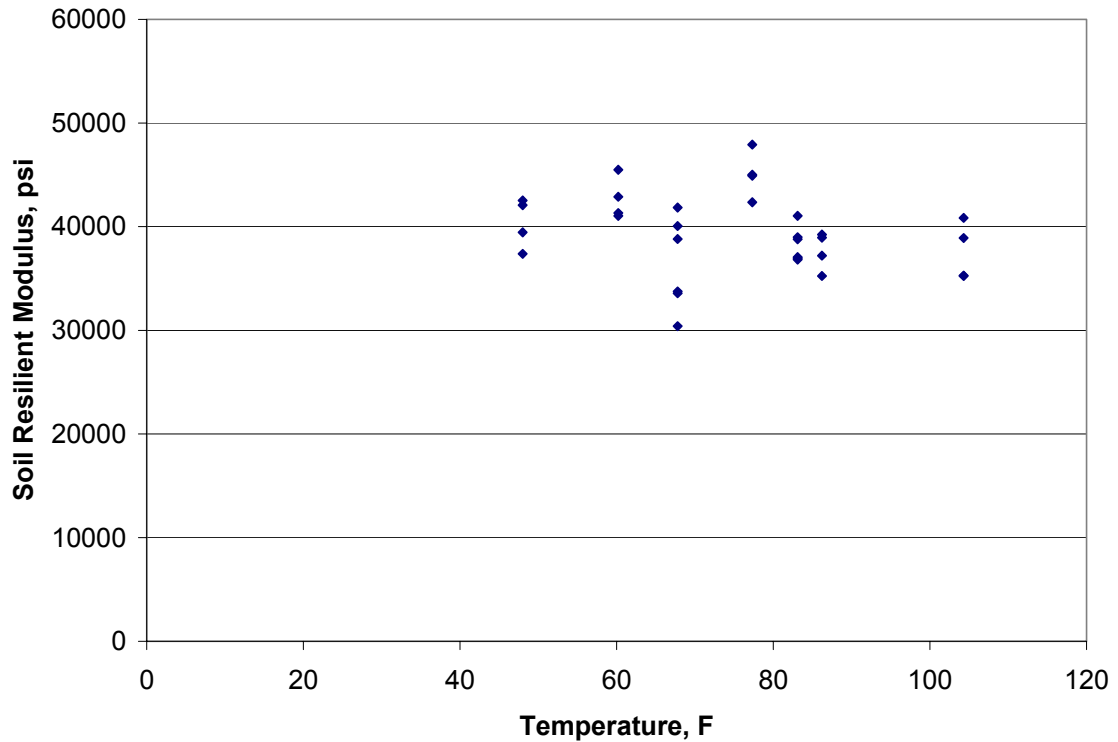
Figure 4-11. Soil resilient modulus and temperature relationship for S10.

Determine Seasons for Analysis

PerRoad requires a specific modulus value and its variability when calculating

mechanistic pavement responses. To quantify a specific modulus value, the temperature

spectrum needed to be analyzed to determine the seasonal temperatures seen 10 inches

deep in the pavement. Beginning with the start of traffic in 2000, temperatures were

collected every minute and compiled into an hourly average temperature before being

stored in a database. While temperatures were compiled every hour, the only

temperatures necessary to complete this analysis were the temperatures measured when

the Track was being trafficked. This was completed by synchronizing the temperatures

to the times trucks were running in the trafficking database from beginning of traffic in 2000 until the end of traffic in 2005.

Once accomplished, the temperature data were transformed into a cumulative distribution plot as seen in Figure 4-12 for section S10. To more precisely quantify the seasonal changes of the HMA modulus, the temperature spectrum for each section was divided into five seasons with the exception of S2 because no temperature relationship was present. A season was defined as one quintile of the temperature data. The average temperature for each season was then specified as the mid-point of each quintile (i.e. the 10th, 30th, 50th, 70th, and 90th percentiles). Table 4-5 shows the seasonal temperature average for each section.
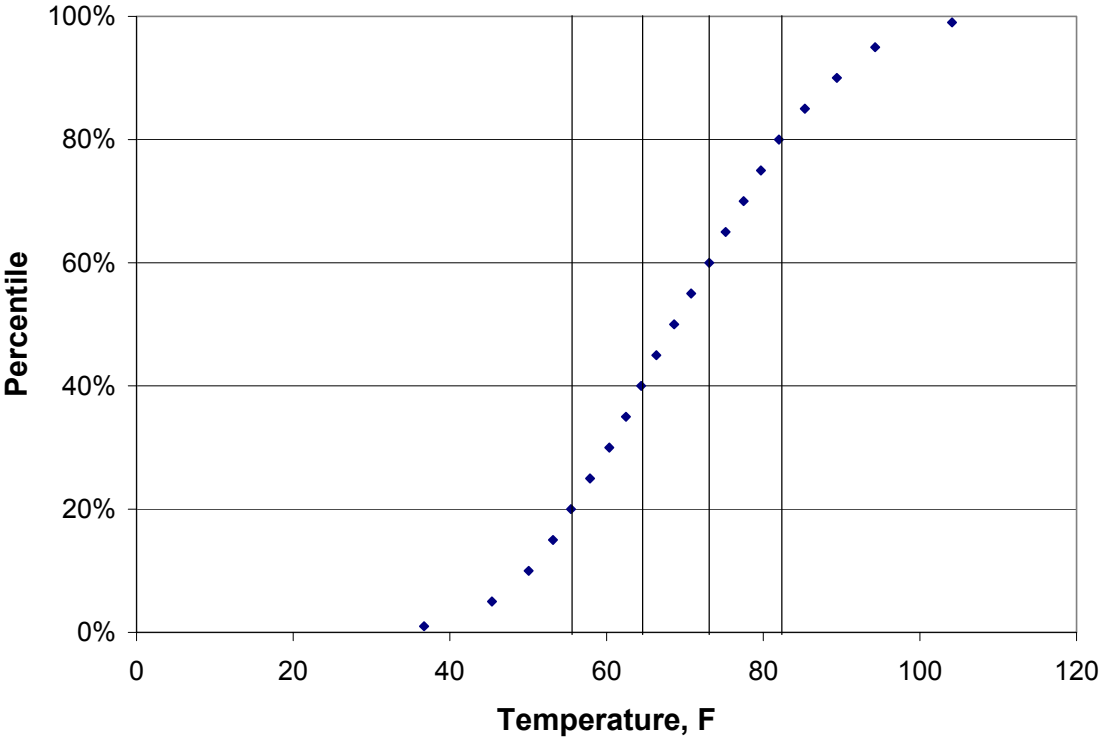
Figure 4-12. Temperature Spectrum for S10.

Table 4-5. Seasonal Average Temperature (°F).

Section	Season 1	Season 2	Season 3	Season 4	Season 5
N11	61	78	87	96	106
N12	49	65	78	89	111
S9	49	61	72	83	102
S10	50	60	69	78	90
S13	49	60	72	82	110

Both the HMA modulus for S2 and the resilient moduli for all of the sections
analyzed at the 2000 Test Track were not found to be temperature dependant. The
methodology for characterizing these values will be explained in the next section.

Find Modulus for Each Season

After the mean temperatures for each section's season were determined, the
moduli for the HMA were calculated using the stiffness-temperature relationships
developed earlier. A relationship between temperature and stiffness could not be
developed for S2; therefore, one HMA stiffness was used to describe the yearly
pavement properties for this section. This stiffness was the average of the
backcalculated material properties. The modulus values for each section are presented
by season in Table 4-6.

Table 4-6. Seasonal HMA stiffnesses (psi).

Section	Season 1	Season 2	Season 3	Season 4	Season 5
N11	325,632	353,382	381,499	415,091	481,960
N12	290,076	354,048	391,323	440,425	510,253
S2	524,178	NA	NA	NA	NA
S9	307,267	326,536	347,369	369,324	398,034
S10	401,203	431,634	459,338	490,588	539,834
S13	214,574	306,422	345,805	390,416	442,719

PerRoad incorporates variability into its analysis by using coefficients of variation; therefore, in order to more accurately characterize the material properties of the pavement, some measure of variability needed to be developed. Only one COV is used to characterize the material property on a non-season specific basis throughout the year. The seasonal analysis with the stiffness-temperature relationship accounts for the variability in the pavement stiffness due to temperature; however, there is no measure of spatial variability within the test section using just the temperature-stiffness relationships.

To account for spatial variability, the data needed to be normalized to one temperature (temperature corrected) to calculate a spatial stiffness COV. This was accomplished by adjusting the temperature-stiffness relationships (Equation 4-4) developed earlier to calculate a stiffness correction factor seen in Equation 4-5.

$$CF = e^{k_2(T_m - 68)} \hspace{4cm} \text{Equation 4-5}$$

Where: CF = stiffness correction factor

k_2 = section specific constant in Equation 4-4

T_m = measured temperature at time of FWD testing, °F

Once the correction factor was calculated, the original stiffness was divided by the correction factor to calculate a temperature corrected stiffness. A visual representation of this concept is seen in Figure 4-13 for section S13. As can be seen, the stiffness values are adjusted back towards a specific stiffness value. The dashed line is the representative of calculating the stiffness value in Equation 4-4 at 68 °F for this section. If the R^2 of the stiffness-temperature relationship were 1.0, all of the corrected

datapoints would line up on the dashed line. The higher the R^2 value of the stiffness-temperature relationship, the closer the corrected points will be to the dashed line.
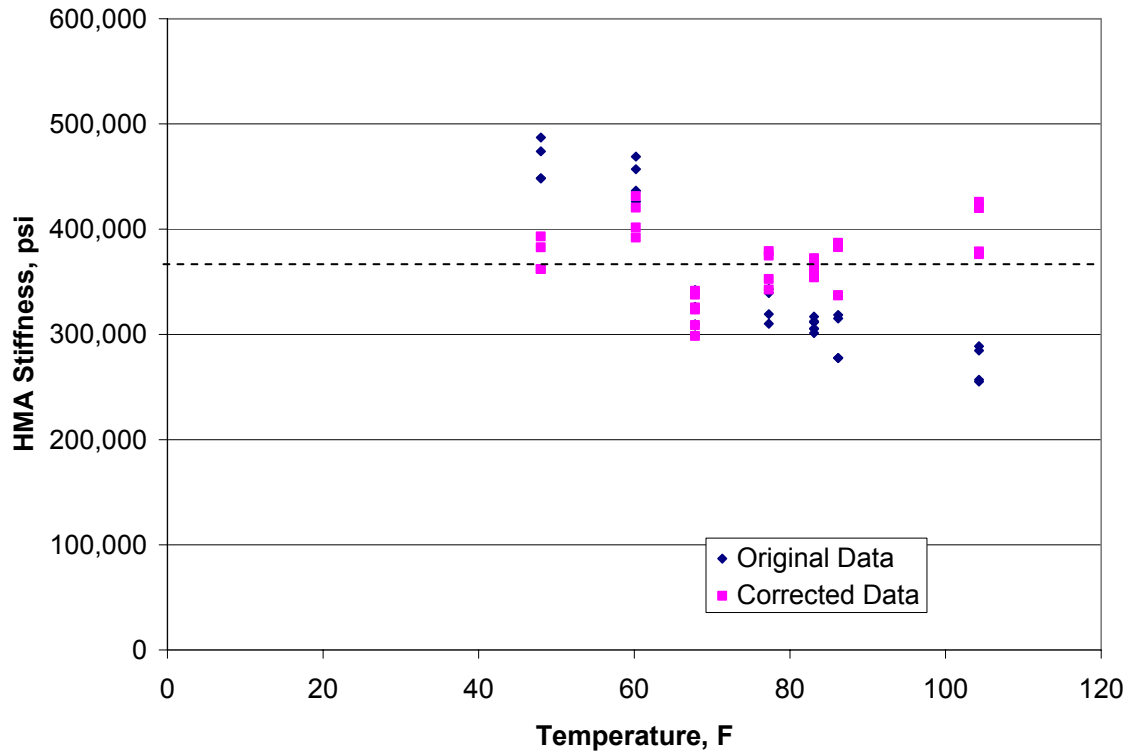
Figure 4-13. Temperature Corrected Stiffnesses.

Once the new temperature corrected stiffnesses were determined, a single spatial coefficient of variation was calculated from the new corrected backcalculation dataset. Table 4-7 shows the COVs for each section based on this methodology. The COV for S2's one season approach was calculated using the HMA backcalculated modulus values.

Table 4-7. HMA Coefficients of Variation.

Section	COV (%)
N11	7.1
N12	15.3
S2	20.3
S9	9.9
S10	14.3
S13	8.9

The resilient modulus values for each section's subgrade were developed similarly to the methodology used to calculate the HMA modulus and COV for section S2. Since a temperature-stiffness relationship could not be developed, an average resilient modulus value and COV were calculated based upon the backcalculated data developed using earlier methodologies described. Table 4-8 shows these datasets. At this point, the material properties of the pavement and soil were adequately characterized for PerRoad to complete its analysis.

Table 4-8. Resilient modulus and COVs by section.

Section	Average M_r (psi)	COV (%)
N11	46,636	5.9
N12	39,417	9.7
S2	31,683	11.7
S9	30,575	10.5
S10	39,417	9.7
S13	34,872	9.1

LOADING CONFIGURATION

Perpetual pavements should be able to withstand trafficking without accumulating fatigue damage. After the twenty years of life, minor surface rehabilitations are to be expected. As discussed earlier, the six test sections chosen for this analysis were done so because they had withstood twenty million or more ESALs without exhibiting signs of fatigue cracking.

These twenty million ESALs were applied during two different Test Track experiments. Each testing cycle consisted of different tracking patterns; therefore, the load spectra for the two testing cycles needed to be individually considered.

78

2000 NCAT Test Track Traffic

The NCAT Pavement Test Track was loaded by approximately 10 million ESALs over a two and a half year period. During the 2000 cycle of testing, four triple trailers (Figure 4-14) with a gross weight of approximately 152 kip loaded the track 16 hours a day, 6 days a week at approximately 45 miles per hour. The exact axle weights for each vehicle can be seen in Table 4-9.

Figure 4-14. Triple trailer used for loading during the 2000 Test Track experiment.

Table 4-9. Loading configurations for the 2000 Track (kips).

	Steer	Tandem	Single				
	Axle 1	Axle 2	Axle 3	Axle 4	Axle 5	Axle 6	Axle 7
Truck 1	11.25	41.20	19.95	20.30	20.15	20.00	20.40
Truck 2	11.45	40.65	19.70	19.90	20.30	20.40	20.00
Truck 3	10.95	39.65	20.40	20.10	21.65	20.35	20.95
Truck 4	11.45	39.50	20.00	20.05	20.30	20.55	19.30

When looking at the loading configurations seen for the four trucks used in the 2000 Test Track, little variation was seen in the axle weights. For the steer axles, all of the weights were between 10 and 12 kips. For the tandem axles, there was only a 1.7

kip difference between Truck 1 and Truck 4. The largest range between single axles was 2.35 kips.

While accurate axle weights for each vehicle were included in the 2000 Test Track traffic database, accurate records needed to determine the percentage of the total ESALs trafficked by each individual truck were not available. For PerRoad to calculate a mechanistic response in the pavement, the program required the user to define what percentage of a particular axle type was in a given 2 kip weight class (i.e. 20-22 kips). Since all the steer axles were in the same weight group, the lack of detailed records did not prove problematic. However, the tandem and single axles had axle weights falling into multiple weight classifications. As explained above, detailed records were not available to precisely determine the correct percentages of the different weight classifications. In order to remain conservative in the analysis, it was assumed that all of the trafficking came from the heaviest weight classification for the tandem and single axles. In other words, all the steer axles weighed between 10-12 kips, the tandem axles weighed 40-42 kips, and the single axles were 20-22 kips.

Once overall weights for each axle type were distributed, the percentage of each axle type had to be considered. Since all four of the trucks had one steer, one tandem, and five single axles, it was assumed that a 1:2:5 ratio could be used to determine axle percentages. Table 4-10 provides the overall load spectrum for the 2000 Test Track.

Table 4-10. 2000 Test Track Load Spectrum

Axle Type	Weight (kips)	Overall Percentage (%)
Steer	10-12	12.5
Tandem	40-42	25.0
Single	20-22	62.5

2003 Test Track Traffic

Complexity arises when assessing the loading configuration of the 2003 Test

Track. While the 2000 Test Track used the same truck configuration throughout the

trafficking cycle, the 2003 Test Track used three different loading configurations: single

box, triple box trailers, and triple flat-bed trailers. Each trailer configuration brought a

new axle configuration and weights to the analysis. For example, a triple box trailer

would still have one steer, one tandem, and five single axles; however, a single box

trailer would contain one steer, two tandems, and no single axles.

While the complexity of additional truck configurations and weights was present,

a detailed account of trucking provided the exact number of laps completed by each

truck type over the course of the 2003 experiment. In this case, 11.43% of the 2003

traffic occurred under single box trailer while the remainder (87.57%) of the trafficking

was completed by triple trailers. Table 4-11 was then developed to quantify the load

spectrum for the 2003 Test Track.

Table 4-11. Load spectrum for the 2003 Test Track experiment.

Axle	Weight (kip)	Percentage (%)
Steer	12-14	15.28
Box Tandem	32-34	3.50
Triple tandem	40-42	13.54
Single	20-22	67.68

Cumulative Traffic

The combination of the two datasets provided a cumulative load spectrum for the

full trafficking of these six test sections from 2000-2005. Since each testing cycle

consisted of 10 million ESALs, it was assumed equal loading applications from each test

cycle occurred; therefore, an average percentile would result in a cumulative load

spectrum for the Test Track cycles. Table 4-12 provides the needed information for

PerRoad analysis.

Table 4-12. Cumulative Load Spectrum for 2000 and 2003 Test Tracks.

Axle	Weight (kip)	Percentage (%)
Steer	10-12	6.25
Steer	12-14	7.64
Tandem	32-34	1.75
Tandem	40-42	19.27
Single	20-22	65.10

MECHANISTIC RESPONSE

With both the material properties of the pavement and soil characterized, the

load spectrum accurately quantified, and cross-sections for each test section constructed,

the needed dataset required for PerRoad to complete its mechanistic pavement analysis

was complete (Figure 4-15). The program used the data created and coupled it with

layered elastic theory to calculate horizontal strain at the base of the bound materials, the

critical location for fatigue cracking.
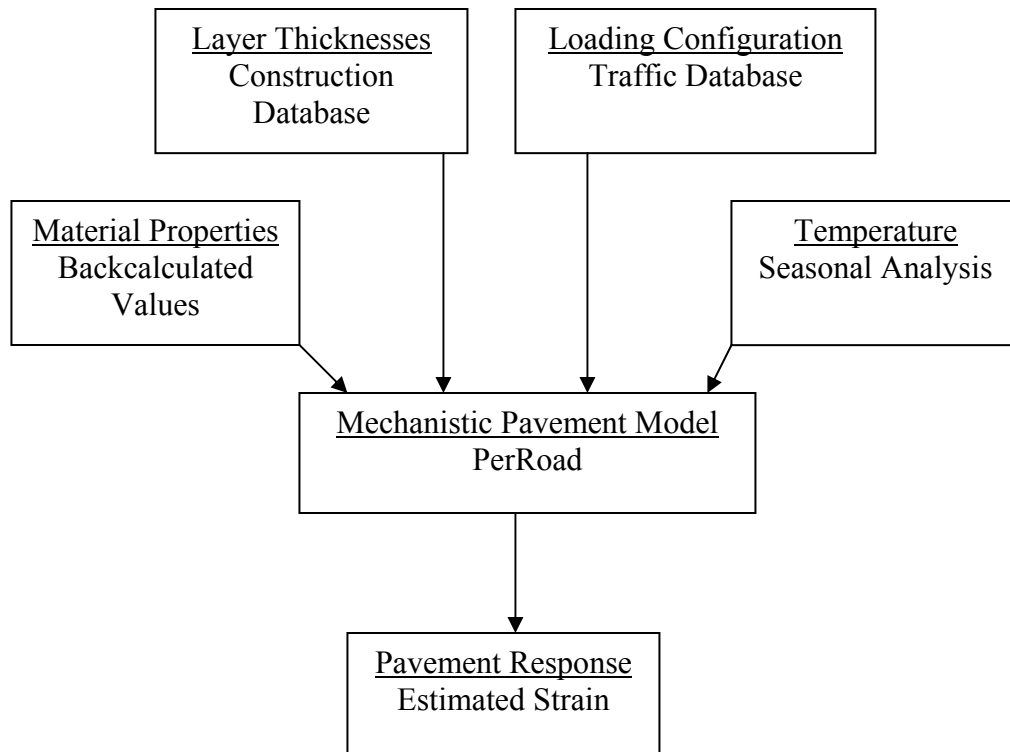
Figure 4-15. PerRoad Flowchart.

Once these strains had been estimated, cumulative distributions of the 5000 estimated strains were developed. Figure 4-16 presents the cumulative distributions for all the sections analyzed in the 2000 Test Track. This plot represents the percentiles of strains experienced at the base of the HMA layer in this section over six years of trafficking between 2000 and 2005.
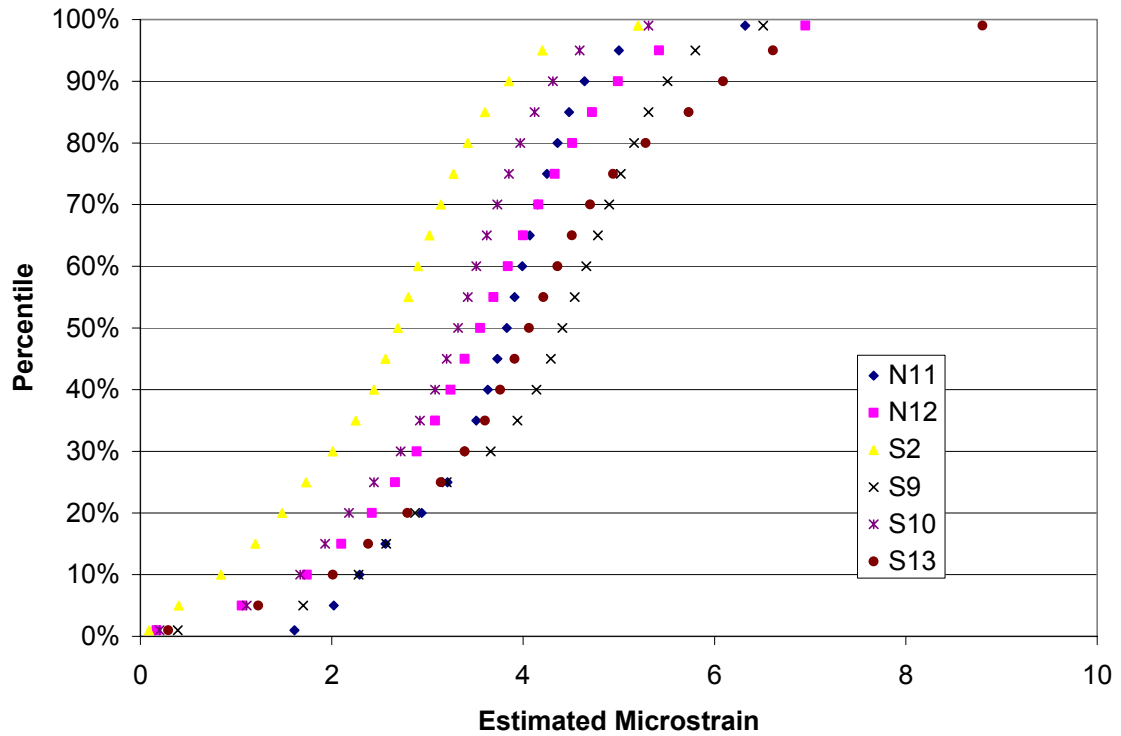
Figure 4-16. Cumulative distributions of strain for 2000 Test Track.

RESULTS AND CONCLUSIONS

When looking at the data in Figure 4-15, it is clear that the prediction of low

strains due to the pavement's thickness and stiffness held true. It is also clear why

fatigue cracking had not occurred during the life of these pavements with some of them

lasting through almost 29 million ESALs. At the 99th percentile, all six sections have

strains below 9 με. The maximum 50th percentile among the six sections is even below

4.5 με. The 99th percentile value is 8 times smaller than the laboratory estimated fatigue

threshold of 70 με. The 50th percentile value is 15.5 times lower than the estimated

laboratory fatigue threshold. Because these strains are so much lower than this

estimated fatigue threshold, it is possible to see that pavements can be placed thinner

than 23 inches with the possibility of having adequate fatigue protection as long as proper construction practices and mix design are considered.

When comparing the individual strain profiles of the sections, Section S2 produced the strain profile with the lowest values. This was due to the stiffness of the mix. When the backcalculated HMA modulus was analyzed, its average HMA modulus was almost 75,000 psi greater than the next highest 50th percentile HMA modulus among the six sections. This value was almost 125,000 psi greater than the third highest 50th percentile HMA modulus. On the two hottest days of testing on this section, two tests returned HMA stiffness values greater than 730,000 psi. This would account for the high average modulus stiffness for the year and the small strains simulated in PerRoad.

SUMMARY

The combination of stiff and thick pavements led to the occurrence of small strains at the bottom of the HMA layer for the 2000 Test Track test sections. The 99th percentile strains were below 10 µε for all six of the analyzed test sections. The calculated strains validate the theory that these sections were overdesigned against fatigue cracking.

For states to build more practical, thinner pavements, pavement structures should experience higher strains than those calculated for the 2000 Test Track sections. To validate this shift to larger strains, pavements were analyzed from other Test Track experiments using thinner pavements and measured strains.

CHAPTER FIVE

DEVELOPING STRAIN DISTRIBUTIONS FOR THE 2003 TEST TRACK

THE 2003 NCAT TEST TRACK EXPERIMENT

The 2003 NCAT Test Track experiment began trafficking on October 21, 2003 and ran through December 17, 2005. Many of the original test sections constructed for the 2000 experiment were removed as new state DOTs were brought into the project and its scope was broadened. One of the most sizable additions to the new experiment was the introduction of eight so-called "structural sections" in the North tangent.

These eight sections (Figure 5-1) were designed to study mechanistic responses in pavements and relate them to the new M-E design scenarios. The structural sections varied in both thickness and binder grade according to the sponsor group's objectives. Mix design information is seen below in Figure 5-2 and Table 5-1.
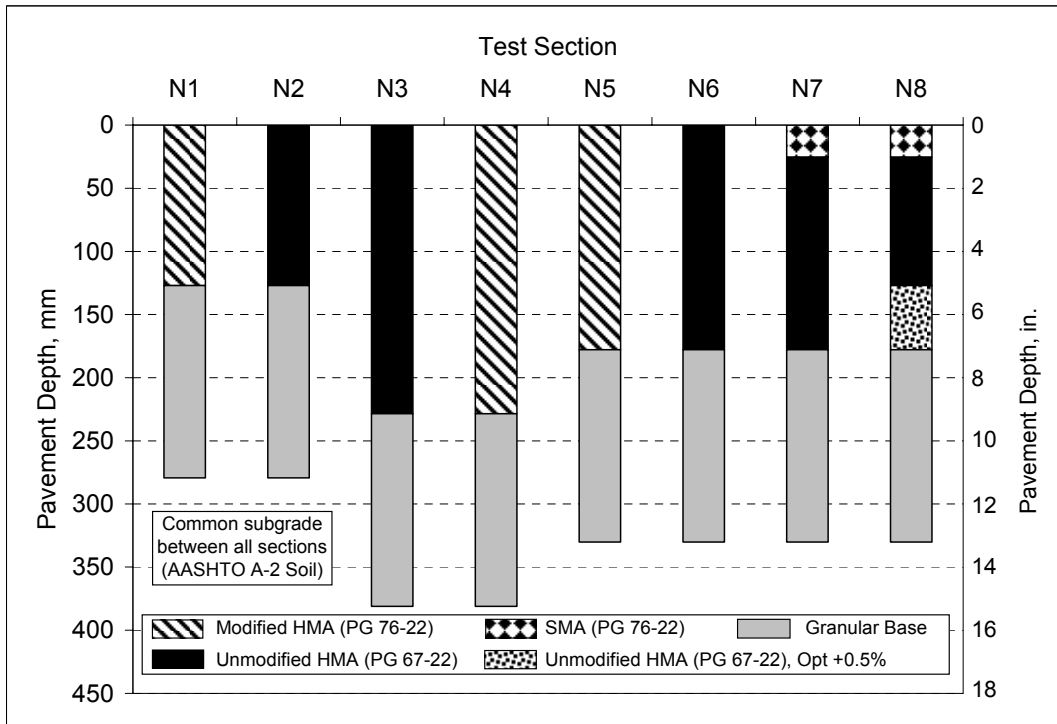
Figure 5-1. Structural Sections at the 2003 NCAT Test Track.
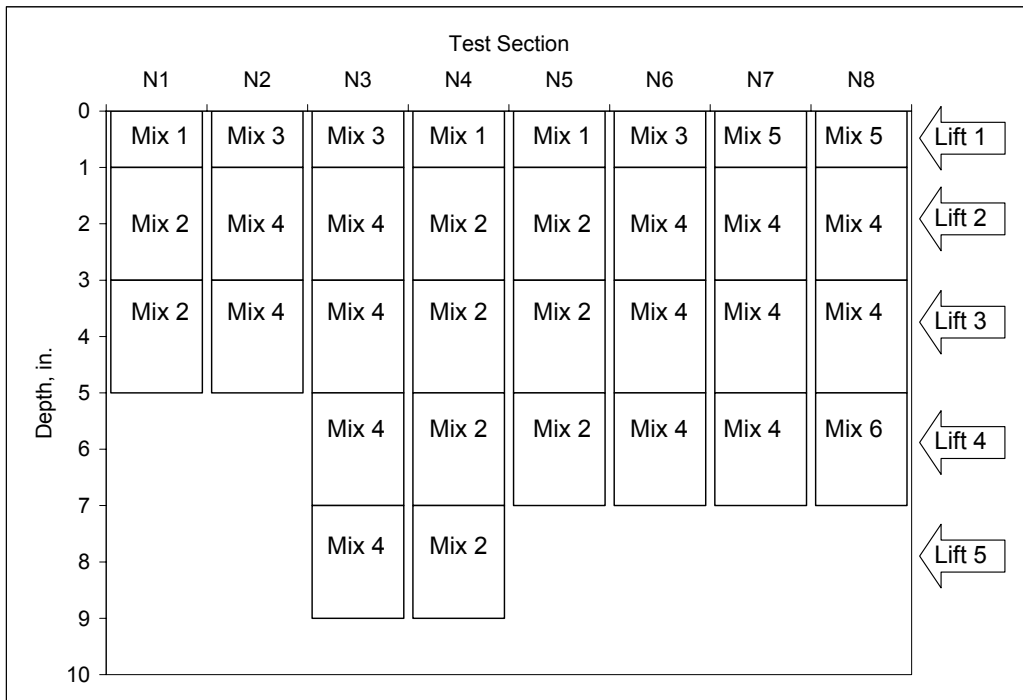
Figure 5-2. HMA Sublayer Mixture Numbering (Timm and Priest, 2006).

Table 5-1. HMA Mix Design Parameters (Timm and Priest, 2006).

Asphalt Mixture	1	2	3	4	5	6
Asphalt PG Grade	76-22	76-22	67-22	67-22	76-22	67-22
Gradation	Wearing	Base	Wearing	Base	SMA	Base
Liquid Antistrip Agent, %	0.5	None	0.5	None	None	None
Design Methodology	Super	Super	Super	Super	Marshall	Super
Compaction Device	Gyratory	Gyratory	Gyratory	Gyratory	Hammer	Gyratory
Compactive Effort, Number of Gyrations	80	80	80	80	50	80
Mixing Temperature, F	345	345	325	325	345	325
Effective Asphalt Content, %	6.13	4.27	6.13	4.27	6.05	4.77
Dust to Asphalt Ratio	0.88	1.10	0.88	1.10	1.50	0.99
Maximum Specific Gravity of Mix	2.474	2.571	2.474	2.571	2.447	2.536
Effective Specific Gravity of Aggregate Blend	2.729	2.766	2.729	2.766	2.687	2.747
Bulk Unit Weight of Compacted Pills, pcf	147.8	153.6	147.8	153.6	145.9	155.5
Tensile Strength Ratio	0.83	0.83	0.83	0.83	0.87	Unknown
Computed Air Voids in Total Mix, %	4.3	4.3	4.3	4.3	4.1	2.5
Voids in Mineral Aggregate, %	17.9	14.5	17.9	14.5	17.9	13.5

While the 2000 Test Track consisted of extremely thick sections, the eight

sections from the 2003 Test Track were considerably thinner, ranging from 5 to 9

inches. The binders used were PG 67-22 and PG 76-22. As thicknesses and binder

grades varied, so did pavement performance. Some sections, such as N1 and N2, quickly

deteriorated due to fatigue cracking while other sections (N3 and N4) withstood the 10

million ESALs of the 2003 experiment without signs of fatigue cracking. These

sections were left in-place for the 2006 Test Track.

Another parameter that set the 2003 Test Track apart from the previous

experiment was its use of embedded pavement instrumentation. These devices collected

dynamic pavement responses under trafficking instead of having to theoretically

estimate the stresses and strains using programs such as PerRoad.

While each structural section consisted of pressure plates, temperature probes,

and asphalt strain gauges, the asphalt strain gauges were the focus of this investigation.

The CTL ASG-152 (Figure 5-3) is a 350 ohm full-bridge 6/6 nylon based "H" gauge.

These gauges have been known to have misaligned wings which might prevent the

gauge from lying flush with the HMA layer; however, most organizations and facilities having used these gauges found they perform well in accelerated pavement testing (APT) experiments if they are installed correctly (Hornyak et al., 2007; Willis, 2008). These devices have also been shown to be precise when measuring strain at the base of bound materials under live traffic (Willis and Timm, 2008).

Figure 5-3. CTL Strain Gauge.

The locations of the strain gauges in each section were surveyed to be centered along the outside wheelpath of the pavement structure. Once the gauge array was centered, a row of three longitudinal gauges was placed with the middle gauge aligned with the center of the wheelpath and the other gauges set two feet to the left and right of the center gauge. Two rows of transverse gauges and a second row of longitudinal gauges were then placed using the same methodology. Each row was placed two feet

downstream of the previous row. A general schematic of the gauge array is shown in Figure 5-4. All the strain gauges used in this analysis were placed at the base of the HMA layer.
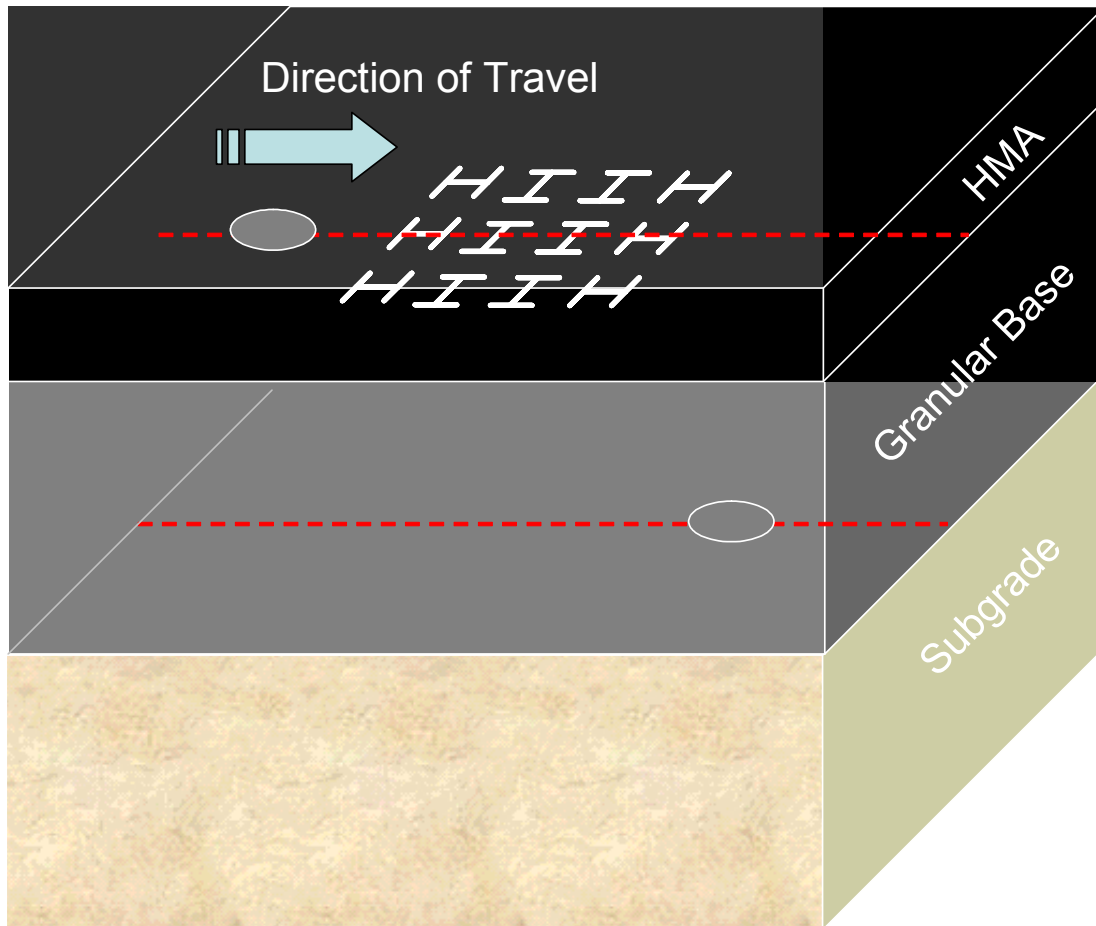
Figure 5-4. 3D Generic Gauge Arrangement (Timm et al., 2004).

Temperature probes were also installed in each test section to measure the continuous temperature gradient of the pavement structures. Probes were built in bundles of four and placed into holes drilled vertically into the shoulder of the pavement. The tips of the four probes were placed at the following depths from the surface: 0 inches, 2 inches, 4 inches, and 10 inches. These temperatures were necessary for estimating continual strain through the research cycles.

GENERAL METHODOLOGY

The methodology for M-E design was again followed as the backbone for the 2003 strain analysis. Unlike the previously mentioned 2000 Test Track methodology, the methodology for the 2003 Test Track (Figure 5-5) did not need to include all the components of basic M-E design due to the collected dynamic strain measurements. For this reason, three components of M-E analysis were eliminated from the methodology: seasonal material property characterization, layer thickness determination, and the use of a mechanistic pavement model.

Seasonal Material Properties Not Needed Due to Measured Response		**Layer Thickness** Not Needed Due to Measured Response

Loading Configuration
Traffic Database

Mechanistic Pavement Model
Not Needed Due to Measured Response

Pavement Response
Measured Strains

Pavement Performance
Variety of Distresses
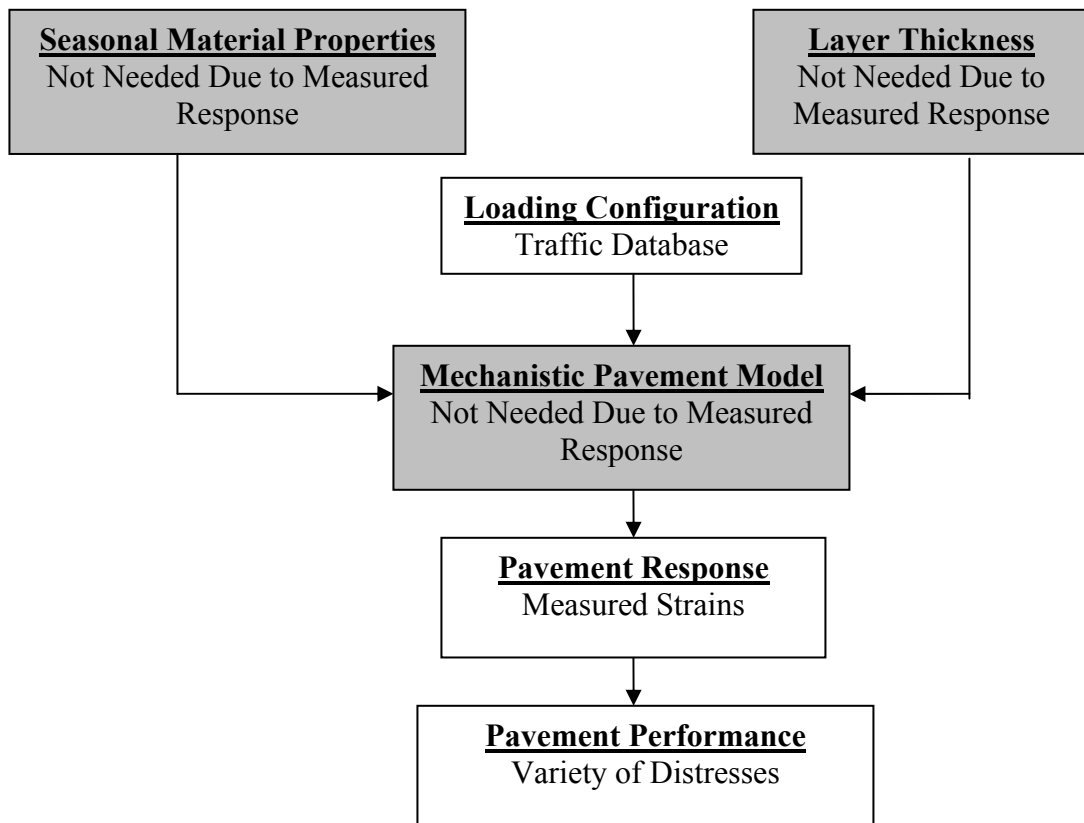
Figure 5-5. 2003 Test Track Analysis Methodology.

The two components of the analysis requiring manipulation and study were the loading configuration and the pavement responses. Detailed trucking databases allowed

precise loading configurations to be analyzed, and weekly measured pavement responses were used to develop continuous strain distributions for the structural sections. These two design components were then linked to the observed pavement performance of the section to make correlations between pavement response and performance.

Seven of the eight structural sections were analyzed using this analysis methodology. Section N8 was originally designed to withstand a loading cycle of 7 million ESALs with a rich bottom layer. The purpose of this experiment was to determine if the rich bottom would help improve the performance of the section in the accelerated load testing conditions. However, N8 was soon found to perform poorly relative to the other 7 in. sections at the Test Track (Willis and Timm, 2007).

A forensic investigation was launched to determine the cause of this pavement deterioration upon the close of trafficking in 2005. Willis and Timm (2007) studied the dynamic strain measurements recorded in the section, a series of trenches cut into the section, and core bond strengths as a way to determining the eventual cause of the pavement failure. Upon the close of the investigation, debonding was determined to cause the premature fatigue cracking in the section (Willis and Timm, 2007).

When debonding occurs in a pavement, the strain profile of the structure changes. Instead of a pavement acting as one monolithic pavement structure, the debonded layers cannot transfer the load to each other, thus causing the upper lifts of the pavement to exhibit higher strain levels. Figure 5-6 shows simulated strains and how debonding changes the strain profile in a pavement with the pavement material properties of N8. Since debonding occurred during trafficking, the strain profile of the structure changed before cracking was visualized at the surface of the pavement. Due to

these changes, it was felt this section would not be appropriate for study; therefore, it was not included in the 2003 strain analysis.
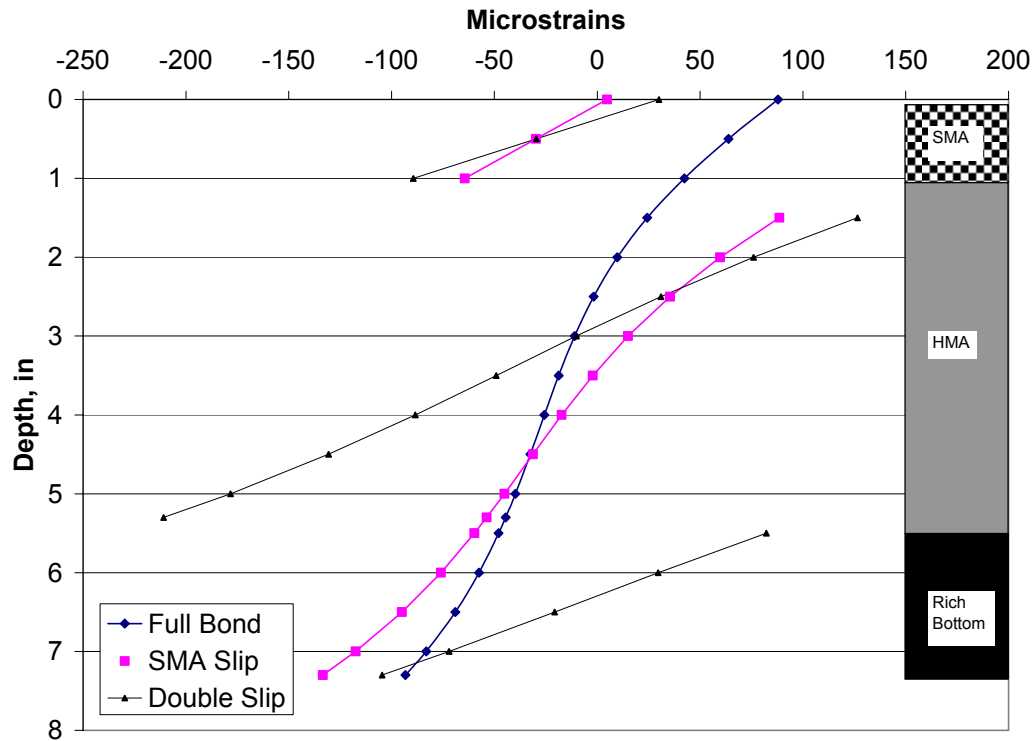
Figure 5-6. Theoretical Strain Profile of 7.3 inch Pavement (Willis and Timm, 2007).

LOADING CONFIGURATION

Trafficking for the 2003 Test Track was conducted similarly to that of the 2000 experiment. A fleet of triple trailer trucks (Figure 5-7) was used to load the pavement with approximately 10 million ESALS in just over two years. Trafficking began in October 2003 and ran through mid-December 2005. When trafficking was initiated, only one truck was used for the first month to initiate some seating and aging of the HMA. Figure 5-8 shows the weight distributions of an example triple truck (Timm et al., 2006).

93

A second vehicle was also incorporated into the trafficking cycle on January 12, 2004. This truck was the combination of a tractor and one box trailer shown in Figure 5-9. The steer axle of this vehicle weighed the same amount as its triple trailer counterpart; however, the tandem axles only weighed between 32 and 34 kips. The exact weights of all the trucks used in the 2003 Test Track are given in Table 5-2.

Figure 5-7. Triple Trailers Used to Traffic the 2003 Track (Timm et al., 2006).
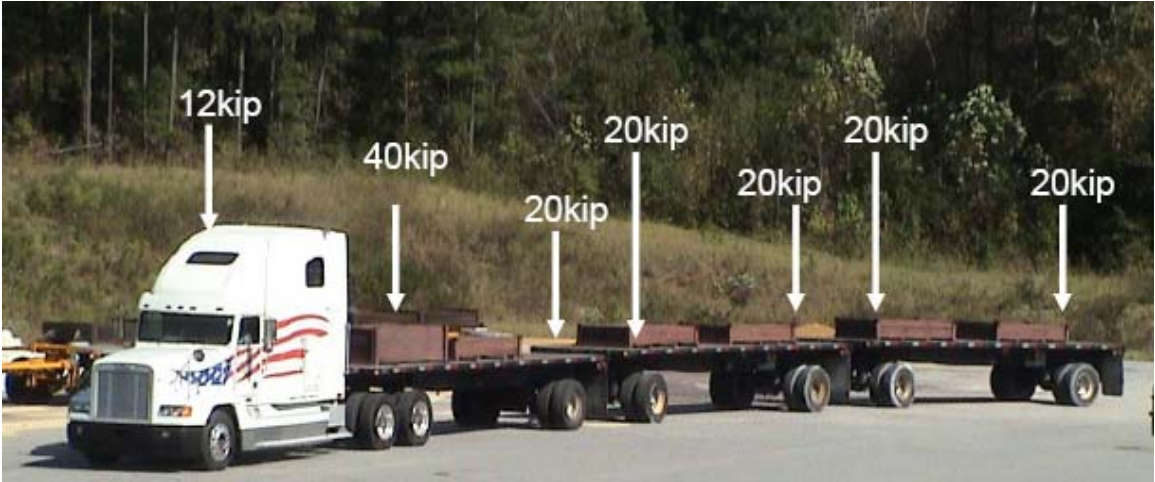
Figure 5-8. Truck Configuration (Priest and Timm, 2006).

Figure 5-9. Box Trailer Used to Traffic the 2003 Track (Priest and Timm, 2006).

Table 5-2. Truck Weights for 2003 Test Track.

	Steer, lb	Tandem, lb		Single, lb				
Truck ID	1	1	2	1	2	3	4	5
1	10,150	19,200	18,550	21,650	20,300	21,850	20,100	19,966
2	11,000	20,950	20,400	20,950	21,200	21,000	20,900	20,900
3	10,550	20,550	21,050	21,000	21,150	21,150	21,350	20,850
4	10,500	21,050	20,700	21,100	21,050	21,050	20,900	21,050
6	11,200	19,850	20,750	20,350	20,100	21,500	19,500	20,300
Average	10,680	20,320	20,290	20,760	20,760	21,310	20,550	20,613
COV	3.9	3.9	4.9	2.2	2.5	1.7	3.6	2.2
	Steer, lb	Drive Tandem, lb		Rear Tandem, lb				
Box	11,550	16,850	17,000	16,800	16,100			

A detailed trucking database was developed to keep track of which truck configuration was being used to traffic the pavement. Table 5-3 provides an example of the trafficking database. Each truck configuration was given a number which correlated to a specific number of axles at precise weights so precise axle counts could be determined per hour during trafficking.

Table 5-3. Example Entry in Trafficking Database.

Date	Hour	Truck	Configuration	Laps
11-12-03	13	2	Triple	13.56

PAVEMENT RESPONSE

Each of the structural test sections was instrumented with strain gauges as shown in Figure 5-10 and temperature probes at depths of 0, 2, 4, and 10 inches. Simultaneous

strain and temperature readings were necessary to determine each section's strain-temperature relationship.

Data Collection

Dynamic strain data were collected monthly from the beginning of trafficking until fatigue cracking was first noticed in April 2004. At this point, data were collected on a weekly basis (Timm et al., 2006).

When data were collected, three passes of each truck were recorded for each section of the structural section using a portable DATAQ dynamic data acquisition system (Figure 5-11). This portable system was connected to a roadside junction box containing the interfaces for both slow and high speed data collection systems. Dynamic responses such as strain and pressure were collected over a high speed system at a frequency of 2,000 Hertz. Temperatures were recorded on a minute-by-minute basis and aggregated into an hourly average for each test section. When the portable data acquisition system was connected to the system interfaces, live data could be streamed to a laptop and recorded for analysis (Timm and Priest, 2006).
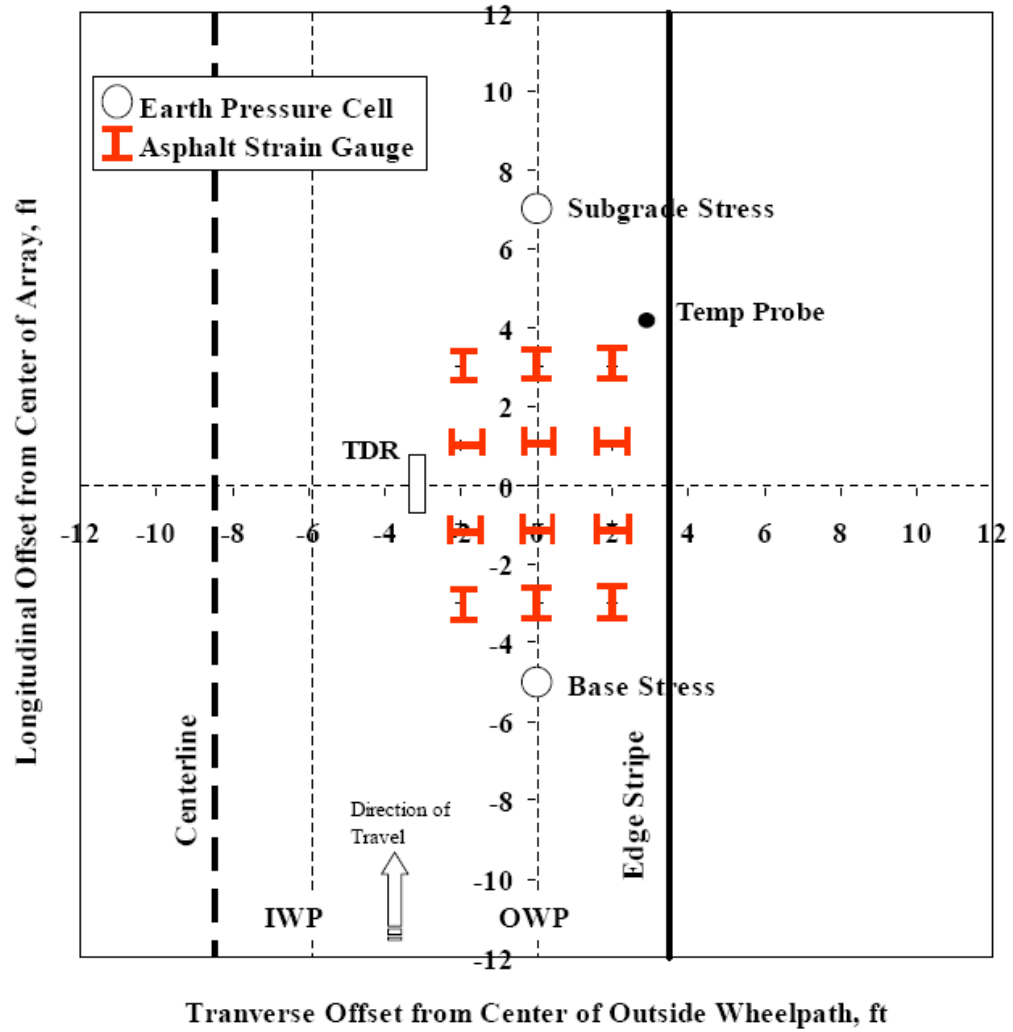
Figure 5-10. Instrumentation Array for the 2003 Test Track.
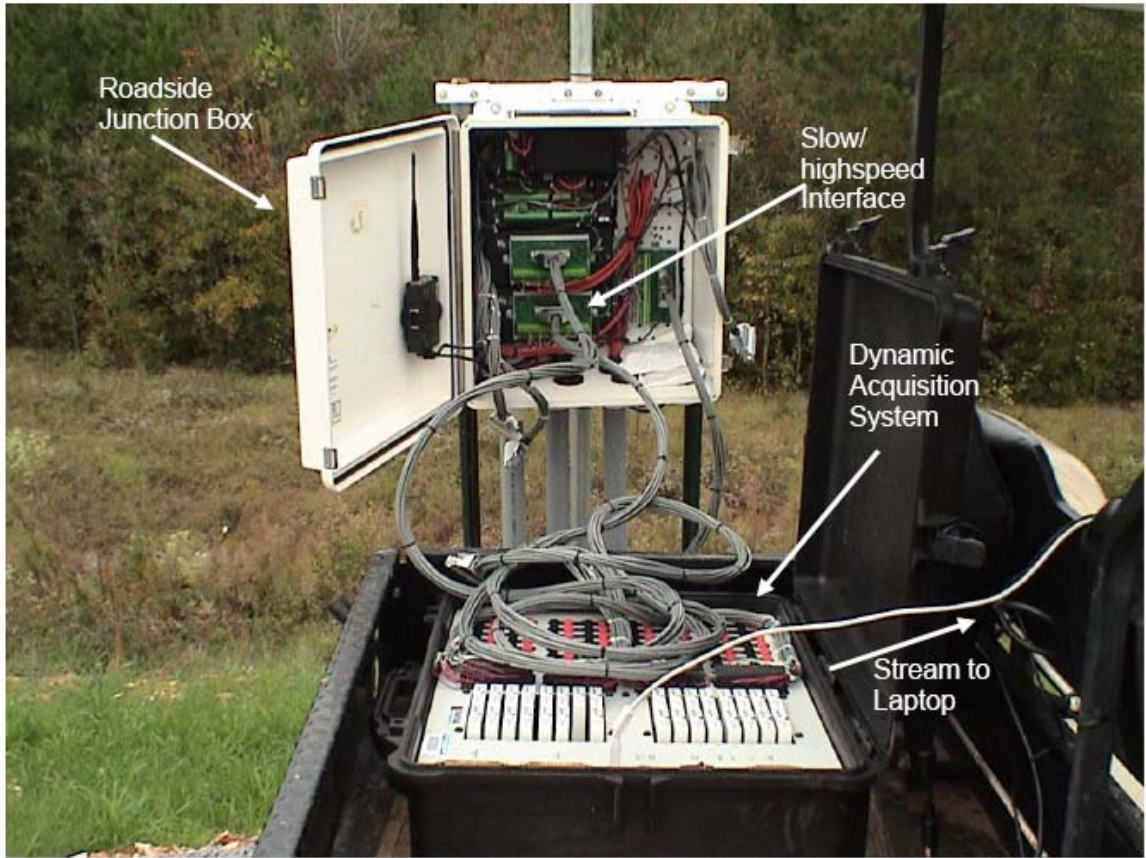
Figure 5-11. Roadside Collection System (Priest, 2005).

Data Processing

Once the data were recorded, they were analyzed in a graphical engineering software package called DADISP. This program would clean and process the trace using algorithms developed at the Test Track. This process is documented by Priest and Timm (2006). A typical strain response in DADISP is shown in Figure 5-12. Figure 5-13 portrays the strain trace's relationship with the passing of a triple-trailer truck.
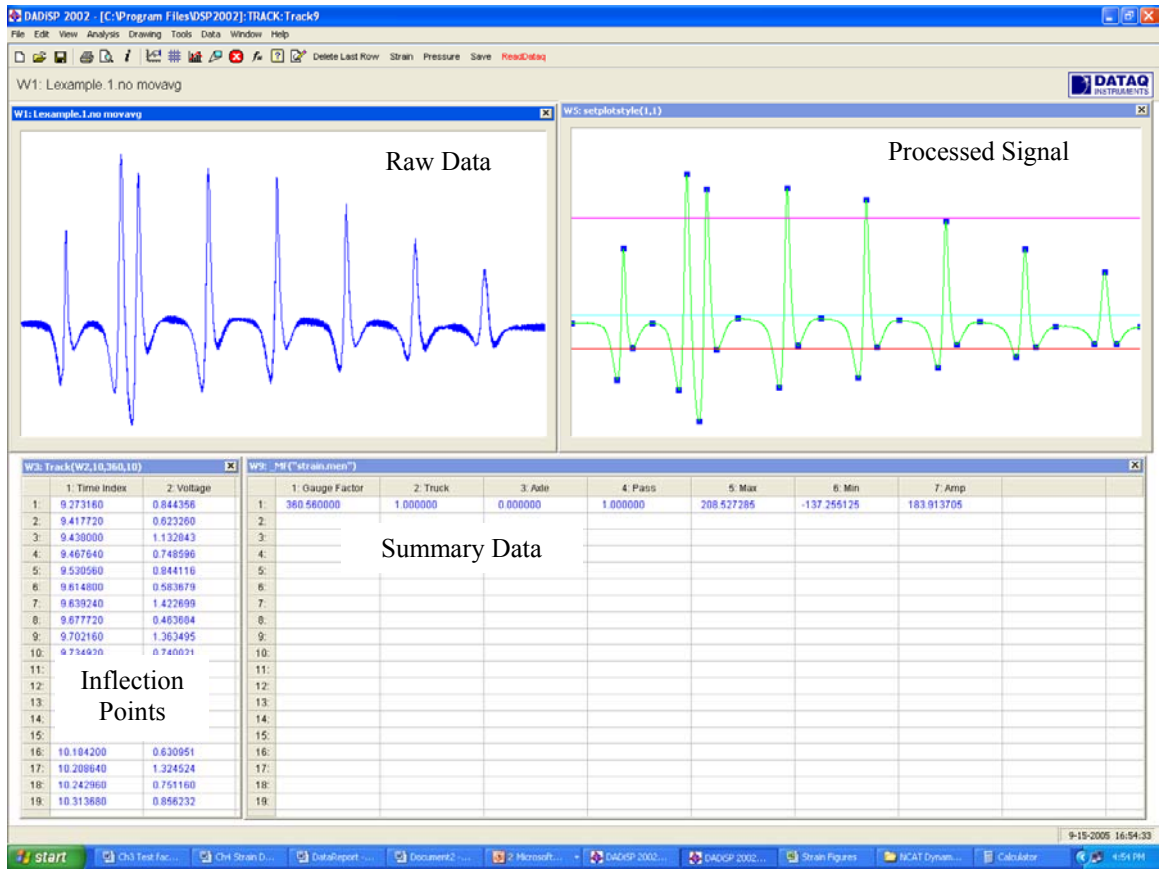
Figure 5-12. DADISP Processing Window (Priest and Timm, 2006).
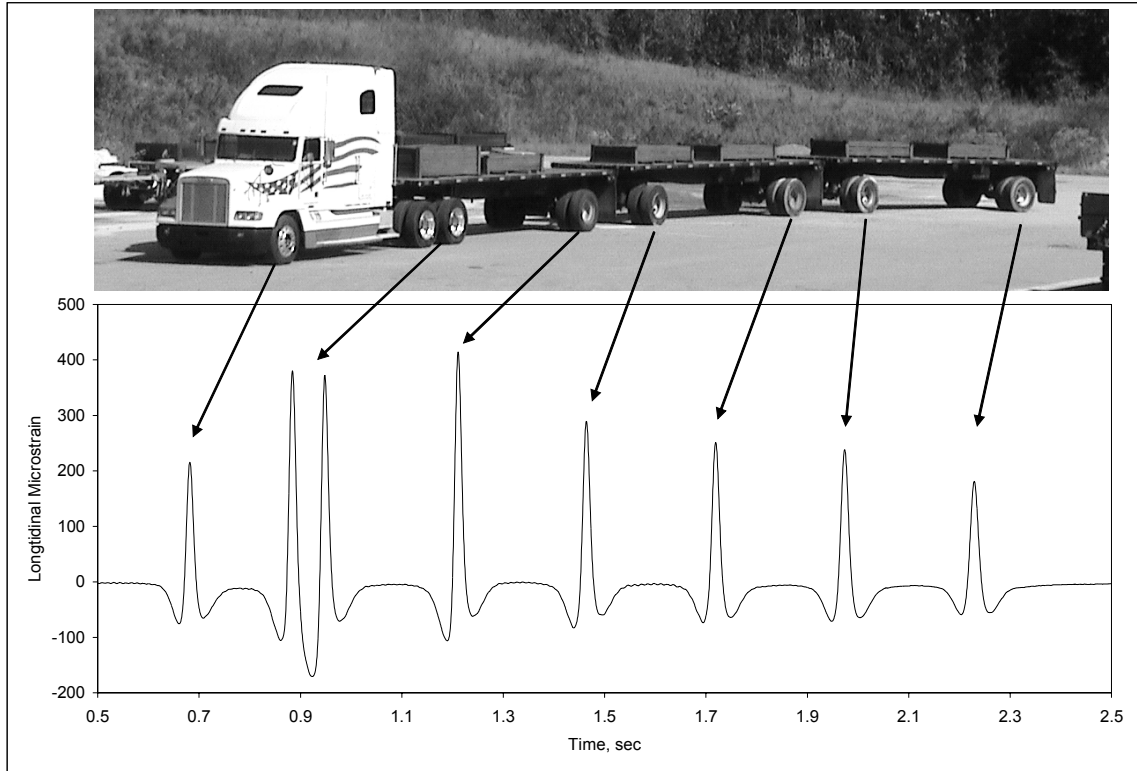
Figure 5-13. Typical Strain Response.

As can be seen, the triple trailer predominantly used at the track consisted of one steer axle, one tandem axle, and five single axles. This axle configuration resulted in eight distinct pavement loadings; however, using the analysis methodology prescribed during the 2003 Test Track, one strain value was calculated using the amplitude of the entire truck pass.

Amplitude (Figure 5-14) was determined by calculating the average of the inflection points (peaks and valleys) during one truck pass. This value was typically at or near the baseline value for the truck pass. The maximum portion of the amplitude was calculated by averaging all the inflection points above the average line. The minimum portion was determined using the same methods for the inflection points below the blue line. The amplitude of each truck pass was defined as the difference

100

between these maximum and minimum averages (Priest and Timm, 2005) and

represented the average strain response over the entire vehicle pass.
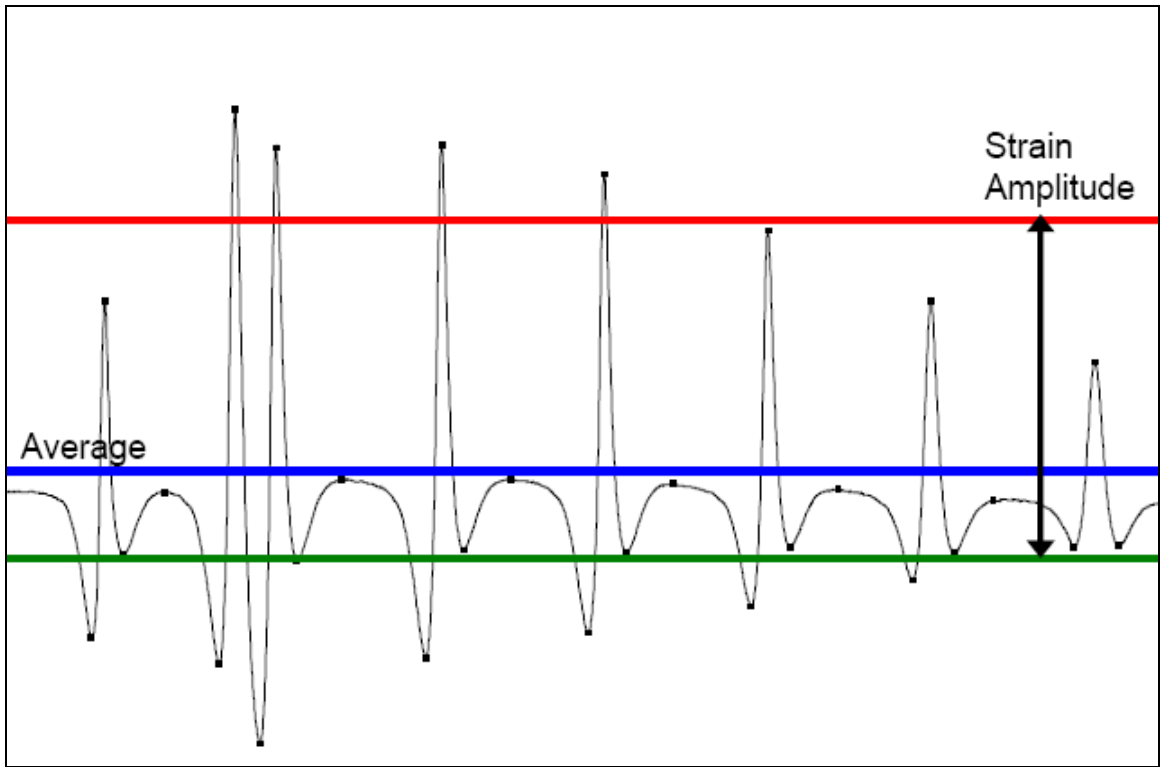
Figure 5-14. Strain Amplitude Illustration (Priest and Timm, 2006).

When each strain trace was processed, its record included the date, section,

gauge identifier, truck number, and pass number for organization of the data. The

dynamic responses recorded were gauge factor (specialized for each strain gauge), truck

pass, minimum reading, maximum reading, and amplitude. These values were all then

entered into a Microsoft Access database where the data could be stored, managed, and

manipulated.

Pavement Performance

Along with dynamic data collection, performance data were collected weekly at the Test Track. On Mondays, trucking was stopped so the Test Track staff could make cracking and rutting measurements.

Cracking was monitored by visually inspecting the pavement (Figure 5-15) and marking where cracking had occurred. When a cracked area or individual crack had been indentified, it was marked with chalk and then recorded using a video camera attached to a boom on a skid-steer tractor. These videos were then digitized, and the coordinates of the cracked areas were recorded. These crack records were developed into crack maps of the structural sections as seen in Figure 5-16. The dark lines are individual cracks while the boxes are cracked areas (Priest and Timm, 2006).

Figure 5-15. Crack Investigation Technique (Priest and Timm, 2006).
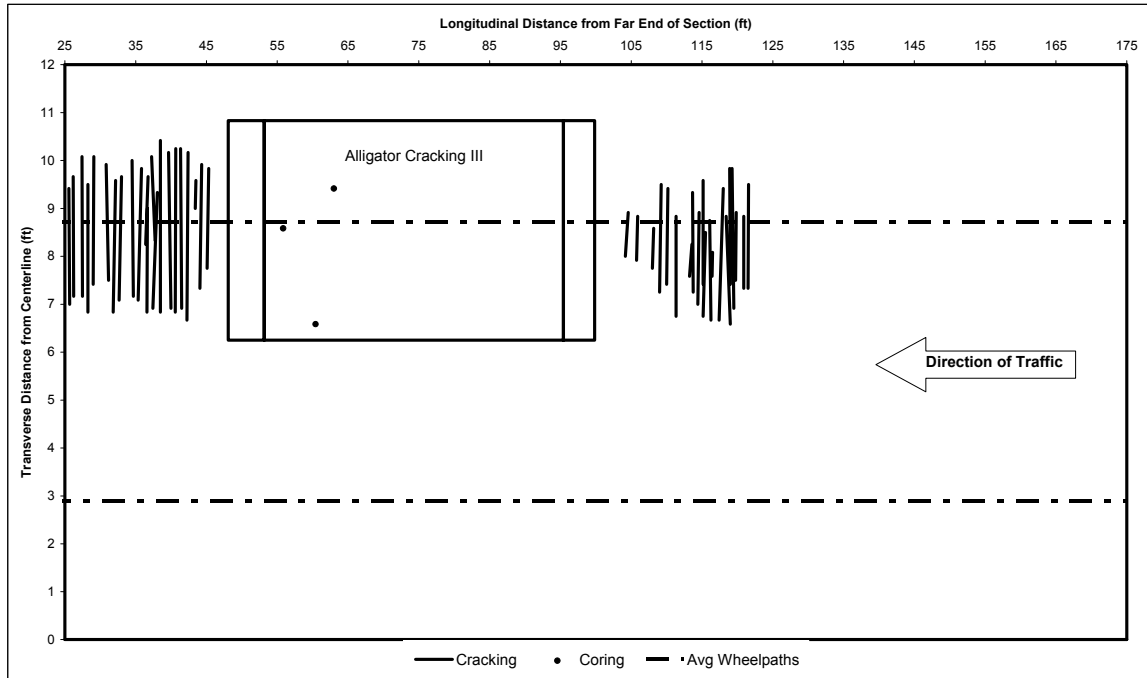
Figure 5-16. Example Crack Map (Priest and Timm, 2006).

Developing Strain-Temperature Relationships

Temperature can be related to both the material properties of HMA (as seen previously) and a pavement's mechanistic response. In order to develop strain distribution plots for each section, hourly strains are necessary; however, measuring and processing continual strain at the Test Track was impractical. Therefore, strain and temperature relationships needed to be developed to calculate an hourly strain value for each vehicle.

In her research at the NCAT Test Track, Priest developed relationships between the mid-depth temperature and measured strains using the following equation (Priest and Timm, 2006):

$$\varepsilon = k_1 T^{k_2}$$ Equation 5-1

Where: ε = longitudinal strain

k_1 = section-specific regression constant

k_2 = section-specific regression constant

T = mid-depth temperature, °F

These relationships were developed for each structural section at the Test Track based upon the loading configuration of the truck: box or triple. The relationships were taken by matching a measured strain to the average hourly temperature at the time of testing. Once matched, as illustrated in Figure 5-17, a statistical correlation could be developed.
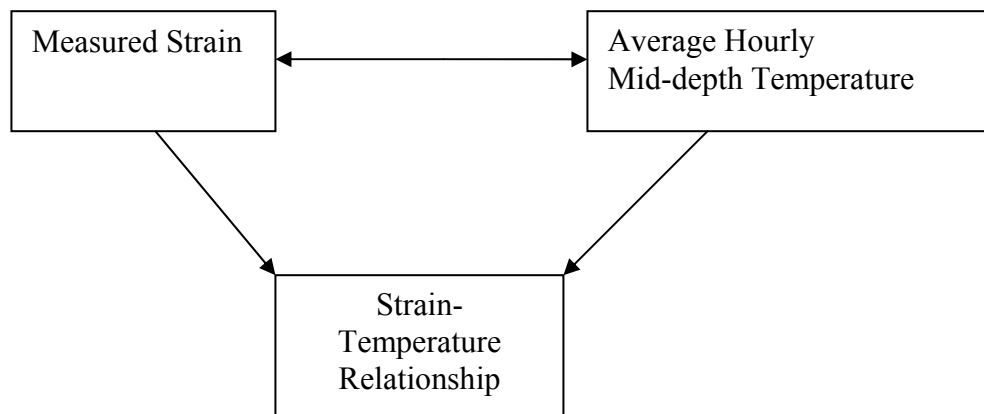
Figure 5-17. Strain-Temperature Relationship Model.

The relationships were developed only until cracking was first visualized due to the erratic nature of pavement instrumentation in distressed areas. These dates are listed in Table 5-4. Examples of the relationships between the mid-depth temperature and recorded strain are presented in Figures 5-18 and 5-19 for triple and box trailers,

104

respectively. The coefficients and R^2 for each relationship are provided in Tables 5-5 and 5-6 by section for both triple and box trailers. The regression coefficients in section N1 for the relationship with the triple trailers are based upon limited data due to the early fatigue cracking in the section. There were not enough data to formulate a relationship between the strain imposed by the box trailer and temperature for this section (Priest and Timm, 2006).
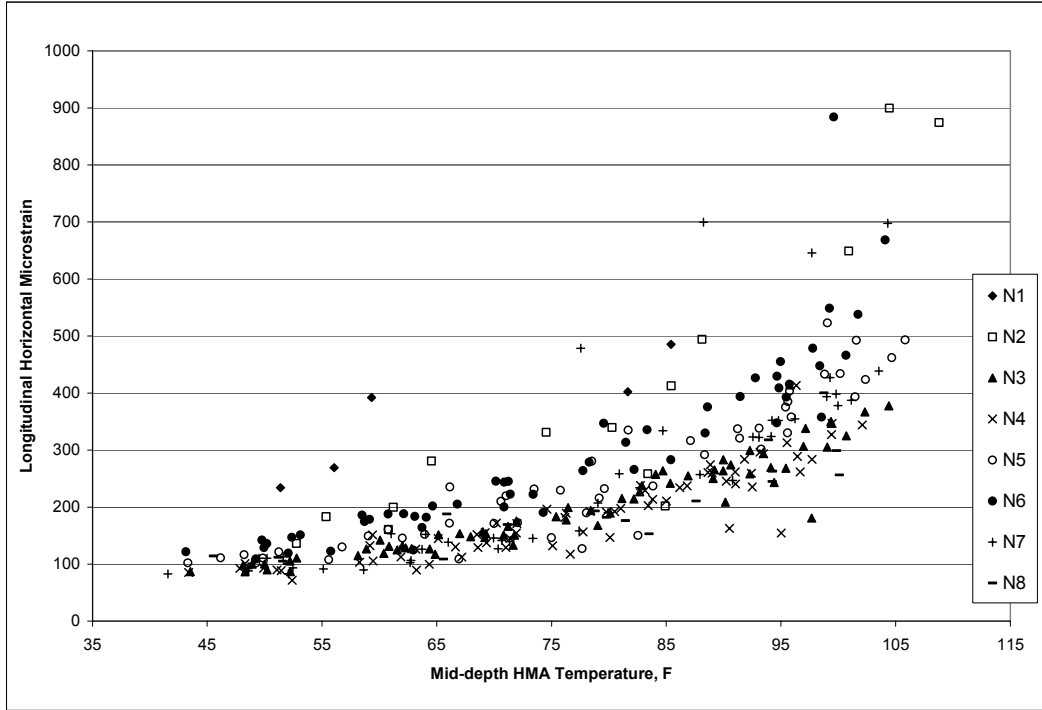
Figure 5-18. Strain-Temperature Relationship for Triple Trailer (Priest and Timm, 2006).
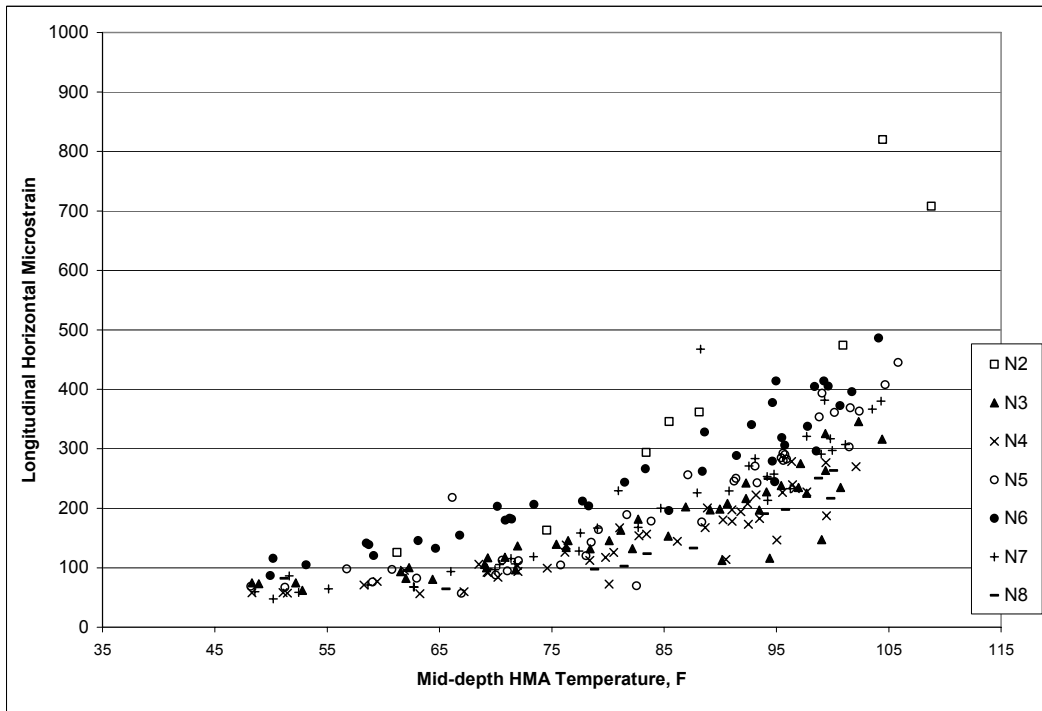
Figure 5-19. Strain-Temperature Relationship for Box Trailer (Priest and Timm, 2006).

Table 5-4. Dates Cracking Observed.

Section	Date
N1	March 22, 2004
N2	June 14, 2004
N3	No cracking at present time
N4	No cracking at present time
N5	February 7, 2005
N6	February 7, 2005
N7	February 7, 2005

Table 5-5. Triple Trailer Strain-Temperature Relationship Coefficients (Priest and Timm, 2006).

Section	k_1	k_2	R^2
N1	4.0439	1.066	0.763
N2	0.0005	3.091	0.877
N3	0.0508	1.899	0.909
N4	0.0211	2.086	0.822
N5	0.0109	2.291	0.881
N6	0.0132	2.293	0.810
N7	0.0022	2.652	0.705

Table 5-6. Box Trailer Strain-Temperature Relationship Coefficients (Priest and Timm, 2006).

Section	k_1	k_2	R^2
N1	NA	NA	NA
N2	3.922E-05	3.579	0.871
N3	5.501E-03	2.332	0.773
N4	1.304E-03	2.632	0.773
N5	1.4404E-04	3.185	0.887
N6	1.852E-02	2.155	0.881
N7	8.310E-04	2.796	0.821

Continuous Pavement Response

While Priest and Timm's work (2006) developed strain-temperature

relationships for the seven structural sections in this study, her work did not continue in

developing cumulative strain distribution plots for each structural section. Figure 5-20

provides the methodology used in developing the strain distributions for this analysis.
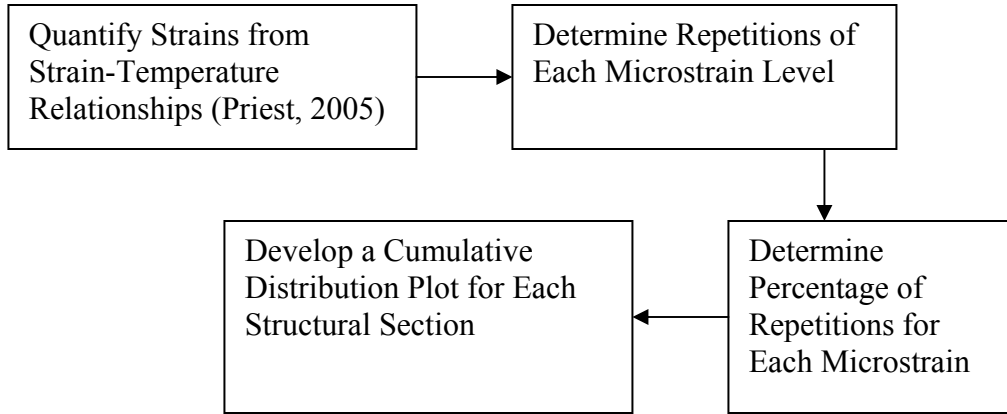
Figure 5-20. Developing Cumulative Strain Distribution Methodology.

Quantify Strains from Strain-Temperature Relationships

Priest and Timm's strain-temperature relationships (2006) were used to quantify

the strain amplitude imposed on a pavement structure during a truck pass at a given

temperature. To then estimate the strain magnitudes experienced in the pavement due to

these loadings, one had to know when the trucks were running, and the average hourly

mid-depth temperature at the time of trafficking (Figure 5-21).
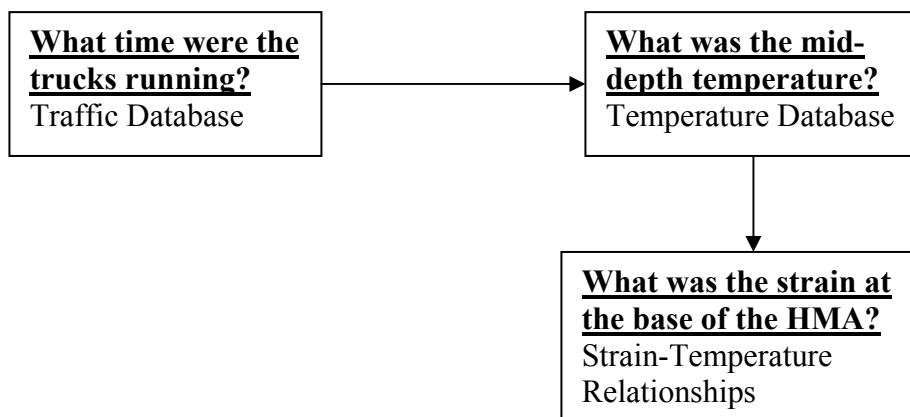
Figure 5-21. Methodology for Estimating Strain.

The traffic database managed by the staff at the NCAT Test Track began keeping detailed records of the trafficking patterns of the fleet in during the 2003 experiment. One of these records included the times the trucks were out on the track.

Sections N3 and N4 were the two sections whose traffic was carried through the 2006 Test Track for this analysis. These two sections, at the end of the 2003 test cycle, had not experienced any fatigue cracking in their pavement structure; therefore, it was decided that their experiment should continue for another 10 million ESALs. At the present time (20 million ESALs), they still have no signs of fatigue cracking.

During the 2006 Test Track experiment, new truck configurations (double trailers) were used which Priest had not accounted for in previous research. Since relationships had not been developed for this new truck configuration, it was decided to use the triple trailer equation to estimate the strain amplitudes produced by the double trailer configuration. The triple trailer equation would produce higher strains than the box trailer equation; thus, it would prove to be more conservative. The differing number of strain events would be accounted for at a later time.

The temperature database for each section at the Test Track also kept track of the temperatures measured from the four temperature probes in the pavement; therefore, every hour, an average hourly temperature was recorded at the surface of the pavement and 2, 4, and 10 inches deep. While the mid-depth temperature was not measured directly, linear interpolation between two measured temperatures was used to estimate the mid-depth temperature.

There were times when either due to datalogger malfunctions or other sources of error that temperatures were not recorded and entered into the temperature database.

When this was the case, average temperatures from the surrounding years were inserted in place of the missing data. For example, near the end of the 2003 Test Track experiment, all of the average temperature data from N3 and N4 were lost after August 12, 2005. To remedy this, the 2004 and 2006 mid-depth temperatures were averaged on an hourly basis and used to estimate strains in the pavement during the fall of 2005.

Once both the traffic and mid-depth temperature databases were complete, the databases were queried in Microsoft Access to match the mid-depth temperatures during times when the trucks were running on the pavement. This query also reported the truck configurations. The temperatures for each section were then used in the previously developed strain-temperature equations to estimate the strains seen at the base of the HMA layer (Table 5-7).

Table 5-7. Estimated Strains Example.

Section	Date	Hour	T_{mid}, °F	Configuration	Microstrain
N1	1-12-2004	13	51.8	Triple	271
N1	1-12-2004	13	51.8	Box	106

Determine Repetitions of Each Microstrain Level

After estimating the strains, it was vital to know how many strain repetitions of that specific strain magnitude were experienced in the pavement. This was completed by knowing the strain previously calculated, the truck configuration from the traffic database, and the number of laps completed each hour. The linkages between databases needed to make this computation are shown in Figure 5-22.

What Is the Truck Configuration? Traffic Database	How Many Strain Events Occur for Each Truck Configuration? Tire Events

How Many Laps Did Each Truck Complete in an Hour? Traffic Database	What Is the Total Number of Strain Repetitions for Each Strain Magnitude at Each Hour?

What Is the Strain Magnitude? Previously Computed Strains
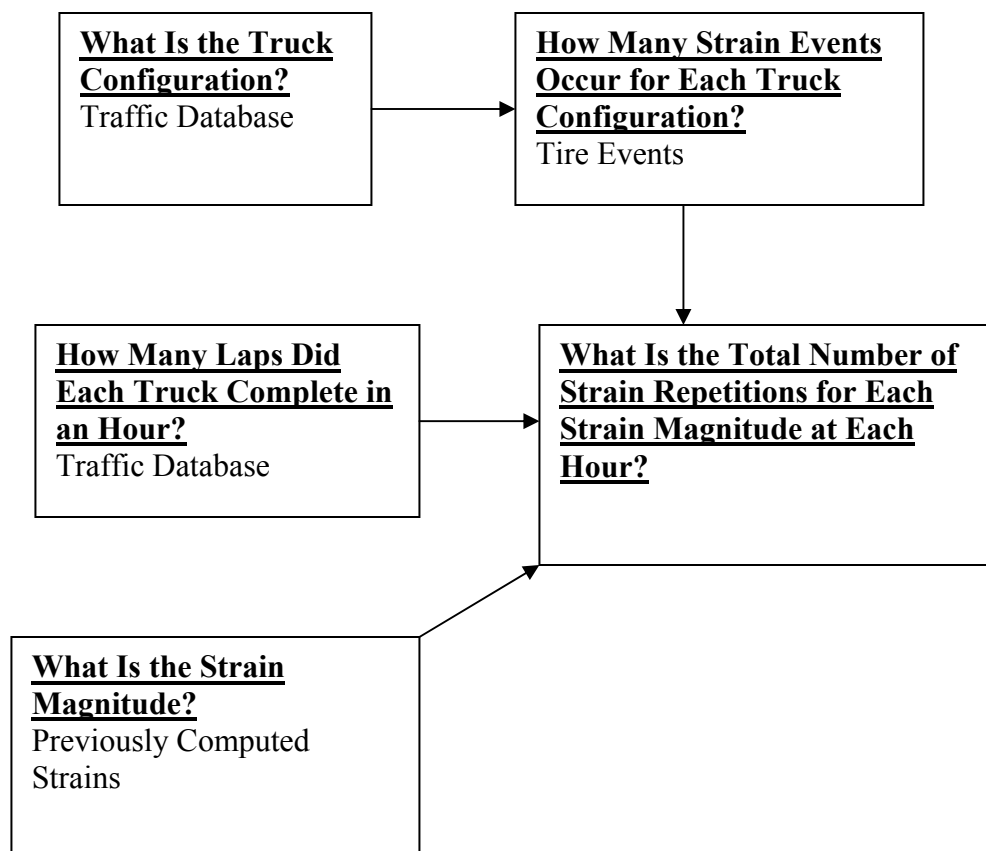
Figure 5-22. Strain Repetition Flowchart.

The truck configuration contributed to the number of strain events caused by an individual truck. If one were to look at the strain traces previously shown in Figure 5-13, one would see that the strain trace had eight strain events that occurred, one for each axle. Using the truck configurations given in the traffic database, Microsoft Excel was used to determine the number of strain repetitions for each vehicle type used at the Test Track. The number of repetitions was calculated based upon the number of axle loadings each truck provided. These values are shown in Table 5-8.

111

Table 5-8. Strain Events Per Truck Configuration.

Truck Type	Steer Axles	Tandem Axles	Single Axles	Strain Events
Single Box Trailer	1	2	0	5
Double Trailer	1	1	3	6
Triple Trailer	1	1	5	8

Once the number of strain events having occurred for each truck was determined, the number of strain events was multiplied by the number of laps completed in one hour to calculate the total number of strain repetitions inflicted by each particular truck in an hour (Table 5-9).

Table 5-9. Total Strain Repetition Calculation Example.

Microstrain	Truck Configuration	Strain Events	Laps	Total Strain Repetitions
271	Triple	8	26	208
105	Box	5	26	130

Determine Percentages for Each Microstrain Level

After the total number of strain repetitions imposed by each truck every hour was calculated, the percentage of total strain repetitions at each microstrain magnitude needed to be determined. This was completed by dividing the number of total strain repetitions each hour by the total number of strain repetitions over the entire performance period of the pavement.

In this study, the performance period was defined as time from construction until crack visualization. It is important to discard strains collected after cracking was visualized for two reasons. First, strains measured in sections where cracking has occurred can be erratic and erroneous (Willis and Timm, 2008). Second, if fatigue cracking is visualized, the pavement can no longer be defined as perpetual. For this

study, it is important to understand the strain profile pre-cracking to analyze the strains

which caused the cracking.

An example of how the percentages were calculated is provided in Table 5-10.

The values used in the example are not those found in the study due to enormity of the

total number of strain repetitions encountered in this analysis phase.

Table 5-10. Example Strain Percentage Table.

Strain Magnitude, Microstrain	Strain Repetitions	Percentage (%)
100	209	20.6
500	302	29.7
200	506	49.7
Total	1017	100

Determining the Cumulative Distribution of Strains

To create a cumulative distribution for the estimated strain values, the strains

were sorted by strain magnitude in ascending order. At this point, a running sum of the

percentage column was calculated to determine the percentiles associated with each

strain magnitude. The previously used example is expanded upon in Table 5-11 to

develop its cumulative distribution function.

Table 5-11. Example Strain Percentage Table.

Strain Magnitude, Microstrain	Strain Repetitions	Percentage (%)	CDF (%)
100	209	20.6	20.6
200	506	49.7	70.3
500	302	29.7	100
Total	1017	100	

Once a the cumulative distributions were determined for each structural section,

the 1st, 99th, and every 5th percentile were manually picked from the completed

spreadsheets to develop cumulative distribution plots. Figure 5-23 and Table 5-12

provide the cumulative distribution functions, by section, both graphically and numerically.
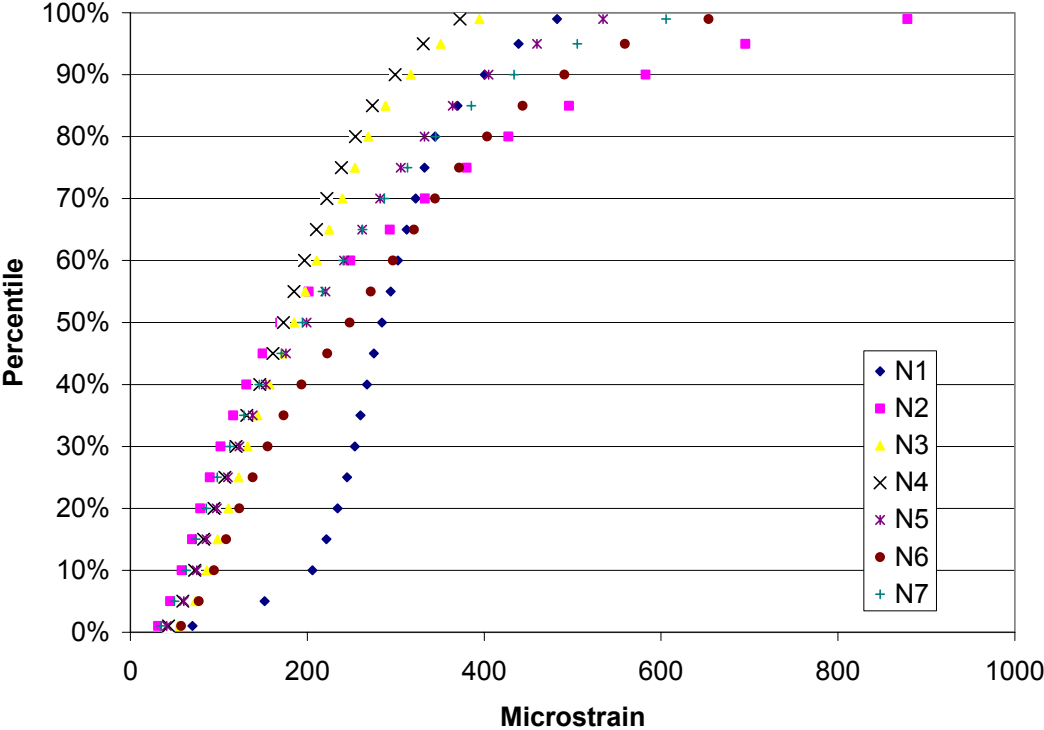
Figure 5-23. Cumulative Distribution Plots for 2003 Test Sections.

Table 5-12. Cumulative Distribution Percentiles for 2003 Test Sections.

Percentile	Tensile Microstrain at Bottom of HMA						
	N1	N2	N3	N4	N5	N6	N7
99%	482	879	395	373	534	654	606
95%	439	695	351	331	460	559	505
90%	400	582	317	299	405	491	434
85%	370	496	289	274	364	443	385
80%	344	427	269	254	332	403	345
75%	332	380	254	239	306	372	313
70%	322	333	240	222	282	344	287
65%	312	293	225	210	262	320	262
60%	303	249	211	197	242	297	241
55%	294	202	198	185	221	272	217
50%	284	169	185	173	199	248	194
45%	275	149	172	161	176	223	171
40%	267	131	157	146	153	193	146
35%	260	116	144	132	138	173	128
30%	254	102	132	119	123	155	112
25%	245	90	122	107	110	138	98
20%	234	79	111	94	98	123	86
15%	222	70	99	83	86	108	74
10%	206	58	86	73	75	94	63
5%	152	45	73	59	60	77	50
1%	70	31	54	43	41	57	35

RESULTS AND CONCLUSIONS

Of the seven sections analyzed in the 2003 Test Track analysis, five of the sections experienced fatigue cracking: N1, N2, N5, N6, and N7. N3 and N4 did not show signs of fatigue cracking, and at the present time (November, 2008), still have not shown indication of fatigue distress.

If one were to compare the cumulative distributions of these sections, one would easily notice that section N4 has the lowest distribution strains at the high end of the cumulative distribution. However, until the 55th percentile strain, its strains are not the lowest. Those are found in N2, but the strains soon escalate in this thinner section.

The other section that did not show signs of fatigue cracking, N3, started out with low strains comparable to those in failed sections; however, from the 25th until the 50th percentile, its strains track very well with sections that failed in fatigue. The 55th percentile seemed to be the breaking point for sections N3 and N4 where failed sections began to escalate into higher strains.

While the breakpoint where the cumulative distribution functions of the cracked sections are greater than those of the non-cracked occurs at the 55th percentile, clear deviations between the sections that performed well and those that did not are present after the 60th percentile where the difference between the maximum non-cracked sectional strain and minimum fatigue cracked sectional strain jumps from 4 $\mu\varepsilon$ at the 55th percentile to almost 30 $\mu\varepsilon$ at the 60th percentile.

If one were to compare the cumulative distribution functions calculated for sections N3 and N4 and compare them to the often used laboratory fatigue thresholds of 70 or 100 $\mu\varepsilon$, one would find that for both sections, less than 10% of the strain measurements fall below 70 $\mu\varepsilon$. In section N3, less than 15% of the strain measurements were below 100 $\mu\varepsilon$, and this value was under 25% for section N4. Therefore, it can be inferred that measured strains in the field can exceed the laboratory fatigue threshold without fatigue damage occurring. This will allow for the design of thinner pavement structures in the future.

At first, when comparing the cracked sections, N1's cumulative distribution function was puzzling. While N1 was clearly the first section to experience fatigue cracking, all four of the other cracked sections exhibited higher strain values near the top of their cumulative distribution functions; however, one had to consider the mid-depth

116

temperatures experienced in the section before the time cracking was seen. Cracking was first seen in section N1 in March of 2004, and all of the other sections lasted until at least June before fatigue cracking was experienced. When looking at the cumulative distributions of the temperatures for the cracked sections (Figure 5-24), it is easier to understand each strain distribution. N1 had relative small temperatures range compared to the other sections, and it was trafficked primarily by one vehicle (the triple trailer). This would lead to the relatively steep cumulative distribution function compared to the non-cracked sections.
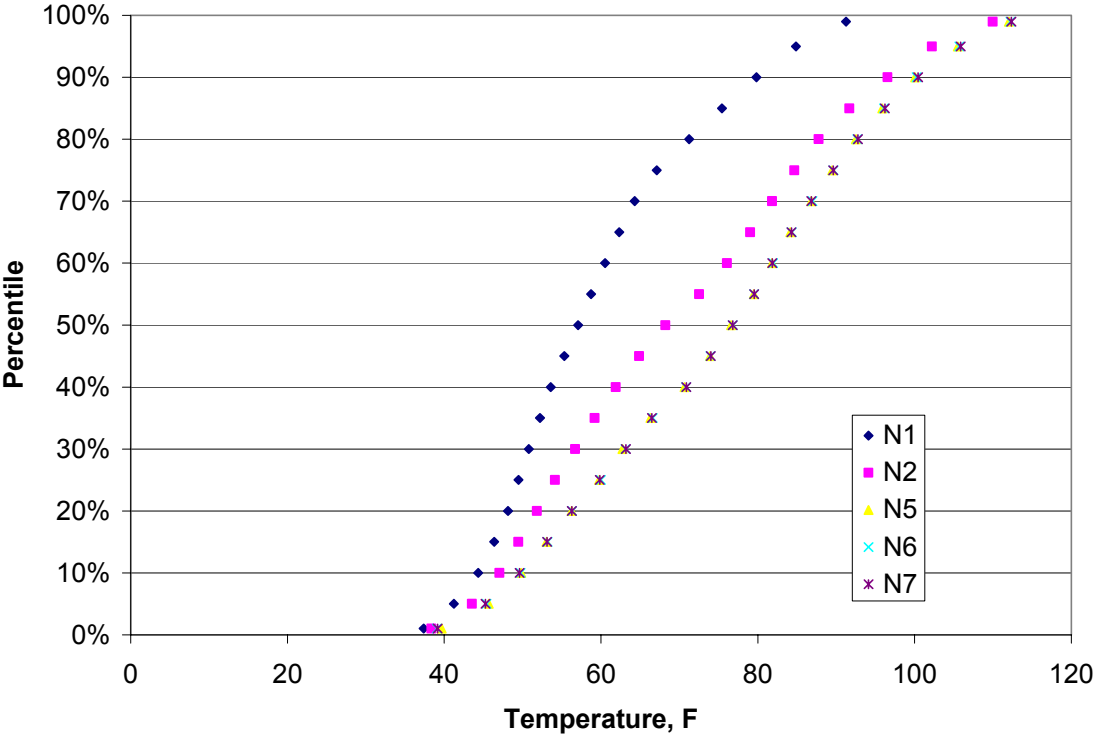
Figure 5-24. Cumulative Distribution of Temperatures for Cracked Sections.

In conclusion, the difference between the cumulative distributions of the cracked and non-cracked sections is the most useful result of this analysis. The strain profiles

117

between the test sections that performed well and those that did not are distinctly different after the 60th percentile strains.

SUMMARY

Based on the limited data from this analysis, it would seem that measured field strains can exceed the laboratory fatigue threshold of 70 $\mu\varepsilon$ and still perform well in fatigue. Sections N3 and N4 provide evidence that well-built sections might be able to designed from higher levels of strain and still be robust enough to withstand trafficking of close to 20 million ESALs.

The idea of developing strain profiles for test sections at the NCAT Test Track is taken a step further in the next chapter. Strain profiles were developed for five newly constructed structural sections from the 2006 experiment, and a new methodology was used to develop a secondary cumulative distribution plot for the two structural sections remaining from the 2003 experiment.

CHAPTER SIX

DEVELOPING CUMULATIVE STRAIN DISTRIBUTIONS FOR THE 2006

NCAT TEST TRACK

THE 2006 NCAT TEST TRACK

The 2006 Test Track experiment began construction in the summer of 2006 and was completed near the end of October the same year. Trafficking of the 46 sections began on November 14, 2006 and is still running at the present time.

Only eight of the original 46 test sections dating back to the 2000 Test Track were left in-place for further trafficking in 2006. As the scope of the project continued to change and new state DOTs became sponsors, the instrumented structural study expanded from eight to eleven section introducing the Missouri and Oklahoma DOTs as section sponsors.

These eleven sections (Figure 6-1) varied in thickness, mix design, and base material. Six of the eleven sections (N1, N2, N8, N9, N10, and S11) were newly constructed for this cycle of testing. Due to their satisfactory performance, sections N3, N4, N6, and N7 were left in-place for further trafficking. A rehabilitation effort was designed to allow section N5 to receive more traffic. A two inch mill and inlay was constructed in this section to alleviate top-down surface cracking.
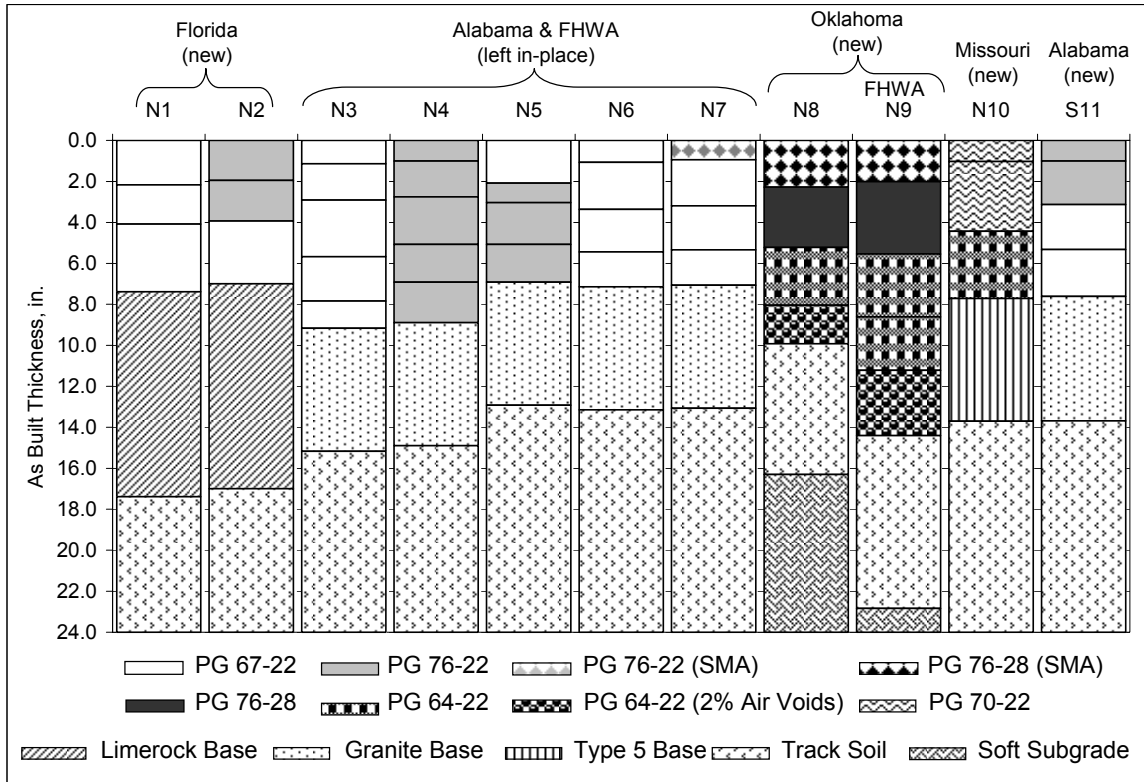
Figure 6-1. Structural Sections at the 2006 NCAT Test Track.

The thicknesses of these eleven sections ranged from 7 to 14 inches in depth, and two of the newly built sections (N8 and N9) were designed by the Oklahoma DOT to be perpetual pavements. These two sections were built on an A-7-6 subgrade material similar to native Oklahoma material. Above the subgrade was an eight inch lift of the typical subgrade material used around the other test sections quarried from the West curve of the Test Track. The pavement structures above the soil are identical in mix design; however, as can be seen in Figure 6-2, the primary difference between the sections is their layer thicknesses. Section N9 was built with an additional four inches of HMA. This additional asphalt comes from an additional three inch lift of PG 64-22 material and a thicker rich-bottom layer.
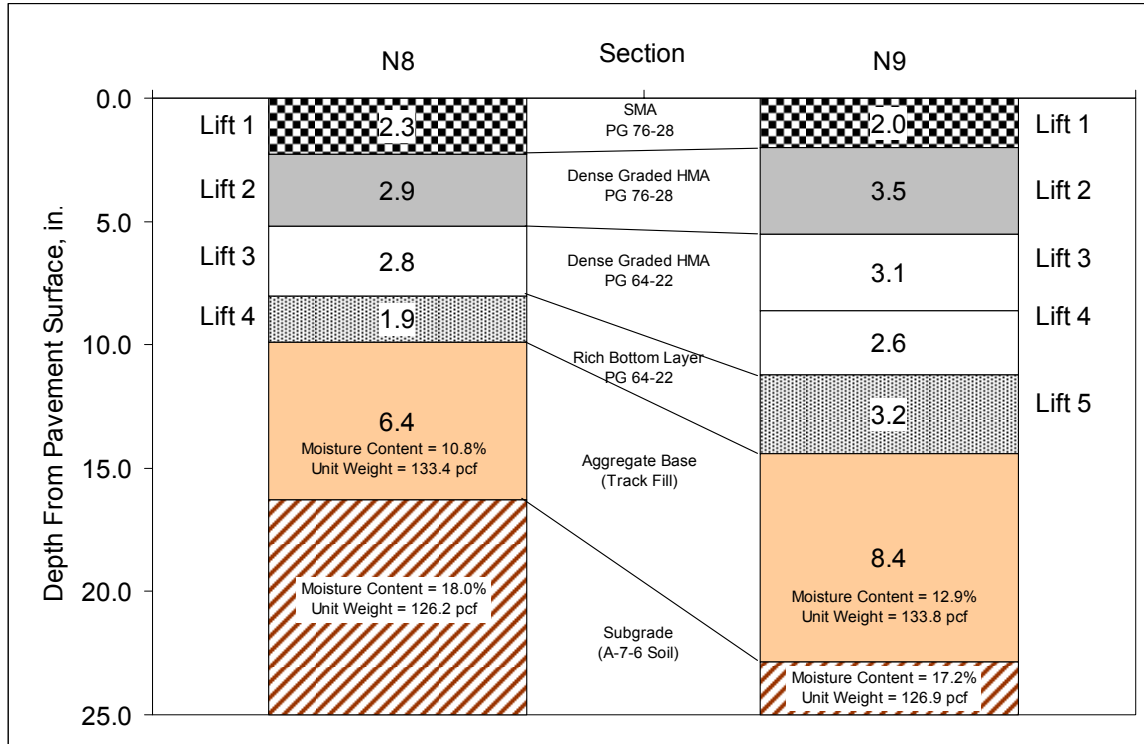
Figure 6-2. Sections N8 and N9 Layer Thicknesses.

The rich-bottom layer was designed using the perpetual design pavement profile consisting of a fatigue resistant base layer, intermediate rut-resistant layers, and a rut-resistant surface layer. This process was completed by designing the rich-bottom layer for 2% air voids, increasing the binder grade closer to the surface, and designing the wearing course of the pavement as an SMA.

Pavement Instrumentation

Like the 2003 Test Track, the 2006 structural study incorporated the use of embedded pavement instrumentation to characterize the dynamic pavement responses of these sections. The same CTL strain gauges were used to capture dynamic strain data as the trucks trafficked each section. Figure 6-3 provides the basic instrumentation array used in the 2006 structural study.

121
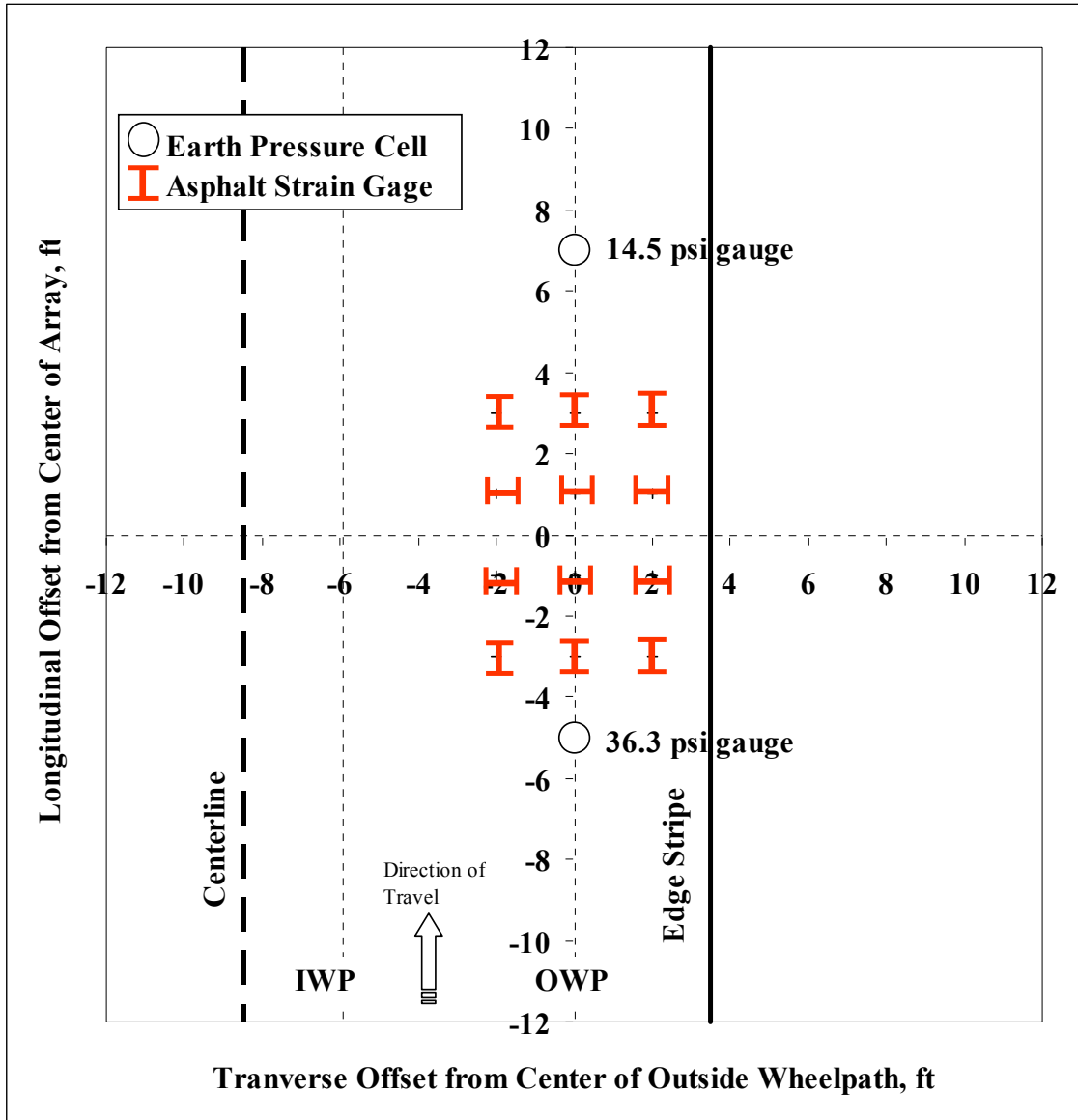
Figure 6-3. Typical Strain Gauge Array.

The strain gauges were centered along the outside wheelpath of the trafficking lane. The wheelpath was determined through a wheel wander study by Priest and Timm (2005) during the 2003 Test Track. The center of the wheelpath was chosen as the center of the gauge array to provide the best chance of encountering a direct hit on the gauge. When the center of the gauge array was located, another gauge was installed two feet to the left and two feet to the right of the centered gauge to capture any wheel

wander which might occur due to human drivers. Once the first row of gauges was installed, three more rows of gauges were installed at two foot intervals on center downstream to measure both longitudinal and transverse strain.

Temperature probes were also installed in each structural section; however, new locations were chosen for tip placement compared to past Test Track experiments. Previous Test Track cycles placed the temperature probe tips at the surface of the pavement and then at depths of 2, 4, and 10 inches. Since strong correlations had been found between the mid-depth temperature of a pavement structure and its material properties and performance, it was thought better to measure the mid-depth temperature than to interpolate it. Thus, a new configuration of temperature probes was designed on a sectional basis where the tips of the temperature probes measured the surface temperature, mid-depth temperature, full-depth temperature, and the temperature three inches into the base material.

GENERAL METHODOLOGY

The general methodology for analyzing the pavement performance of the 2006 NCAT Test Track (Figure 6-4) was once again structured around the M-E design flowchart. Much like the 2003 Test Track analysis, the seasonal material properties and layer thicknesses were not necessary components of the investigation due since dynamic pavement responses were collected that spanned multiple seasons. Measuring dynamic strains at the base of the HMA also alleviates the need to use a mechanistic pavement model to predict pavement response.
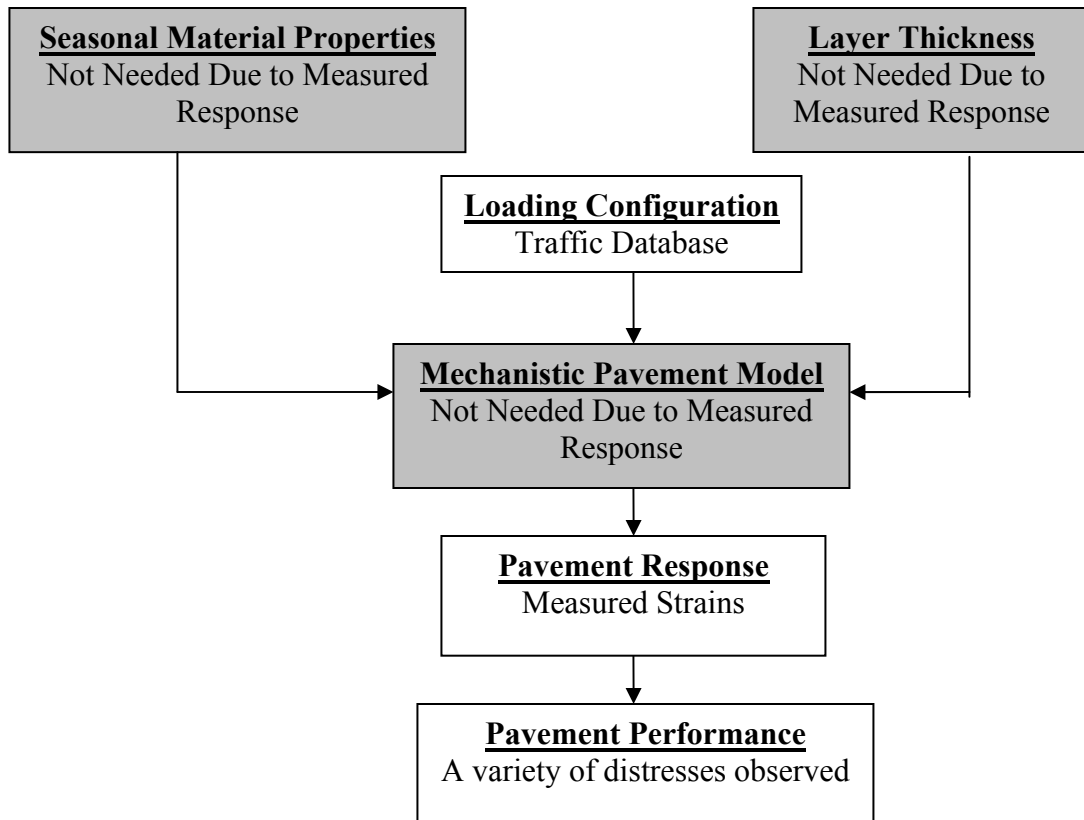
Figure 6-4. 2006 Test Track Flowchart for Data Analysis.

The loading configurations used at the 2006 Test Track came from the trafficking database kept by the NCAT Test Track staff. This database included the truck configuration, hour of trafficking, and number of laps completed in that one hour. This data was used to determine the number of axle repetitions per hour during trafficking.

The pavement response analysis correlates measured strains by axle type to temperature. When strong relationships between temperature and strain were correlated, the continuous temperature database was used to estimate strains during times of trafficking.

Finally, once the loading data and strain data were combined to develop a cumulative strain distribution for the sections being analyzed, the performance of the section needed to be linked to the pavement response to challenge the theory that pavements which deteriorate due to fatigue cracking have different strain distributions than those which remain intact.

SCOPE

Eleven structural sections were in-place at the 2006 Test Track; however, as previously mentioned, only six of the sections were newly constructed. To remain consistent with previous analysis methodologies, a test section could only be analyzed until the point when fatigue cracking was visualized. At this point, it was no longer classified as perpetual.

All six of the newly constructed sections were a part of the 2006 investigation; however, only two (N3 and N4) of the left in-place sections had not experienced fatigue cracking. Since sections N5, N6, and N7 had already shown signs of fatigue cracking, they were not incorporated into this analysis procedure.

LOADING CONFIGURATION

Trafficking at the 2006 Test Track was conducted in a similar manner to the methodology described in Chapter 5. Four triple flat-bed trailer trucks (Figure 6-5) and one triple box trailer (Figure 6-6) loaded the pavement from 5:00 AM until approximately 10:40 PM Tuesday through Saturday accumulate 10 million ESALs over

the two and a half years of trafficking. While the 2003 Test Track incorporated the use

of a single box trailer, the 2006 Test Track did not use this loading device.

Figure 6-5. Triple Flat-Bed Trailer.

Figure 6-6. Triple Box Trailer.

Table 6-1 provides the axle weights for each of the five trucks under normal loading conditions. There were occasions during the testing cycle when either due to a specialized study or due to mechanical malfunction that trailers were removed from their given tractor. This left the tractor pulling either a single flat-bed trailer or a combination of double flat-bed.

Table 6-1. Truck Weights for 2006 Test Track.

	Steer, lb	Tandem, lb		Single, lb				
Truck ID	Axle 1	Axle 2	Axle 3	Axle 4	Axle 5	Axle 6	Axle 7	Axle 8
1	10,150	19,200	18,550	21,650	20,300	21,850	20,100	19,966
2	11,000	20,950	20,400	20,950	21,200	21,000	20,900	20,900
3	10,550	20,550	21,050	21,000	21,150	21,150	21,350	20,850
4	10,500	21,050	20,700	21,100	21,050	21,050	20,900	21,050
5	11,200	19,850	20,750	20,350	20,100	21,500	19,500	20,300
Average	10,680	20,320	20,290	20,760	20,760	21,310	20,550	20,613
COV	3.9	3.9	4.9	2.2	2.5	1.7	3.6	2.2

A detailed trucking database was organized similarly to that of the 2003 Test Track. Queries were conducted in this database to determine the number of repetitions by axle type for each hour of traffic as shown in Table 6-2.

Table 6-2. Example Trucking Database.

Date	Truck	Hour	Laps
2-2-07	4	6	13.5
2-2-07	4	7	27
2-2-07	4	8	27

PAVEMENT RESPONSE

Each new structural test section was instrumented with strain gauges as shown previously in Figure 6-3. Temperature probes were placed vertically in these sections to measure the pavement temperature at the surface, mid-depth, full-depth, and three inches into the subgrade. The two sections left in-place from the previous Test Track experiment had some combination of the 12 strain gauges still functioning and temperature probes at the surface and depths of 2, 4, and 10 inches. Similar to the methodology described in Chapter 5, simultaneous strain and temperature readings needed to be recorded to develop strain and temperature relationships for each test section.

Data Collection

During the 2003 Test Track, strain data were only captured monthly until the first instance of fatigue cracking. Upon this occurring, data collection was then shifted to a weekly event. To fully capture the pavement responses of the structure before

cracking or rutting initiated, a data collection scheme was developed that involved

capturing strain measurements on a weekly basis. During the course of a season, data

were collected in both the mornings and afternoons in an attempt to fully capture the

temperature spectrum seen at the Test Track.

While data were collected in 2003 using a portable DATAQ unit, the

introduction of a new wireless network allowed data to be collected in a location off the

Test Track for safety. Both high speed data (strain and pressure) and slow speed data

(temperature) could be streamed to computers inside the NCAT Test Track office from

remote roadside boxes (Figure 6-7) at each test section.

Figure 6-7. Remote Roadside Boxes.

The data collection methodology involved capturing three passes of each vehicle on every structural test section. The collectors would begin with test section N1 and then proceed through the structural sections collecting data on a section and then moving to the next.

At the beginning of the experiment, the high speed data were captured at a frequency of 2,000 Hertz; however, this frequency seemed to be hindering the network's capacity to stream data well. Therefore, the frequency of the high speed data collection was reduced to 1,000 Hertz with no detriment to the experiment.

Unlike the 2003 Test Track where an average hourly temperature was correlated to the strain, the introduction of the slow speed wireless network allowed for live temperatures to be streamed while strains were being recorded. With this ability, the precise pavement temperatures during the trafficking period could be determined, rather than using an hourly average temperature.

Data Processing

Once the data were recorded, a team of data processors would take the raw data traces and generate strain amplitudes using the DADISP software previously described in Chapter 5. Unlike the previous experiment, it was decided to analyze strain by axle type instead of by truck pass. In other words, for every truck pass, a steer axle, tandem axle, and a single axle strain were processed. While this methodology was more labor intensive than the previously used one, it provided a better understanding of the pavement's interaction with the different axle types.

When analyzing the pavement's reaction by axle, each steer and tandem axle was processed for every truck pass; however, of the five trailing single axles, only the axle with the "best hit" was processed. The "best hit" was defined as the axle yielding the highest recorded strain. This was believed to be the axle which most directly hit a strain gauge. The best hit single axle is circled in Figure 6-8.
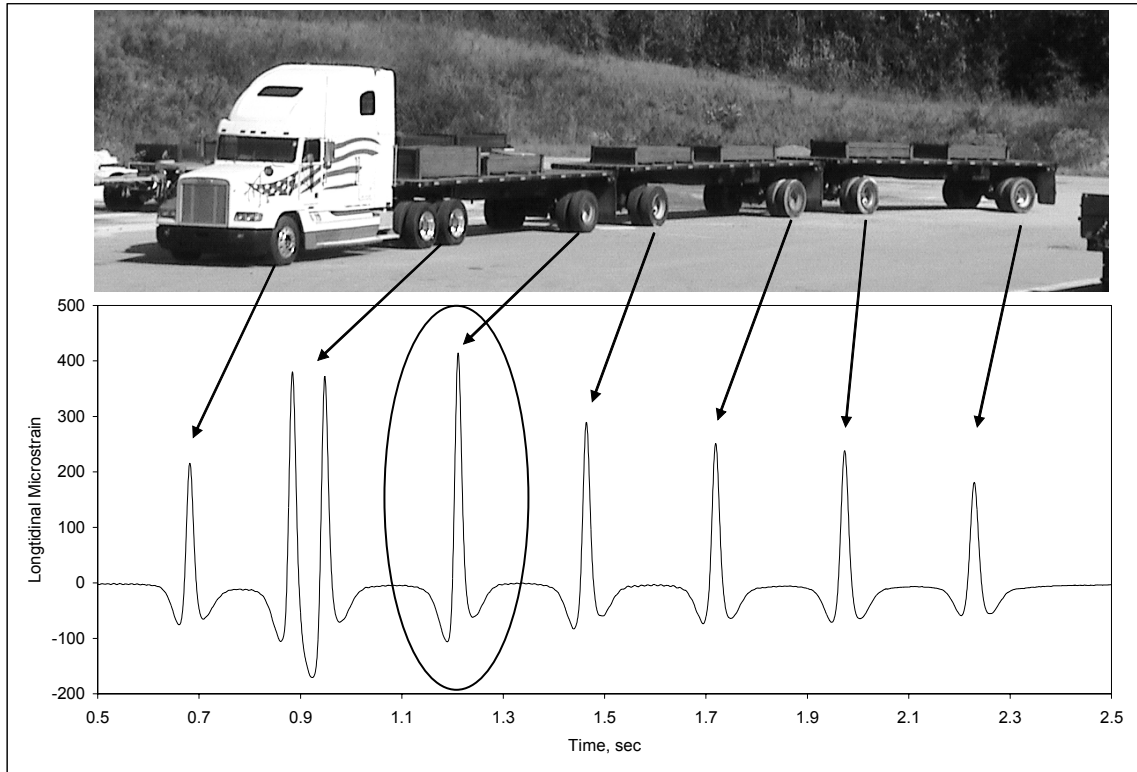
Figure 6-8. "Best Hit" Single Axle.

Figure 6-8 also shows that the strain trace for the triple trailers predominantly used at the Test Track consisted of eight individual strain events. These were the results of one steer axle, one tandem, and five single axles loading the pavement. A double trailer resulted in six strain events, and a single trailer had four. In each case, no matter how many single axles were present, only the best hit was processed.

131

Each axle strain was defined as amplitude. This terminology was defined earlier, but can roughly be described as the difference between the average peak value and the average trough value.

Each strain value was processed and recorded. Before being entered into the strain database, the data were put through a rigorous screening process to ensure the data were of a high quality. This process entailed searching for negative amplitudes, finding outliers (one or two datapoints vastly higher than the other readings), and ensuring that duplicate gauges were recording microstrains within the standard of precision set at the NCAT Test Track (Willis and Timm, 2008).

Once these checks were completed, the data were entered into a strain database. Each strain entry included the following: date, test section, gauge number, gauge factor, truck number, axle type, pass number, maximum reading, minimum reading, and the amplitude. These values were stored in a Microsoft Access database for further manipulation and analysis.

Pavement Performance

Pavement performance was once again monitored and recorded as previously mentioned in Chapter 5. When trafficking was stopped on Monday, visual inspections of the pavement were conducted to mark cracks and cracked regions of the structural sections. These markings were then videotaped and digitized into crack maps. These maps showed the extent of fatigue cracking in each section. These maps also provide a cracking timeline for the structural sections.

When developing strain-temperature relationships and cumulative strain profiles, it is of upmost importance that the data represent strain levels prior to cracking. When fatigue cracking occurs, the pavement is no longer considered perpetual and the strain gauge readings can become erratic and inconsistent. Therefore, the crack mapping data were used to determine the cut-off date for both the strain-temperature relationships and cumulative strain distributions. These dates are provided in Table 6-2.

Table 6-2. Date of Crack Visualization.

Section	Date
N1	April 9, 2007
N2	April 23, 2007
N3	Did not crack
N4	Did not crack
N8	April 28, 2008
N9	Did not crack
N10	June 23, 2008
S11	January 28, 2008

Developing Strain-Temperature Relationships

When the strain-temperature relationships were developed, a strain had to be matched to a temperature at a given pavement depth. These relationships were developed because it was impractical to continuously measure and process strain. In order to complete this task, parameters had to be set as to what strains and temperatures would be used to develop the relationships.

The 2003 Test Track strain-temperature relationships were developed using only longitudinal strains. When analyzing the data, longitudinal strains were typically larger than transverse strains at the same lateral offset. In another study, Willis and Timm (2008) simulated the effects of wheel wander on strain levels (Figure 6-9). As a truck

133

wandered further from a strain gauge, the transverse gauge consistently experienced
lower strains than its longitudinal counterpart; therefore, the longitudinal gauges were
less influenced by wander and would better represent what is occurring at the base of an
HMA layer under trafficking. Hence, longitudinal strains were used to develop strain-
temperature relationships for the 2006 Test Track.
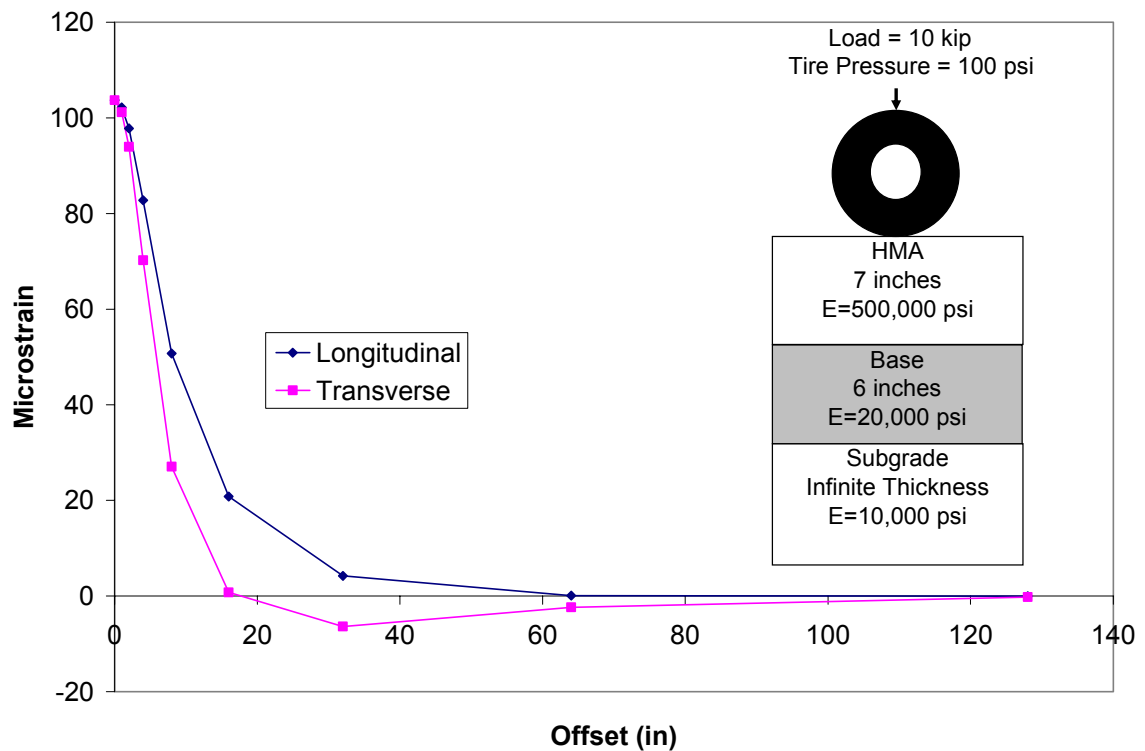
Figure 6-9. Effect of lateral offset on strains.

The next decision as to which strains to use in developing the strain-temperature
relationships was what magnitude strain to incorporate in the analysis. While great care
was taken to ensure only quality data were included in the strain databases, voltage
spikes, faulty gauges, and processing errors occur in data processing. If the maximum
longitudinal strain were chosen to develop the strain-temperature relationships, these
errors might drive the strain temperature relationship development.

134

To determine the appropriate strain choice for the relationships, cumulative strain distributions were developed for each section by day. An example is seen in Figure 6-10. Upon examining three days worth of data, on a day-by-day basis, the 95th percentile strain was determined to be conservative, yet appropriate. The 95th percentile strain would eliminate processing errors and voltage spikes (as seen in the N2 example), but if all the data were captured and processed correctly, the 95th percentile would be close to the maximum strain measurement. Total Access Statistics in Microsoft Access was used to determine the 95th percentile strain for each section by axle type and by day.
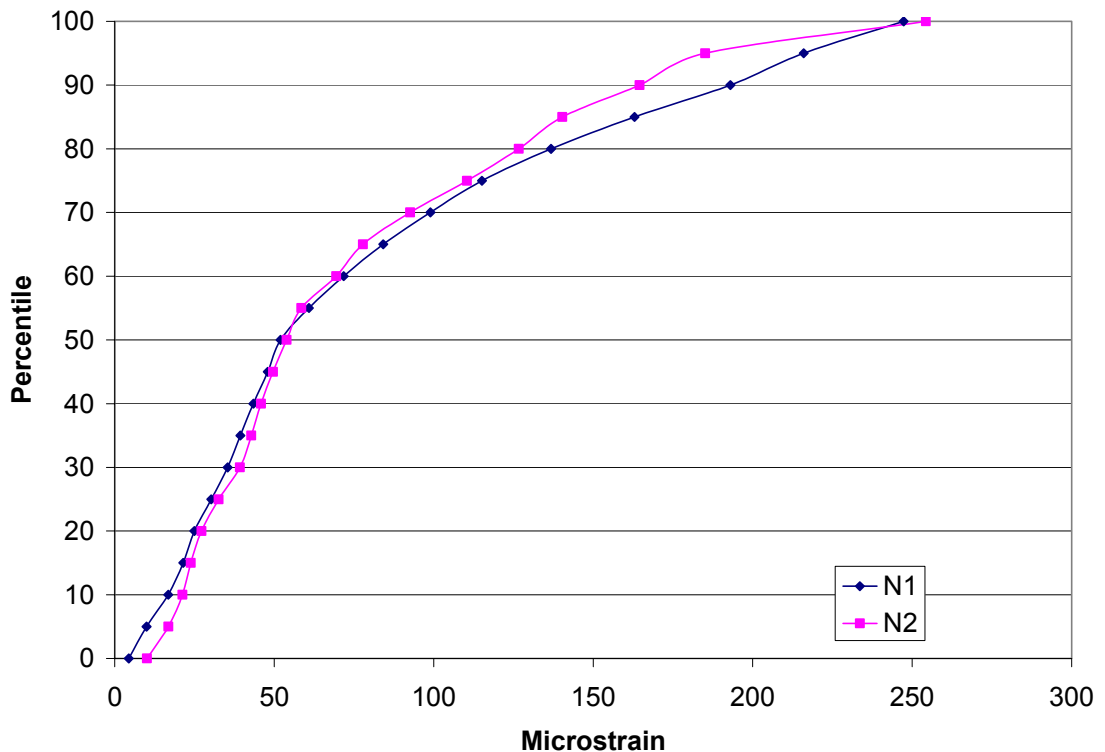
Figure 6-10. Cumulative Distribution of Tandem Strains for November 10, 2006.

Previous researchers at the NCAT Test Track (Priest, 2005) developed strain-temperature relationships based on the mid-depth temperature. To remain consistent with the previous research, the mid-depth temperature was once again used to develop

135

new strain-temperature relationships. The mid-depth temperature was directly measured

in the newly constructed sections (N1, N2, N8, N9, N10, and S11), and linear

interpolation was used to determine the mid-depth temperature for the sections

remaining from the 2003 experiment (N3 and N4).

Figure 6-11 provides the methodology for developing the strain-temperature

relationship. Queries were first developed in Microsoft Access which matched the 95th

percentile strain for each axle and section to the temperature measured at the time of

testing recorded in another database. These matched recordings were then exported to

Microsoft Excel where non-linear regression was used to determine the best relationship

between the 95th percentile longitudinal strain and the mid-depth temperature.

```
┌────────────────────────┐        ┌────────────────────────────┐
│ Determine 95th         │        │ Determine Mid-Depth        │
│ Percentile Strain for  │        │ Temperature for Each Section│
│ Single, Tandem, and    │        │ at Time of Testing         │
│ Steer Axles by Section │        │                            │
└────────────────────────┘        └────────────────────────────┘
               \                    /
                \                  /
              ┌────────────────┐
              │ Microsoft      │
              │ Access/Excel   │
              └────────────────┘
             /        │         \
            /         │          \
┌──────────────┐ ┌──────────────┐ ┌──────────────┐
│ Steer Axle   │ │ Tandem Axle  │ │ Single Axle  │
│ Strain-      │ │ Strain-      │ │ Strain-      │
│ Temperature  │ │ Temperature  │ │ Temperature  │
│ Relationship │ │ Relationship │ │ Relationship │
└──────────────┘ └──────────────┘ └──────────────┘
```
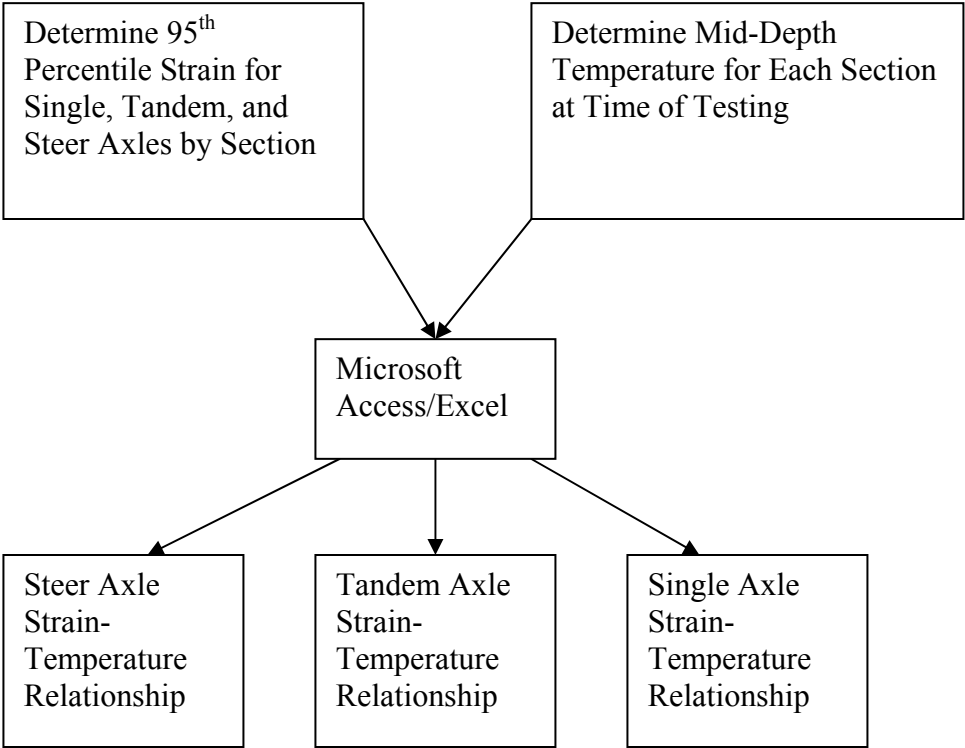
Figure 6-11. Relationship Development Methodology.

In order to determine the best fit equation, Microsoft Excel was used to fit power, exponential and polynomial functions to the data. The exponential equations returned the most consistently high R^2 values. Therefore, equation 6-1 was used as the backbone for the strain-temperature relationships in 2006.

$$\varepsilon = k_1 e^{k_2 T}$$ Equation 6-1

Where: ε = strain, microstrain

k_1 = sectional constant

K_2 = sectional constant

T = temperature, F

Examples of the relationships developed for the steer, tandem, and "best hit" single axle are graphically provided in Figure 6-12, 6-13, and 6-14, respectively. Tables 6-3, 6-4, and 6-5 provide the coefficients for each section's equations and the R^2 values.
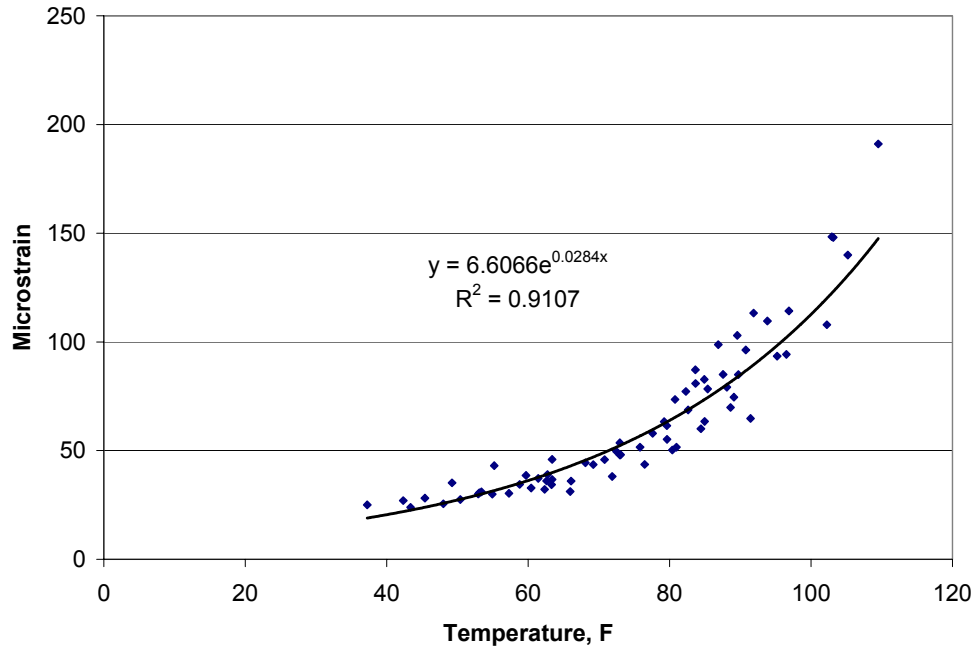
Figure 6-12. Strain-Temperature Relationship for Steer Axles in N9.
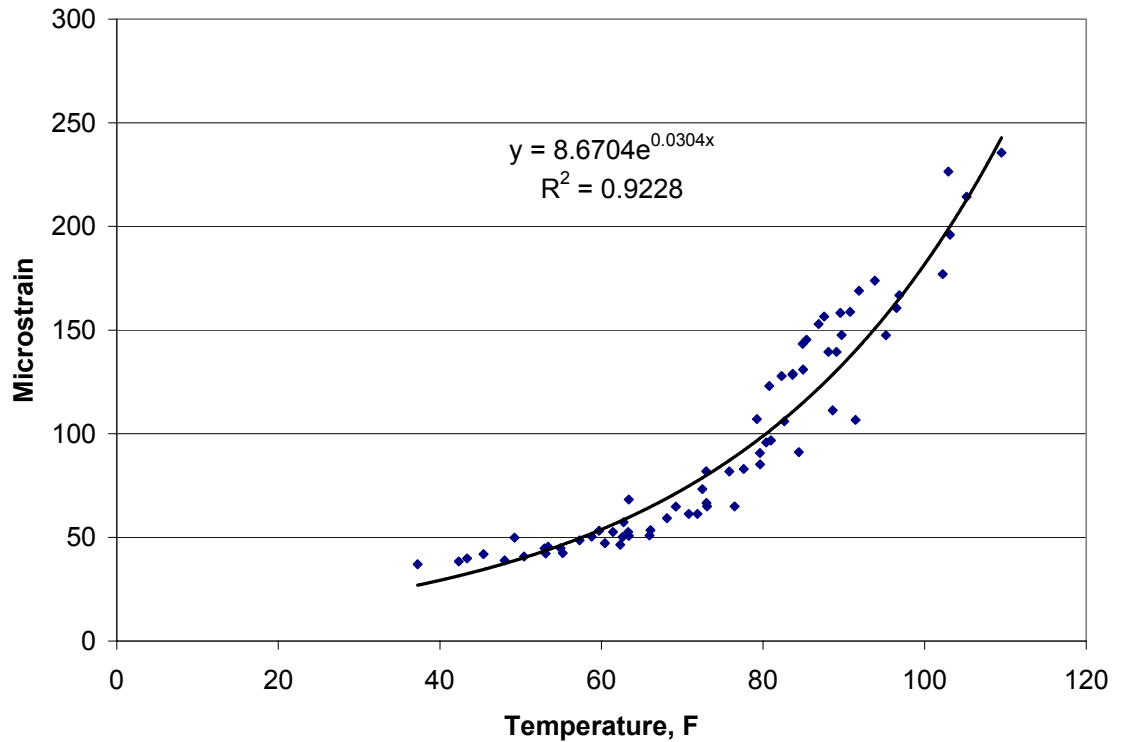
Figure 6-13. Strain-Temperature Relationship for Tandem Axles in N9.
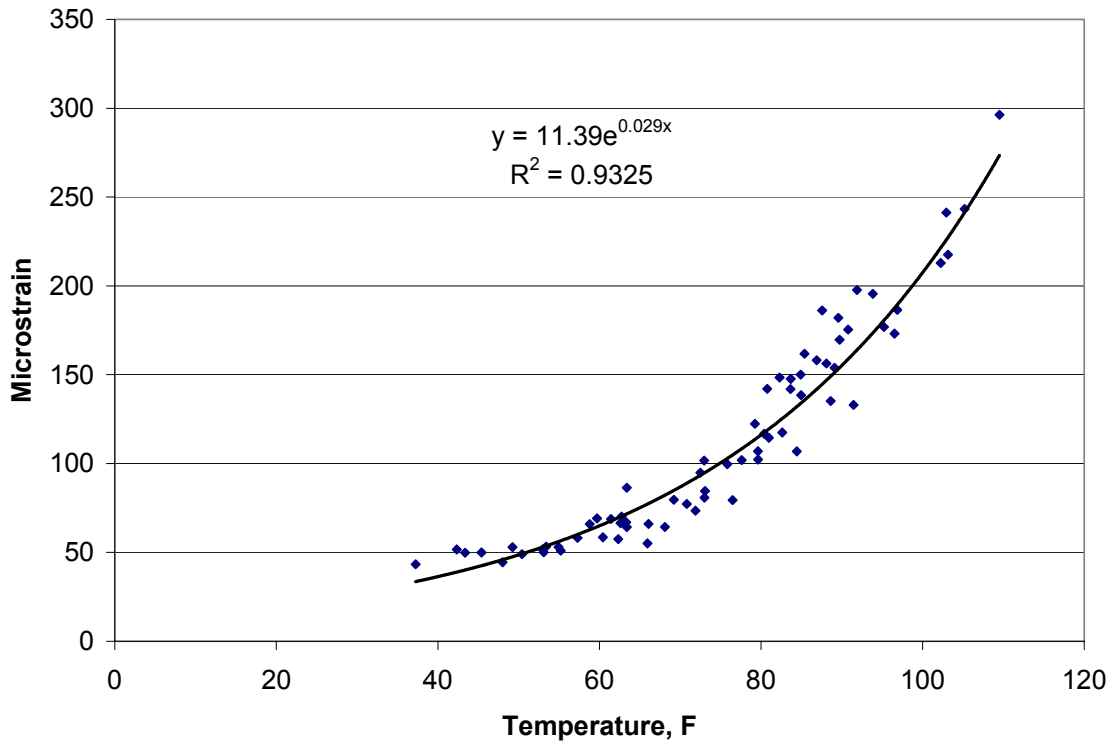
Figure 6-14. Strain-Temperature Relationship for "Best Hit" Single Axles in N9.

Table 6-3. Equation Coefficients by Section for Steer Axles.

Section	k_1	t-stat k_1	k_2	t-stat k_2	R^2
N1	21.580	7.30	0.0272	-3.82	0.84
N2	24.605	7.54	0.0264	-3.45	0.81
N3	10.543	13.15	0.0316	-7.51	0.80
N4	17.631	12.10	0.0225	-5.16	0.79
N8	12.521	12.07	0.0350	-7.51	0.87
N9	6.6066	15.77	0.0284	-8.20	0.91
N10	20.677	11.10	0.0323	-6.62	0.69
S11	14.607	15.87	0.0370	-10.02	0.75

Table 6-4. Equation Coefficients by Section for Tandem Axles.

Section	k_1	t-stat k_1	k_2	t-stat k_2	R^2
N1	46.342	10.20	0.0211	-3.00	0.86
N2	40.794	7.62	0.0236	-3.16	0.82
N3	33.896	16.52	0.0216	-5.80	0.86
N4	33.186	13.93	0.0209	-5.33	0.86
N8	16.995	16.09	0.0341	-9.90	0.96
N9	8.6704	19.60	0.0304	-10.39	0.93
N10	21.737	12.83	0.0349	-8.01	0.85
S11	31.807	20.24	0.0312	-12.21	0.91

Table 6-5. Equation Coefficients by Section for Single Axles.

Section	k_1	t-stat k_1	k_2	t-stat k_2	R^2
N1	45.850	9.71	0.0231	-3.76	0.88
N2	49.126	7.40	0.0226	-2.78	0.80
N3	41.417	21.62	0.0212	-7.55	0.90
N4	41.112	15.13	0.0203	-5.35	0.87
N8	21.169	12.07	0.0319	-7.51	0.96
N9	11.390	20.33	0.0290	-10.38	0.93
N10	31.626	13.11	0.0320	-7.75	0.82
S11	40.070	21.40	0.0293	-12.46	0.90

When looking at the equational coefficients, the thicker sections (N8 and N9) had the lower k_1 values in all three analyses. At lower thicknesses, the k_1 increased somewhat with the exception of S11 which was thinner than N3 and N4; however, these two sections have oxidized and become stiffer over the course of the previous trafficking cycle. The k_2 coefficients in the equation give the slope or rate of strain increase with temperature.

As can be seen in the Tables, sections N3 and N4 have high k1 coefficients; however, the low k_2 coefficient means that strain does not increase much with temperature. The opposite is seen in section N9. The k_1 value is lower than any other section, but it has the one of the highest k_2 values. All three of these sections were free of fatigue cracking. The two sections with the most fatigue cracking (N10 and S11) had comparatively high k_1 and k_2 coefficients; thus, as temperatures increase in these two sections, the strain magnitudes will escalate greatly.

Continuous Pavement Response

To determine the continuous pavement responses, a similar methodology to that outlined in Chapter 5 was followed. The major difference between the two

methodologies was that the 2003 data analyzed strains by truck instead of by axle.

Figure 6-15 outlines that methodology using the strain-temperature relationships for

each section previously developed in this chapter to estimate the strains in the pavement.
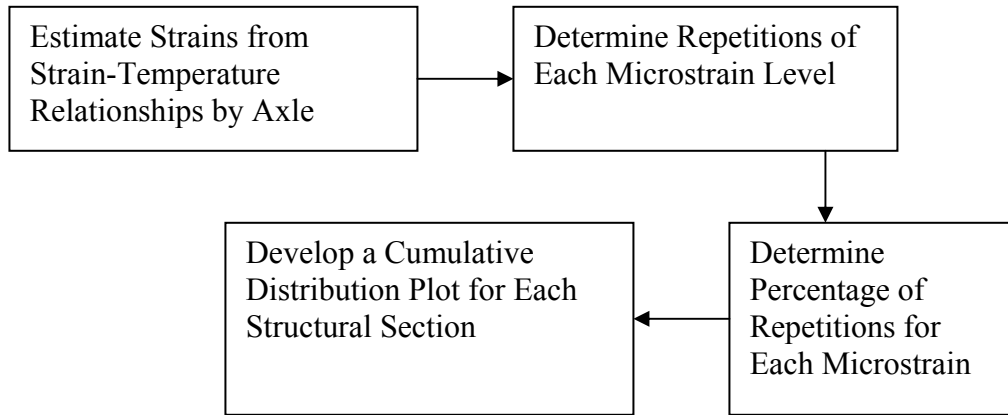
Figure 6-15. Developing Cumulative Strain Distribution Methodology.

Estimating Strains from Strain-Temperature Relationships

To estimate a strain response at the base of the HMA layer in the given test

sections, the methodology prescribed in Figure 6-16 was followed. Microsoft Access

queries matched trafficking data to mid-depth temperature data on an hourly basis.

Once matched, the estimated strains could be calculated using the previously developed

strain-temperature relationships. Table 6-6 gives an example of the estimated strain
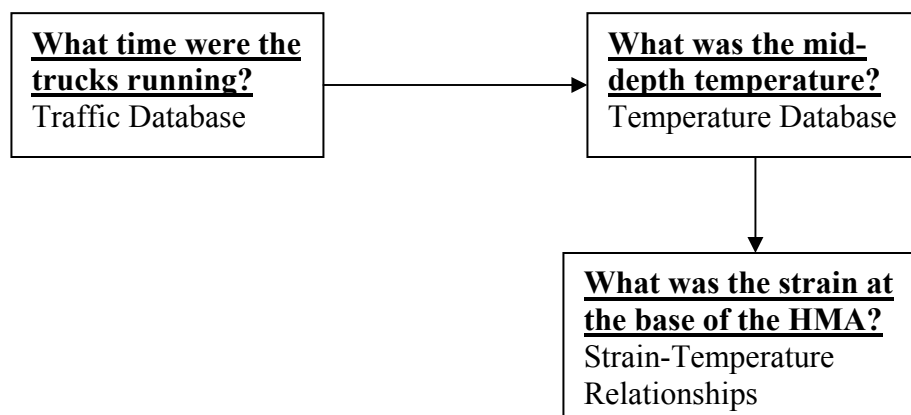
database.

Figure 6-16. Methodology for Estimating Strain.

Table 6-6. Example of Estimated Strain Database.

Section	Date	Hour	T_{mid}	ε_{Steer}	ε_{Tandem}	ε_{Single}
N1	11-10-2006	10	64.2	123.6	179.4	201.8

Developing the strain-temperature relationships by axle allowed for new truck configurations to be included in the track analysis. For example, in the 2003 Test Track analysis, a double trailer had to be considered a triple trailer because there were not relationships developed for it; however, in an axle analysis, the number of single axle repetitions is changed, not the type of vehicle.

This was useful in analyzing the data from both N3 and N4. In the 2003 Test Track analysis, the strains for both N3 and N4 were carried through August 1, 2008 since they had not experienced fatigue cracking at that time. In order to fully capture the strain spectrum of these two sections, the 2003 trafficking data were added to the 2006 data so strains could be estimated through both cycles of testing.

The only concern with going back into the 2003 Test Track was the tandem axle weight. When the box trailer was used in 2003, the axle weights were only between 33

and 34 kips, compared to the 40 kips of the flat-bed trailers. The relationships developed for the 2006 Test Track were based upon 40 kip tandem axles; thus, the strains estimated by the box trailers used in 2003 would be overestimated.

While this might seem important, only 3.5% of the total axles from the 2003 Test Track were box tandem axles. This value would become even smaller with the incorporation of the 2006 data. The tandem axles also typically imposed the second largest strains when it came to axles, singles being the most prolific and having the greatest strains. The result of this overestimation would be a slight shift to the right at the smaller strains in the cumulative distribution graphs between 2003 and 2006. Since this shift occurred in the smaller strains for a minimal percentage of axles, the overestimation did not seem detrimental to the study.

Upon completing the estimation of strains, the strains could be graphically analyzed by hour and day to understand the true temperature susceptibility of the pavement. Figure 6-17 provides a graphical representation of strain over the life of test section N1.   The gaps in the data are Thanksgiving break, Christmas break, and weekends. This section was one of the first sections to exhibit cracking; therefore, the early cut-off date in the graph. Figure 6-18 shows the range of strains on a typical day at the NCAT Test Track for section N1. These strain estimations were used in developing continuous pavement responses for each section.
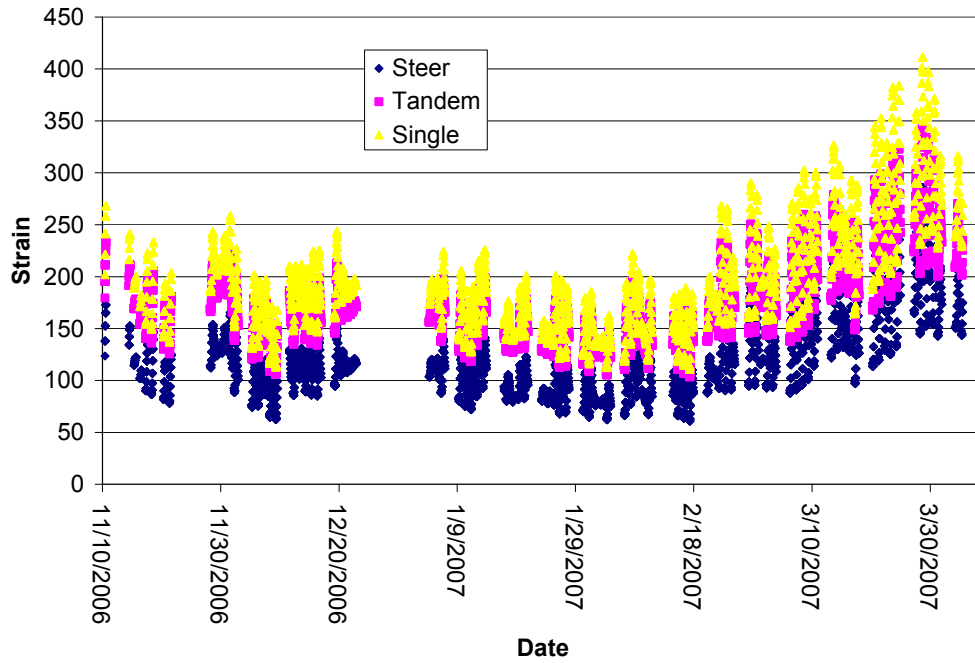
Figure 6-17. Strain by Date for Section N1.
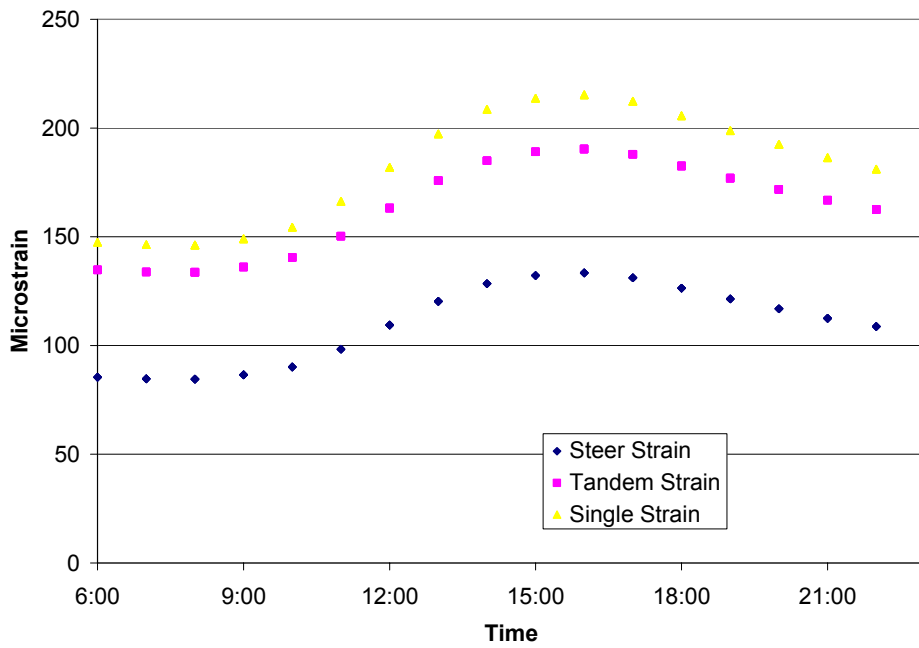
Figure 6-18. Hourly Strain Distribution for Section N1.

Determine Repetitions of Each Microstrain Level

Figure 6-19 graphically portrays the methodology used determine the total number of strain events for each microstrain level. Once strains had been estimated for each mid-depth temperature and linked to a specific truck, queries were developed in Microsoft Access which linked the truck configuration to the truck number and the number of laps completed by that truck. Once the truck configuration was known, the number of axle events could be determined using Table 6-7.

```
┌─────────────────────┐         ┌─────────────────────┐
│ What Is the Truck   │         │ How Many Strain     │
│ Configuration?      │  ────▶  │ Events Occur for    │
│ Traffic Database    │         │ Each Axle?          │
│                     │         │ Tire Events         │
└─────────────────────┘         └──────────┬──────────┘
                                           │
                                           ▼
┌─────────────────────┐         ┌─────────────────────┐
│ How Many Laps Did   │         │ How Many Axle       │
│ Each Truck Complete │  ────▶  │ Events for Each     │
│ in an Hour?         │         │ Truck at Each       │
│ Traffic Database    │         │ Strain Magnitude?   │
│                     │         │                     │
└─────────────────────┘         └──────────┬──────────┘
                       ┌──────┘            │
┌─────────────────────┐│        ┌──────────▼──────────┐
│ What Is the Strain  ││        │ What Is the Total   │
│ Magnitude?          ││        │ Number of Strain    │
│ Previously Estimated│         │ Repetitions for Each│
│ Strains             │         │ Strain Magnitude at │
│                     │         │ Each Hour by Axle   │
│                     │         │ Type?               │
└─────────────────────┘         └─────────────────────┘
```

Figure 6-19. Strain Repetition Flowchart.

145

Table 6-7. Strain Events Per Truck by Axle Type.

Truck Type	Steer Events	Tandem Events	Single Events
Single Box	1	4	0
Single Trailer	1	2	1
Double Trailer	1	2	3
Triple Trailer	1	2	5

Having determined the number of strain events per truck, the number of strain events for each axle was multiplied by the number of laps to determine the total number or strain repetitions for each axle type. For example, if a double trailer completed 13 laps in one hour, this would account for 13 steer events, 26 tandem events, and 39 single axle events. These data were matched with the previously estimated strains to determine the number of strain events at each microstrain level. An example of how the database was managed is seen in Table 6-8.

Table 6-8. Strain Repetitions Example.

Truck	Laps	Steer Strain	Steer Reps	Tandem Strain	Tandem Reps	Single Strain	Single Reps
Double	13	100	13	200	13	300	39
Triple	26	120	26	220	26	320	130

Determine Percentages of Each Microstrain Level

After the total number of strain repetitions imposed by each axle type every hour was calculated, the percentage of total strain repetitions at each microstrain magnitude needed to be determined. This was completed by dividing the number of total strain repetitions by axle each hour into the total number of strain repetitions over the entire life of the pavement. The life of the pavement was defined as from construction until crack visualization.

An example of how the percentages were calculated is provided in Table 6-9. The values used in the example are not those found in the study due to enormity of the total number of strain repetitions encountered in this analysis phase.

Table 6-9. Example Strain Percentage Table.

Strain Magnitude	Strain Repetitions	Percentage (%)
100	13	5.3
120	26	10.5
200	13	5.3
220	26	10.5
300	39	15.8
320	130	42.1
Total	247	100.0

Determining the Cumulative Distribution of Strains

To create a cumulative distribution for the estimated strain values, the strains were sorted by strain magnitude in ascending order. At this point, a running sum of the percentage column was calculated to determine the percentiles associated with each strain magnitude. The previously used example is expanded upon in Table 6-10 to develop its cumulative distribution function.

Table 6-10. Example Strain Percentage Table.

Strain Magnitude	Strain Repetitions	Percentage (%)	CDF (%)
100	13	5.3	5.3
120	26	10.5	15.8
200	13	5.3	21.1
220	26	10.5	31.6
300	39	15.8	47.4
320	130	52.6	100.0
Total	247	100	

Once the cumulative distributions were determined for each structural section, the 1st, 99th, and every 5th percentile were manually picked from the completed

spreadsheets to develop cumulative distribution plots. Figure 6-20 and Table 6-11

provide the cumulative distribution functions by section both graphically and

numerically.
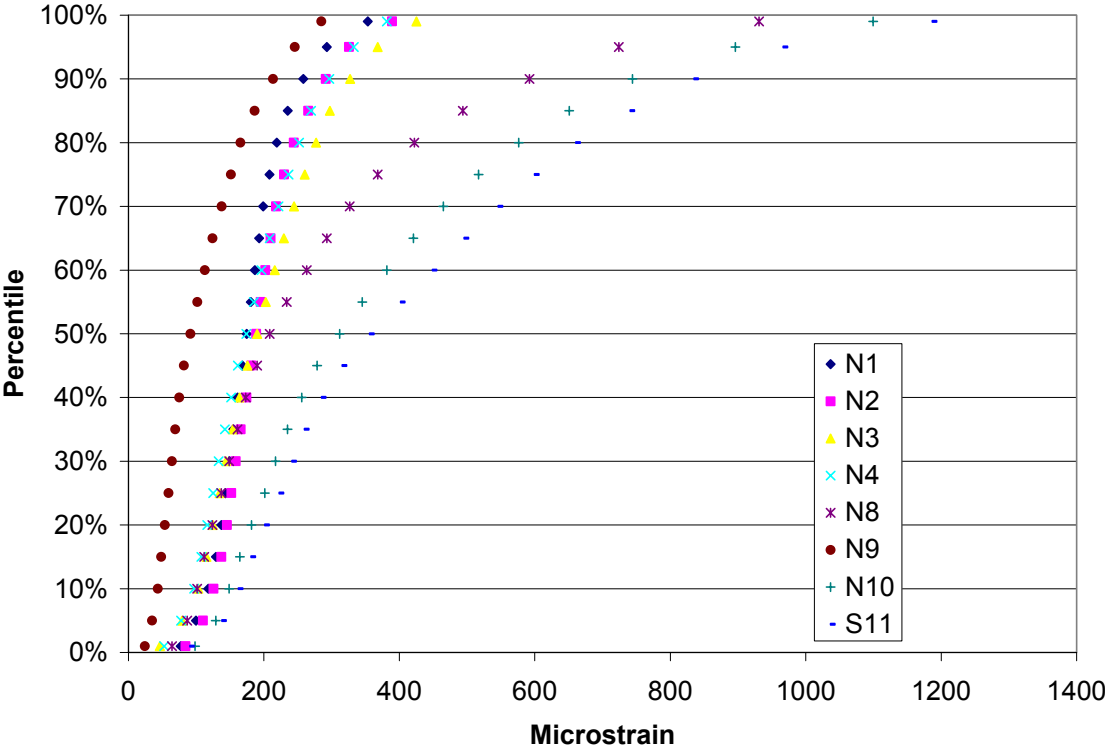
Figure 6-20. Cumulative Distribution of Strains for 2006 Structural Sections.

148

Table 6-11. Cumulative Distribution of Strains for 2006 Structural Sections.

Percentile	N1	N2	N3	N4	N8	N9	N10	S11
99%	353	389	425	381	931	285	1100	1187
95%	293	326	368	333	724	246	896	967
90%	258	291	327	296	592	214	744	835
85%	235	265	298	270	494	186	651	741
80%	219	244	277	252	422	166	576	661
75%	208	230	260	236	368	151	517	600
70%	199	218	244	221	327	138	465	546
65%	193	210	229	209	293	124	421	496
60%	187	202	216	197	263	113	382	449
55%	181	195	203	185	234	102	345	402
50%	175	189	190	174	208	92	312	356
45%	168	181	176	162	190	82	279	316
40%	161	175	164	152	173	75	256	285
35%	155	166	154	142	161	69	235	260
30%	149	158	144	133	149	64	217	242
25%	143	152	135	125	137	59	201	223
20%	137	145	125	116	124	54	182	201
15%	129	137	115	108	112	49	165	181
10%	118	126	103	97	101	43	149	163
5%	100	110	79	78	87	35	129	138
1%	77	84	46	53	64	24	98	91

RESULTS AND CONCLUSIONS

When comparing the strain distributions of the 2006 Test Track, there is a clear distinction between sections that were resistant towards fatigue cracking and those that were not. Three of the eight analyzed sections experienced fatigue cracking (N8, N10, and S11). Section N1 and N2's experiments were cut-off early because of observed cracking; however, forensic investigations have shown that the cracking experienced in these two sections were top-down cracking and not bottom-up fatigue. The three other sections (N3, N4, and N9) have not experienced bottom-up cracking at this point.

The two sections that failed early in fatigue (N10 and S11) had strain profiles that behaved very similarly. Even at the 5th percentile strain, both sections have strain

measurements above 125 microstrain, and the values continue to escalate from that point.

Section N8 is another section that eventually experienced fatigue cracking. Unlike sections N10 and S11, N8's early strain profile reflects those of the non-cracked sections very well. Section N8 was specifically designed to perform in a perpetual manner; however, while thick, it was also built on a very poor subgrade material which may have influenced the structure's ability to disperse strain. At the 50th percentile strain, there is a 20 microstrain difference between this section and the maximum strain value of a section that did not experience fatigue cracking. As the percentiles get closer to the 99th, these discrepancies continue to increase.

The remaining five sections did not experience bottom-up fatigue cracking during the 2006 trafficking cycle. Sections N3 and N4 were two test sections that experienced 19 million ESALs of traffic without showing signs of fatigue damage. These two sections had the highest strains of the non-cracked sections under the most traffic.

N9, the fourteen inch perpetual section, experienced the lowest strain values of any section during the 2006 Test Track. N1 and N2 followed N9 in low strain values, but these strain profiles were based on minimal data due to early top-down cracking. Since N1 and N2 had strain profile below those of N1 and N2, these sections would not have failed due to bottom-up fatigue cracking.

If one were to compare the cracked profiles versus the non-fatigue cracked profiles, a clear breakpoint occurs around the 45th percentile. At this point, the cracked sections begin to diverge greatly from the non-cracked sections. N3 and N4's strain

150

profiles represent the least conservative strain profiles that were able to withstand trafficking without fatigue cracking. These two sections have also received double the traffic of any other section in the 2006 study. Therefore, these two sections should be considered when determining the uppermost bound for a field-based measured fatigue threshold.

SUMMARY

Once again, distinct differences were found in the cumulative distribution plots of the sections that cracked and those of the uncracked sections. Three sections (N3, N4, and N9) remained in-tact for at least 9 million ESALs. These sections all exhibited lower strains at the upper ends of their cumulative strain distributions. The breakpoint occurred at approximately the 45th percentile strain.

At this point, cumulative strain distributions had been developed for 21 test sections at the Test Track over three cycles of testing. These plots needed to be compared to each other across all 21 test sections to develop strain criteria for perpetual pavements. These distributions also needed to be compared to laboratory fatigue thresholds to determine if a relationship between the two could be developed.

CHAPTER SEVEN

RESEARCH FINDINGS

INTRODUCTION

This chapter presents two different data comparison analyses that were conducted on the data developed from each Test Track experimental cycle. The first procedure compares the strain distributions developed from the previously mentioned methodologies to laboratory fatigue endurance limits tested under the National Cooperative Highway Research Program's (NCHRP) Project 9-38. The second data analysis procedure compares all three sets of cumulative distributions to each other to create acceptable measured strain criteria for perpetual pavement design.

LABORATORY TESTING

In association with NCHRP Project 9-38, fatigue testing was conducted on the base mixes from the structural sections at the 2003 NCAT Test Track. Beam fatigue specimens were created using the average gradation and asphalt contents of the 19.0 mm mixes. As previously seen in Chapter 4, two different mixes were used as the base HMA layers in the first seven sections of the 2003 experiment. Therefore, only two mixes were tested to characterize all seven test sections. The tests used samples compacted to 7% air voids at the optimum asphalt content. The precise methodologies

used for the testing are documented elsewhere (Prowell et al., 2008).The fatigue

endurance limits and their 95% lower bound confidence limits are presented in Table 7-

1. These results were extrapolated from laboratory testing using a Three-Stage Weibull

equation (Prowell et al., 2008).

Table 7-1. Fatigue Endurance Limits for 2003 Test Sections.

Section	Average Extrapolated Beam Fatigue, με	95% Confidence Lower Bound, με
N1	220	146
N2	172	151
N3	172	151
N4	220	146
N5	220	146
N6	172	151
N7	172	151

LABORATORY TESTING AND FIELD DATA COMPARISON

One of the goals of this research was to determine if a relationship existed

between the laboratory fatigue endurance limits determined under NCHRP 9-38 and the

cumulative strain distributions developed in the previous chapters. This was

accomplished using three phases of data comparisons.

The first phase was conducted by comparing the endurance limit to a strain

calculated using the strain-temperature equations developed in Chapters 5 and 6. The

comparison temperature was the prescribed testing temperature for AASHTO T321.

The second phase compared the magnitude of the laboratory fatigue threshold

data to measured field strain distributions. The 95th percentile confidence interval lower

bound strain was graphically inserted onto a cumulative distribution plot to determine

where this value fell on each section's cumulative strain distribution, and that value was compared to the section's fatigue performance.

The final analysis comparison between the laboratory fatigue thresholds and the developed strain distributions was conducted by comparing the 95th percentile confidence interval lower bound to the entire strain distribution. A fatigue ratio, between the measured strain values and laboratory-established threshold, was developed to make this comparison.

The 95% confidence interval lower bound was chosen to be the basis of comparison between the laboratory fatigue and field strain data. 220 $\mu\varepsilon$, the predicted average beam fatigue value for the PG 76-22 binder mix, was more than double the previously listed fatigue limits in mixes. This value might be due to a high reading or an erroneous test; therefore, it was felt that using the 95% confidence lower bound was more appropriate for comparisons. The 95% confidence interval lower bound also brought the inclusion of mix variability to the analysis; therefore, it proved to be a more conservative estimate of the fatigue threshold.

Phase One – Comparison of Fatigue Threshold to Modeled Strain Levels

The fatigue tests were conducted at 20°C (68°F). Comparative inquiries were conducted to calculate the estimated strains at the test temperature for both the 2003 and 2006 Test Tracks using the strain-temperature relationships previously developed and discussed in Chapters 5 and 6. These strains are presented in Table 7-2.

154

Table 7-2. Strains at 20°C Estimated from Predicted Fitted Models.

Section (Year)	Strain at 20°C		
	Box, με	Triple, με	
N1 (2003)	NA	363	
N2 (2003)	142	231	
N3 (2003)	103	153	
N4 (2003)	87	140	
N5 (2003)	99	172	
N6 (2003)	165	210	
N7 (2003)	111	159	
	Steer, με	Tandem, με	Single, με
N1 (2006)	137	195	221
N2 (2006)	148	203	228
N3 (2006)	90	147	175
N4 (2006)	81	137	163
N8 (2006)	135	173	185
N9 (2006)	46	69	82
N10 (2006)	186	233	279
S11 (2006)	181	265	294

When analyzing the 2003 Test Track estimated strain relationships, one would see that at 20°C, five of the six section's average box trailer produced a microstrain magnitude below its lower confidence limit fatigue threshold. However, when the heavier triple trailers were considered, six of the seven test sections were above the 95th percentile threshold strain. While two (N3 and N4) of the 2003 test sections did not fail in fatigue, one of these two sections had a strain magnitude larger than its fatigue endurance limit confidence limit at the associated test temperature.

While fatigue testing has not been conducted on the base HMA layers of the 2006 Test Track at this time, if one were to assume similar lower bounds for the fatigue thresholds (i.e. 150 microstrain) for these sections, a similar trend would be seen. Only

two sections (N10 and S11) experienced higher strains than the lower bound fatigue limit under the steer axle. The three sections that did not crack were at least 60 microstrain below this value for their steer axles. However, when analyzing the 40 kip tandem axle at the test temperature, the only sections still below the estimated lower bound fatigue endurance limit were the three sections that did not crack (N3, N4, and N9).

A final look at the single axles for the 2006 Test Track shows seven of the eight sections measuring strains higher than the lower bound fatigue endurance limit. The only section measuring strain amplitudes below this value is section N9 which was 14 inches thick. To understand this phenomenon, one would only have to look back to the strain-temperature relationships developed for this section. Both the k_1 and k_2 values were small compared to the other sections. This showed that section N9, unlike many of the others, did not experience as much strain variation due to temperature.

Phase One - Analysis Results

No clear relationship could be developed between the 95th percentile confidence interval lower bound, the computed strain at 20 °C, and pavement performance. There were cases where test sections (N3) did not fatigue crack; however, their average strain for the triple trailer at laboratory testing temperature was above the designated fatigue threshold. Further investigations needed to be conducted to develop the link between laboratory fatigue thresholds, measured field strains, and pavement performance.

156

Phase Two – Location of Fatigue Thresholds on Cumulative Distribution Plots

Another method for comparing the laboratory fatigue thresholds to the previously developed strain data was to superimpose the 95th percentile confidence interval lower bound strain onto each section's cumulative strain distribution. The cumulative distributions and fatigue threshold for the PG 67-22 mix are shown in Figure 7-1 while Figure 7-2 shows the data for the PG 76-22 mixes.
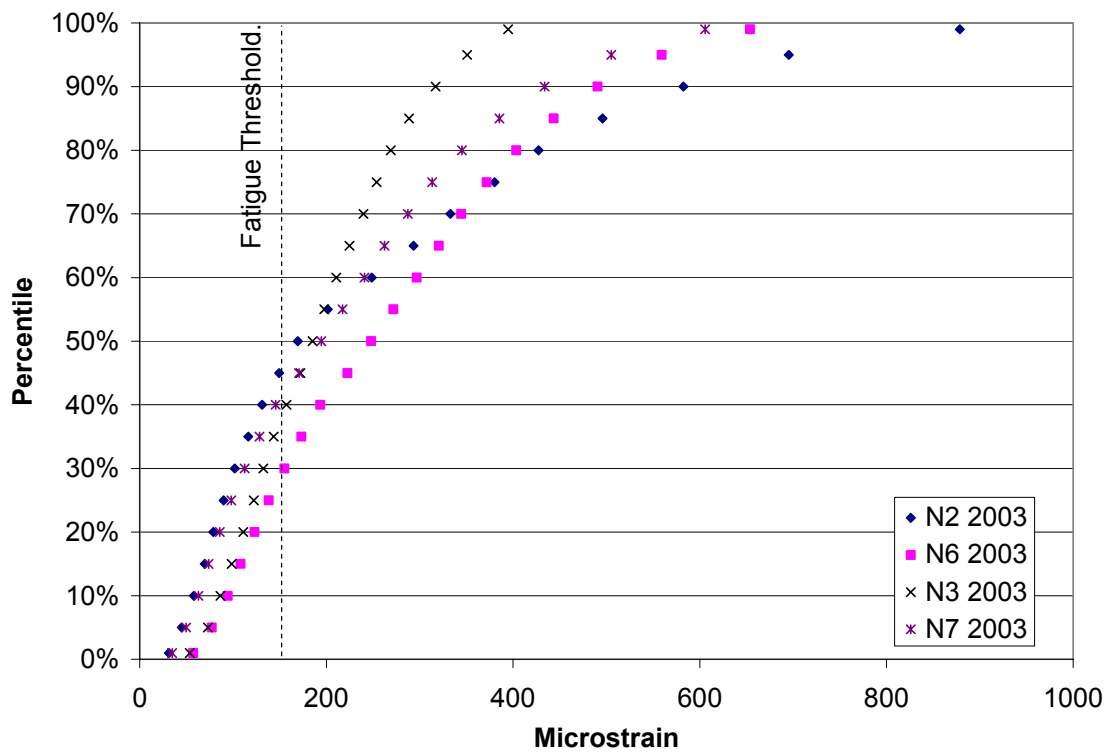
Figure 7-1. Endurance Limits for PG 67-22 Mix.
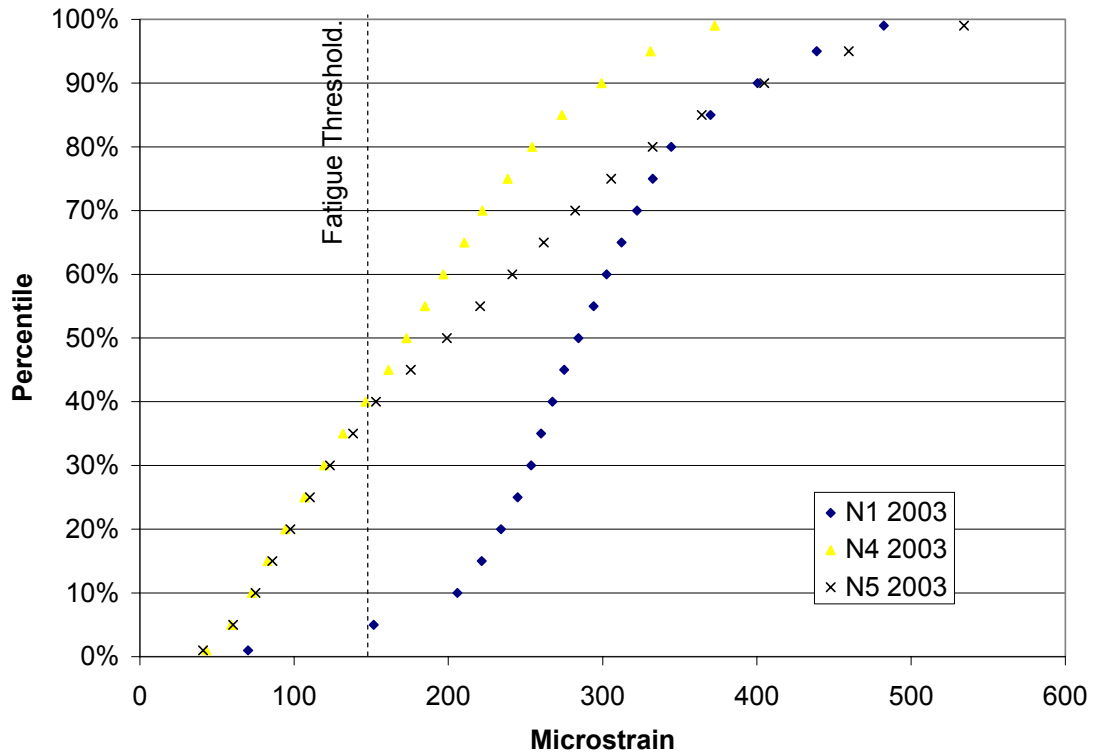
Figure 7-2. Endurance Limits for PG 76-22 Mix.

When comparing the 2003 strain distributions with their lower bound fatigue limit, it was difficult to find a relationship between the laboratory and field data using this methodology. As can be seen, there is no clear correlation between the lab fatigue threshold, where this threshold occurs on the strain distribution, and the section's performance.

For example, Section N4 in 2003 had 40% of its strains below the given laboratory fatigue threshold, and it performed well in the field. Conversely, section N2 had 45% of its strains below the laboratory fatigue threshold, but it failed quickly due to fatigue cracking.

Both base HMA mixes for the 2003 Test Track had similar fatigue properties (i.e. fatigue thresholds near 150 με). Since fatigue data had not been developed from the

2006 Test Track's base mixes, it was assumed that these mixes had similar fatigue properties for continuation of the analysis. Figure 7-3 displays these data.

The 2006 data finds similar discontinuities between the field and laboratory using this methodology. N2 experienced no fatigue cracking; however, it had fewer strains measured below its fatigue threshold than did section N8 which experienced fatigue distress.
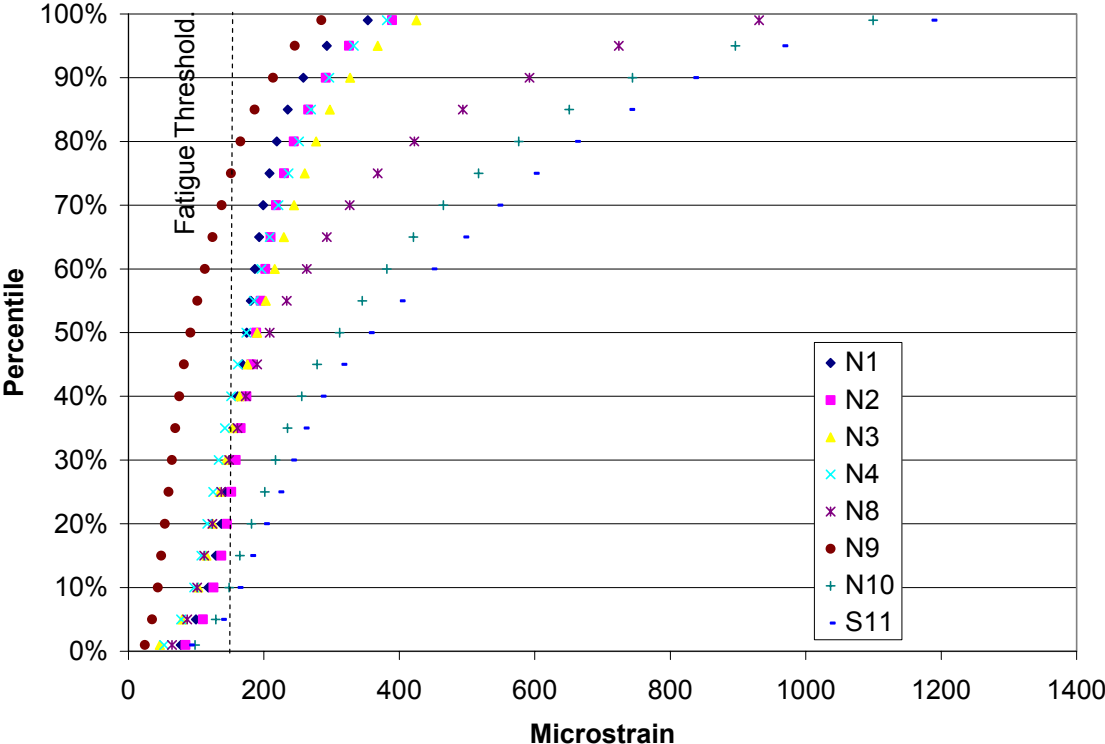
Figure 7-3. Endurance Limits for 2006 Test Sections.

Phase Two – Analysis Results

It was the desire of this research to determine if a relationship existed between the laboratory fatigue thresholds, the measured strain data, and pavement performance. In order to correlate these three parameters together for comparison across the analyzed test sections, Table 7-3 was developed.

Table 7-3. Comparison of Cumulative Strain Distribution and 95% Confidence Interval Lower Bound.

Section	Percentile of Fatigue Threshold	Performance
N1 2003	8th	Fatigue cracked
N2 2003	45th	Fatigue cracked
N3 2003	57th	No cracking
N4 2003	40th	No cracking
N5 2003	37th	Fatigue cracked
N6 2003	29th	Fatigue cracked
N7 2003	42nd	Fatigue cracked
N1 2006	31st	Top-down cracking
N2 2006	22nd	Top-down cracking
N3 2006	33rd	No cracking
N4 2006	38th	No cracking
N8 2006	31st	Fatigue cracked
N9 2006	74th	No cracking
N10 2006	11th	Fatigue cracked
S11 2006	8th	Fatigue cracked

As seen in this table, there is no correlation between the percentile where the fatigue threshold occurred along a section's cumulative distribution and its fatigue performance; however, a trend was noticed in certain cumulative strain distributions.

If one were to specifically compare N2 and N4 from 2003 again, no correlation between the locations of the fatigue threshold on their cumulative strain distributions and performance could be developed. However, above the fatigue threshold, N2's strain distribution begins to flatten out while N4's strain distribution continues on a gradual slope. Since the lower strains were similar between the two sections, it seemed the

160

strains above the fatigue threshold contributed to the deterioration of section N2. This makes sense since one would expect that higher strains contribute more to pavement damage. Therefore, a third analysis phase was developed to try to bridge the laboratory and field data using the entire cumulative distribution rather than just particular points on the distribution.

Phase Three – Ratio Comparison

While the two previous phases this research analysis did not find any relationship between field and laboratory fatigue data, both analysis procedures were limited to one point either on the cumulative strain distribution or on the strain-temperature relationship curves. The third phase of comparisons included comparing the entire cumulative strain distribution of each section to the fatigue threshold by the use of a fatigue ratio (Equation 7-1). The fatigue ratio is a way to express how far the strain distribution extends above the fatigue threshold.

$$R_n = \frac{\varepsilon_n}{\varepsilon_f}$$

(Equation 7-1)

Where: R_n = ratio at the nth percentile

E_n = strain at the nth percentile, microstrain

ε_f = fatigue threshold, microstrain

This ratio was calculated for each test section from the 50th to the 99th percentile on a 5 percent increment. These ratios are tabulated in Tables 7-4 and 7-5. The sections that did not experience fatigue cracking are italicized.

161

Table 7-4. Ratio by Percentile for 2003 Test Sections.

Percentile	N1 2003	N2 2003	N3 2003	N4 2003	N5 2003	N6 2003	N7 2003
99%	3.22	5.86	2.63	2.48	3.56	4.36	4.04
95%	2.93	4.64	2.34	2.21	3.06	3.73	3.37
90%	2.67	3.88	2.11	2.00	2.70	3.27	2.89
85%	2.47	3.31	1.92	1.82	2.43	2.96	2.57
80%	2.30	2.85	1.79	1.70	2.22	2.69	2.30
75%	2.22	2.53	1.69	1.59	2.04	2.48	2.09
70%	2.15	2.22	1.60	1.48	1.88	2.30	1.91
65%	2.08	1.96	1.50	1.40	1.75	2.14	1.75
60%	2.02	1.66	1.40	1.31	1.61	1.98	1.60
55%	1.96	1.34	1.32	1.23	1.47	1.81	1.45
50%	1.90	1.13	1.23	1.15	1.33	1.65	1.30

Table 7-5. Ratio by Percentile for 2006 Test Sections.

Percentile	N1 2006	N2 2006	N3 2006	N4 2006	N8 2006	N9 2006	N10 2006	S11 2006
99%	2.36	2.60	2.83	2.54	6.21	1.90	7.33	7.91
95%	1.95	2.17	2.45	2.22	4.83	1.64	5.97	6.45
90%	1.72	1.94	2.18	1.98	3.95	1.42	4.96	5.57
85%	1.57	1.77	1.98	1.80	3.29	1.24	4.34	4.94
80%	1.46	1.63	1.85	1.68	2.82	1.10	3.84	4.40
75%	1.39	1.53	1.74	1.58	2.45	1.01	3.45	4.00
70%	1.33	1.45	1.63	1.48	2.18	0.92	3.10	3.64
65%	1.29	1.40	1.53	1.39	1.95	0.83	2.80	3.30
60%	1.24	1.35	1.44	1.31	1.76	0.75	2.54	2.99
55%	1.21	1.30	1.35	1.23	1.56	0.68	2.30	2.68
50%	1.16	1.26	1.27	1.16	1.39	0.61	2.08	2.37

It was seen that a distinct difference was found between the ratios of the sections that failed and the ratios of those that did not. At the 99th percentile, all the sections exhibiting fatigue cracking had ratios greater than 3.2, and the sections that performed well were all under 2.85. This gap between the ratios of cracked and uncracked sections continues until the 55th percentile.

Phase Three – Analysis Results

Based upon these limited data, it is proposed that control points could potentially be set along strain distributions using the fatigue ratio to help eliminate fatigue cracking

during perpetual pavement design. These control points (Table 7-6) were based upon the section that remained in-tact while returning the highest fatigue ratio during the 2003 and 2006 Test Track analyses (i.e., N3 using the by truck analysis).

Table 7-6. Fatigue Control Points for Fatigue Crack Prevention.

Percentile	Maximum Fatigue Ratio
99%	2.83
95%	2.45
90%	2.18
85%	1.98
80%	1.85
75%	1.74
70%	1.63
65%	1.53
60%	1.44
55%	1.35
50%	1.27

Laboratory Versus Field Summary

While it was difficult to determine a relationship between the laboratory fatigue threshold, field pavement responses, and pavement performance using just one location on either a strain distribution or strain-temperature model, it was possible to propose a new perpetual pavement design concept using the entire strain distribution as a basis for comparison. While more data are needed from differing mix designs to validate the concept of a fatigue ratio, data from the 2003 and 2006 Test Tracks support the concept of using control points set by multiples of the laboratory fatigue 95th percentile confidence interval lower bound to govern fatigue design.

FATIGUE CRITERIA ANALYSIS

The primary objective for this research was to recommend strain criteria to control fatigue cracking in perpetual pavements; therefore, the final analysis for this dissertation involved setting these criteria based on strain values from three cycles of testing at the Test Track. In the 2000 Test Track, no fatigue cracking was seen; however, the strains at the bottom of the HMA were estimated to be extremely low. Both the 2003 and the 2006 Test Track experiments, some of the thinner test sections proved to be less resistant to fatigue cracking; however, test sections were still built thinner than 24 inches and resisted fatigue distresses. Figure 7-4 displays cumulative strain distributions from all three test cycles. Only one section from the 2000 Test Track was chosen for display due to the comparatively low strains. The 2000 Test Track sections proved to be overdesigned for fatigue cracking which was the original intention of the 2000 test sections.

Table 7-7 describes the performance of each section shown in Figure 7-4. N3 and N4 2003 designate the cumulative distributions developed using the methodology for that particular experiment (i.e., strains based on complete truck passes). N3 and N4 2006 were developed on an axle-specific basis. Figure 7-5 describes the methodology used in developing strain criteria for this analysis.
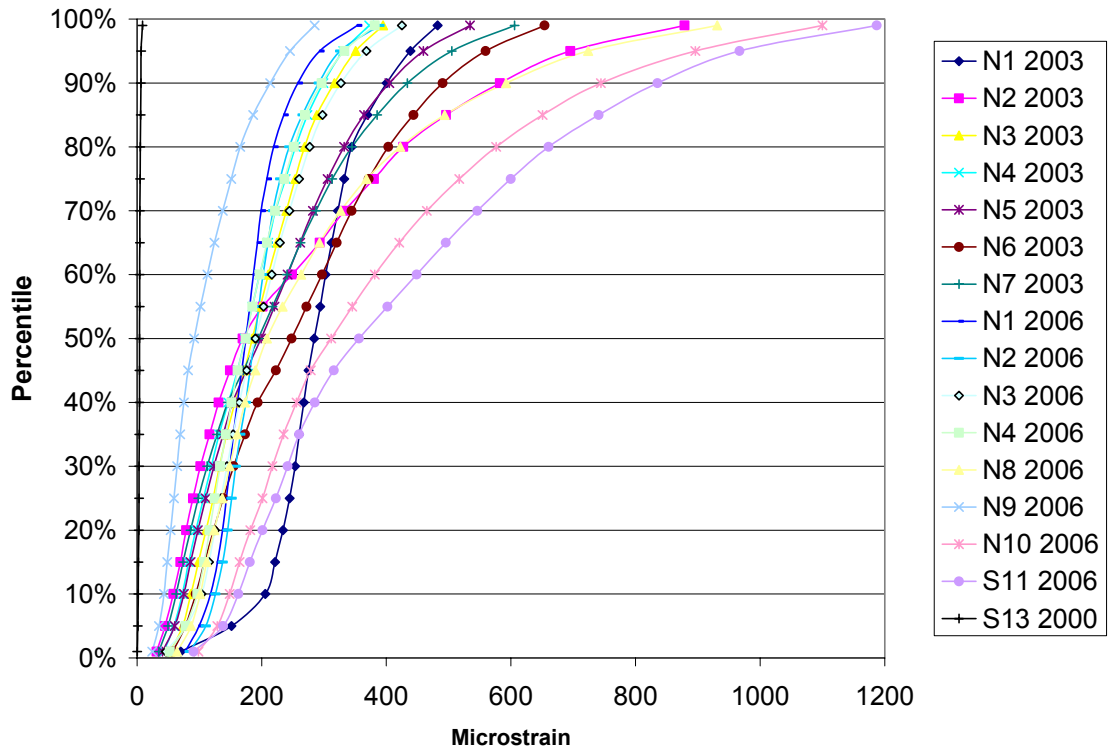
Figure 7-4. Cumulative Distributions from Three Test Cycles.

Table 7-7. Section Performance.

Section	Performance
S13 2000	Did not crack
N1 2003	Fatigue cracking
N2 2003	Fatigue cracking
N3 2003	Did not crack
N4 2003	Did not crack
N5 2003	Fatigue cracking
N6 2003	Fatigue cracking
N7 2003	Fatigue cracking
N1 2006	Top-Down cracking
N2 2006	Top-Down cracking
N3 2006	Did not crack
N4 2006	Did not crack
N8 2006	Fatigue cracking
N9 2006	Did not crack
N10 2006	Fatigue cracking
S11 2006	Fatigue cracking

| **Are There differences between the pavement responses of fatigue cracked sections and non-fatigue cracked sections?** |
| Compare Cumulative Distributions Developed in Chapters 4, 5, and 6 |

| **If differences can be found, what sections are appropriate for use in developing strain criteria for perpetual pavements?** |
| No Fatigue Cracking |
| Extended Trafficking |
| Not Overdesigned |

| **Can one strain distribution be developed as a criteria for perpetual pavement design?** |

Figure 7-5. Strain Criteria Development Methodology.

Cracked Versus Uncracked Comparisons

Comparisons were made between the cracked and non-cracked sections, and it was discovered that deviations between cracked and uncracked sections strain profiles occur after approximately the 55th percentile. Beyond this percentile, the fatigue cracked sections always exhibited a higher strain level.

Figures 7-6 and 7-7 provide two different graphical representations of this breakpoint and the differences seen between the cracked and uncracked strain profiles. The first figure (7-6) shows the highest strain at each percentile for the non-fatigue cracked sections and the lowest strain at each percentile for the fatigue cracked sections (i.e., the worst of the un-cracked sections and the best of the cracked sections).   As one can see, the strains for the fatigued sections were continually below those that did not

experience fatigue cracking until approximately the 55th percentile. The second figure

shows the same data in a different way. Figure 7-6 shows the difference between the

maximum strain from the non-fatigue cracked sections and the minimum strain from the

fatigue cracked sections for each percentile (i.e., the difference between the squares and

diamonds in Figure 7-5). One sees that the cracked strains exceed the non-cracked

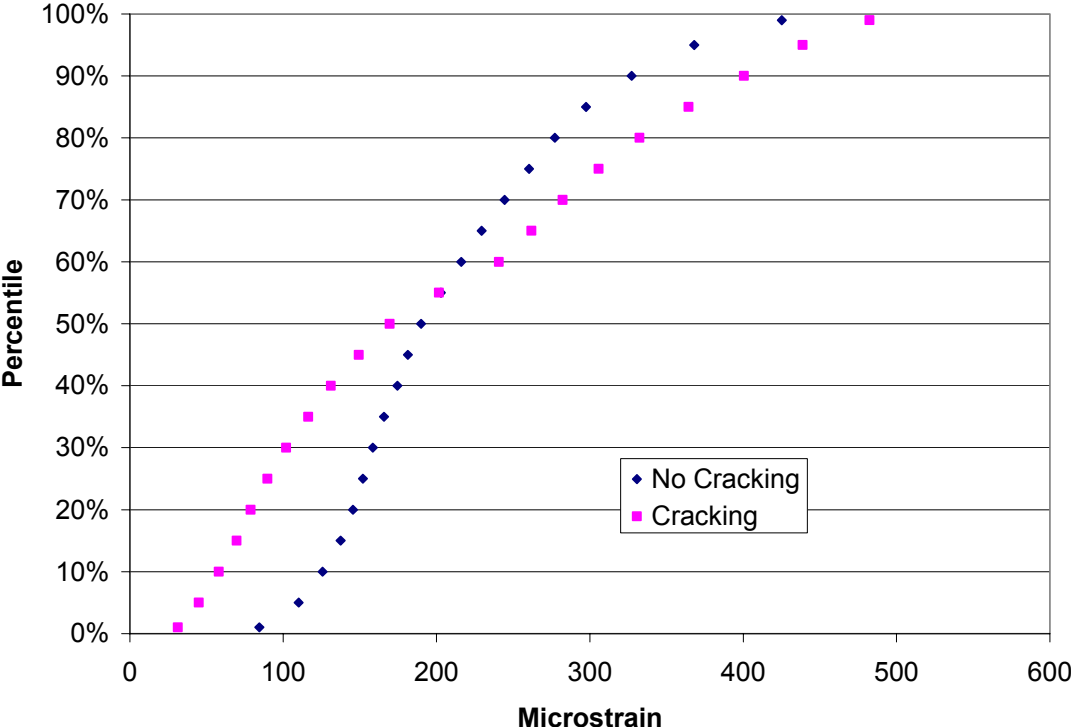strains permanently after approximately the 55th percentile.

Figure 7-6. Highest Uncracked Strain Versus Lowest Cracked Strain.
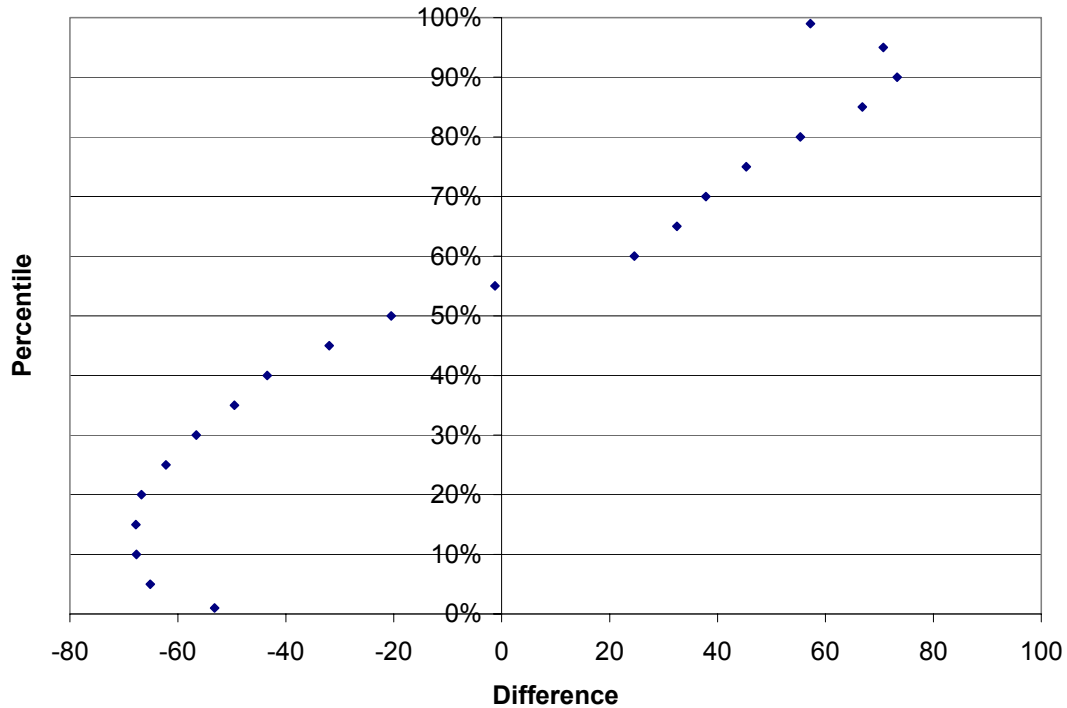
Figure 7-7. Minimum Fatigued Strain minus Maximum Non-Fatigued Strain by Percentile.

These two plots lead one to believe that fatigue cracking was governed by the higher strains in each section's strain distribution, as discussed above in the other analyses. There were many cases where fatigued sections had lower strains than non-fatigued sections, but these occurred in the bottom 55% of their cumulative distribution plots. After the 55th percentile, the slopes of the fatigued sections and non-fatigued sections experience measured strain differences outside of the allowable gauge tolerance specified for the NCAT Test Track (± 15 $\mu\varepsilon$). Since fatigue cracking was governed by the higher strains in the strain profiles, a new approach was developed for setting fatigue criteria for perpetual pavements.

The previously displayed cumulative distributions showed that picking one value on which to base strain performance in the field on was not practical. If one were to

168

choose the 50th percentile strain as a limit, data had shown sections with higher strains performed better than sections with lower strains. If one were to choose only a 99th percentile strain as a fatigue limit, the data might not be truly representative. For example, if a section were designed with the 99th percentile strain of 400 $\mu\varepsilon$ and a 50th percentile strain of 395 $\mu\varepsilon$, the 99th percentile strain might be appropriate for design. However, since the 50th and 99th percentile strains are relatively close to each other, the number of axles attributed to this high microstrain level makes design impractical. To alleviate these issues, a strain upper bound (or series of checkpoints at different percentiles) was developed using the cumulative distributions of sections that had performed well, but had not been overdesigned.

Strain Criteria Development

Eleven of the analyzed sections from the three Test Track experiments had not experienced fatigue cracking as of November 2008. Six of these sections were from the 2000 Test Track experiment. These sections were designed for thicknesses between 24 and 25 inches and carried at least 20 million ESALs of traffic without deteriorating; therefore, the combination of thickness and stiffness proved to decrease the strain magnitude incurred at the base of the HMA layer to below 10 microstrain. These sections were overdesigned for fatigue cracking and, therefore, were considered a lower bound for fatigue thresholds.

During the course of the 2003 Test Track, continuing into the 2006 research cycle, two sections (N3 and N4) were able to withstand 19 million ESALs without fatigue cracking. These two sections were analyzed by using the strain imposed for an

169

entire truck pass for their six years of traffic. The strains seen in these two sections were much higher than those seen from the previous Test Track cycle; therefore, the combination of higher strains and extended trafficking made them ideal for consideration in the development of strain criteria for perpetual pavements.

The 2006 Test Track experiment had three new test sections that did not fail in fatigue cracking. Sections N1 and N2 did crack; however, their failure mechanism was due to top-down cracking, not fatigue. Their short lifespan due to this deterioration caused them to be non-factors in developing the new perpetual pavement strain criteria.

Section N9 was the other newly constructed section that did not experience any sort of pavement distress. While this section did not crack it did experience higher strains than those seen in the 2000 Test Track investigation. The relatively low traffic (only 9 million ESALs as of November 2008), however, made it truly difficult to validate its status as a perpetual pavement. This strain profile would need to see more development as traffic was continually added to the pavement. Once this occurs, it could then be used in validating new fatigue criteria.

Sections N3 and N4 were also trafficked in the 2006 Test Track experiment. In this test cycle, a new methodology was developed for processing strain data by axle instead of by truck pass. Since these two sections had been in-place for approximately 19 million ESALs without any signs of fatigue cracking, the by-axle analyses (i.e., 2006) for these two sections could be used in developing the new fatigue criteria.

Figure 7-8 shows the four cumulative strain distributions which were adequate for developing fatigue criteria for perpetual pavements. These four profiles came from

170

two different sections where by-truck (2003) and by-axle (2006) analyses were conducted on each test section.

As can be seen, when comparing the by-truck and by-axle analyses for the test sections, very few differences were found. The slight shift to the right in the 2006 data at the lower percentiles was explained previously in Chapter 6 as being due to differences in tandem axle weights between the two Test Track experiments. But overall, arriving at very similar distributions validated both approaches to characterizing the cumulative distribution.
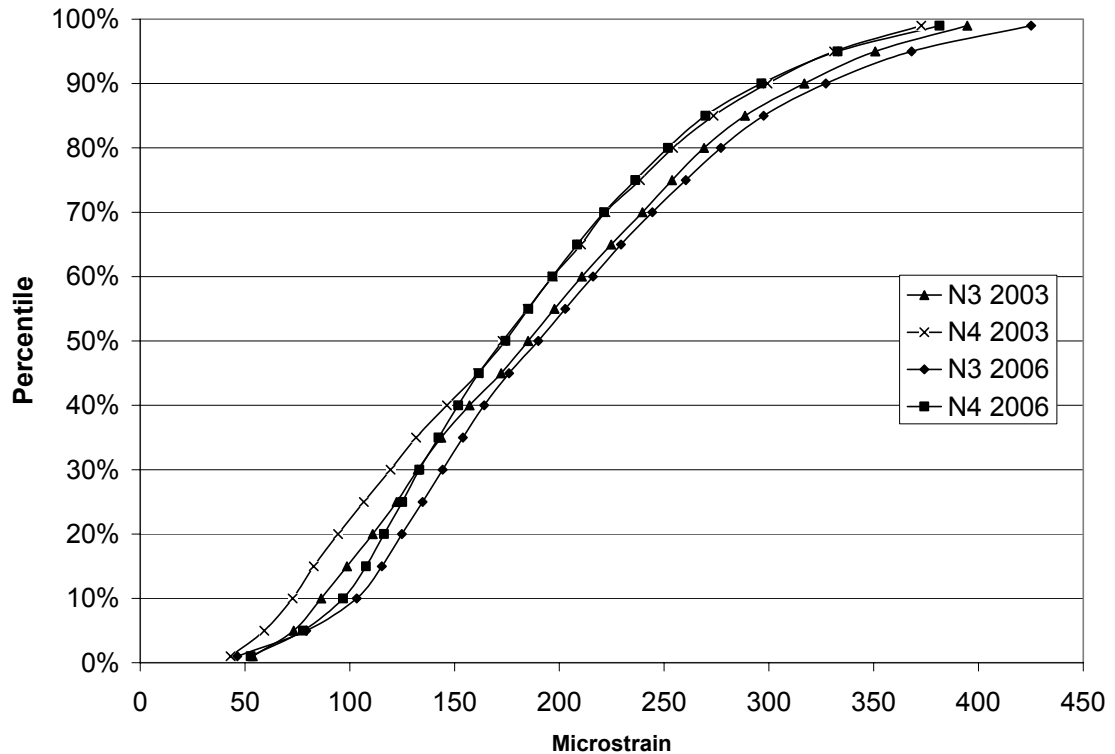

Figure 7-8. Strain Profiles for Sections Used in Fatigue Criteria Development.

While the strain profiles between analysis types were similar for the same section, it was also evident that the differences between the sectional strain profiles might be negligible as well. Previous research had found gauge precision at the NCAT

171

Test Track to be approximately 30 µε between duplicate strain gauges (Willis and Timm, 2008).

An average of all four strain distributions was taken at each percentile and plotted in Figure 7-9. Also plotted in this figure were bands at ±15 µε from the average to allow for 30 µε of gauge variability. As seen, all four strain distributions developed for N3 and N4 fell within the precision of the gauge at the upper end of the cumulative distributions; therefore, the average strain distribution of all four plots adequately characterized the strain profile of a perpetual pavement. The exact values for each percentile are listed below in Table 7-8.
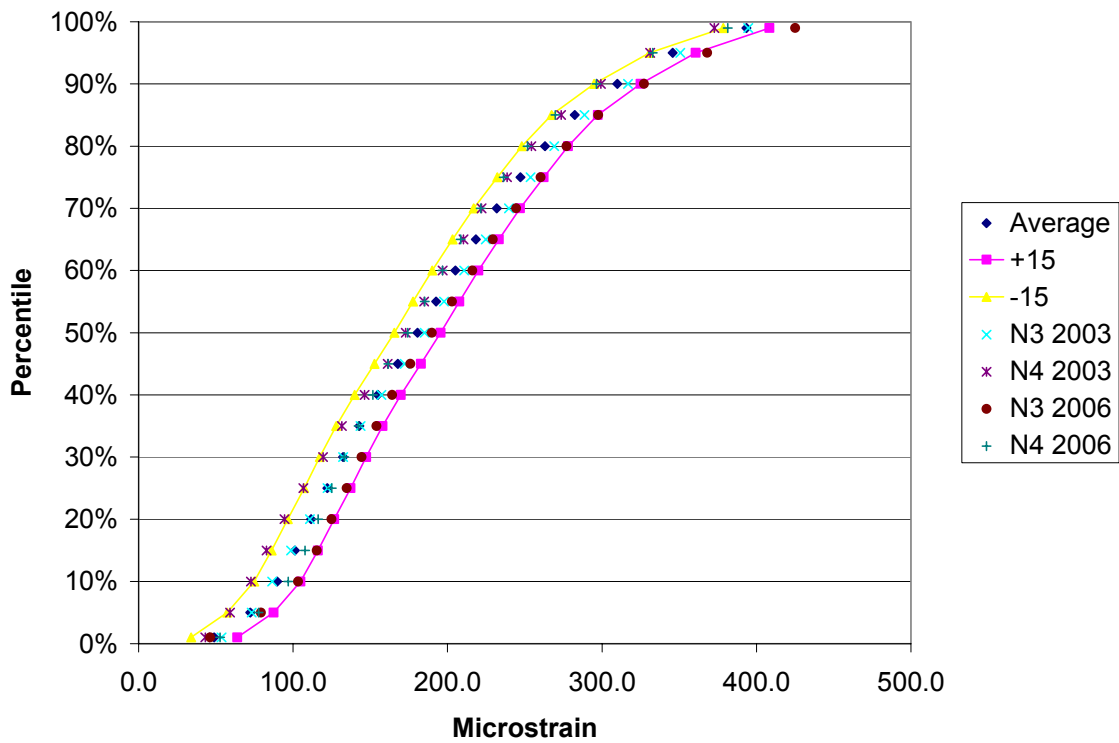
Figure 7-9. Average Strain Distribution with Confidence Bands.

Table 7-8. Strain Criteria for Perpetual Pavements.

Percentile	Fatigue Limit
99%	394
95%	346
90%	310
85%	282
80%	263
75%	247
70%	232
65%	218
60%	205
55%	193
50%	181
45%	168
40%	155
35%	143
30%	132
25%	122
20%	112
15%	101
10%	90
5%	72
1%	49

Strain Criteria Summary

It was determined by comparing the cumulative distribution plots of test sections across three Test Tracks that fundamental differences (i.e. differences of greater than ±15με) were seen in the strain profiles of sections that fatigue crack and those that do not. Using four strain profiles developed for sections N3 and N4, an average strain distribution was calculated. When gauge variability (±15 με) was considered, all four profiles fell within the gauge tolerance of the average strain distribution. Therefore, the average strain profile was determined to be an upper bound for strain criteria in flexible perpetual pavement design.

CHAPTER EIGHT

CONCLUSIONS AND RECOMMENDATIONS

SUMMARY

M-E design has advanced the concept of limiting horizontal strain at the base of the HMA layer in flexible pavements to prevent fatigue cracking and limiting vertical strain in the subgrade to prevent structural rutting. If these two distresses can be avoided, then the pavement could be classified as perpetual. Though both distresses are important, this research focused on the horizontal strain limit related to fatigue. The problem with perpetual pavement design in fatigue has been where should this strain limit, or fatigue threshold, be set.

Two analyses were conducted to research the concept of field validated strain criteria for perpetual pavements. The first analysis was conducted by comparing the laboratory-predicted fatigue threshold with field measured strains and pavement performance. In this study, the most practical link between these three parameters was found by taking a ratio of the nth percentile and the predicted fatigue threshold. The ratios of the non-fatigued sections were smaller than those of the fatigued sections. Therefore, control points (Table 8-1) were set as maximum ratios between field measured strains and the laboratory fatigue endurance limit.

174

The second analysis compared strain distributions for structural test sections across three Test Track research cycles to observed pavement performance. As with the fatigue ratio concept, differences were found in the strain profiles of the sections that experienced fatigue cracking and those that did not. Four test sections were deemed appropriate for inclusion in developing strain criteria for perpetual pavements. The average strain of these four sections was set as the upper bound for these criteria (Table 8-1).

Table 8-1. Conclusions

Percentile	Maximum Fatigue Ratio	Upper Bound Fatigue Limit
99%	2.83	394
95%	2.45	346
90%	2.18	310
85%	1.98	282
80%	1.85	263
75%	1.74	247
70%	1.63	232
65%	1.53	218
60%	1.44	205
55%	1.35	193
50%	1.27	181
45%		168
40%		155
35%		143
30%		132
25%		122
20%		112
15%		101
10%		90
5%		72
1%		49

CONCLUSIONS

Based upon the research conducted in this dissertation, the following conclusions can be made concerning strain criteria for perpetual pavements and laboratory estimated fatigue limits, field measured strain, and observed pavement performance relationship.

- Fatigue cracked sections had wider strain distributions than those that did not experience cracking. After the 55th percentile strain, all of the sections experiencing fatigue cracking had greater strain magnitudes than those that had no cracking.

- The higher magnitude strains in each section's distribution govern its fatigue cracking potential. Many sections which eventually experienced fatigue cracking had lower strains before the 55th percentile than those sections which stayed in-tact.

- Assuming mix designs and trafficking patterns are similar to those analyzed in this research, pavement structures whose measured cumulative strain distributions are below the upper bound shown in Table 8-1 should be able to withstand fatigue cracking.

- When trying to develop relationships between laboratory fatigue thresholds and field measured strains, one should consider using the entire strain distribution. Correlations between laboratory fatigue endurance limits, measured strains, and pavement performance were difficult to develop using a singular point. One analysis was conduced comparing the 95th percentile confidence interval lower bound to strains calculated at 20°C from previously developed strain-temperature relationships. A second analysis

176

investigated the location of the 95th percentile confidence interval lower bound along each section's cumulative strain distribution. Neither of these investigations found meaningful relationships between laboratory testing, field strains, and pavement performance.

- The fatigue ratio concept was the most successful form of linking field measured strains, laboratory fatigue endurance limits, and pavement performance. This ratio was calculated by dividing the nth percentile by the 95th percentile confidence interval lower bound. When this ratio was calculated for sections in the 2003 and 2006 Test Tracks, the ratios of cracked and uncracked sections differed. After the 55th percentile strain, the differences in the cumulative distributions could not be accounted for by gauge variability; thus, the ratios calculated from these strain values were concluded to be measurably different. Maximum control points for this ratio were developed by taking the section whose ratios were the highest, yet still stayed in-tact.

RECOMMENDATIONS

Strain Criteria

It is recommended that more research be conducted in developing strain criteria for perpetual pavement design. As more states begin to implement M-E design, it is imperative that they have viable strain criteria on which to base perpetual pavement design. As was seen from the cumulative distributions, one strain value does not

accurately quantify what the pavement is experiencing. The strains at the higher end of

a pavement's cumulative strain distribution need to be controlled. It is recommended

that upper bounds for strain distributions be set instead of using one fatigue design

endurance limit. One proposed upper bound is given in Table 8-1. The use of an upper

bound strain distribution will allow pavement engineers to design thinner pavements that

still perform well in the field.

Laboratory, Field, and Performance Relationship

It is recommended that more research be conducted on the concept of fatigue

ratios. The control points developed were based upon limited data (two mix designs);

therefore, they should be provisionally implemented until further research validates their

accuracy. If these fatigue ratio control points are seen as viable, a secondary set of

strain criteria has been established for M-E perpetual pavement design. Once a mix has

undergone fatigue testing and its endurance limit tested, a new strain distribution profile

would be created for the pavement by multiplying the 95th percentile confidence interval

lower bound by the fatigue ratio.

REFERENCES

Al-Qadi, I.L., H. Wang, P.J. Yoo, and S. H. Dessouky. "Dynamic Analysis and In-situ Validation of Perpetual Pavement Response to Vehicular Loading," Transportation Research Board 2008 Annual Meeting, CD-ROM.

American Association of State Highway and Transportation Officials. *AASHTO Guide for Design of Pavement Structures*. Washington, D.C., 1993.

American Association of State Highway and Transporation Officials: *Mechanistic-Empirical Pavement Design Guide, Interim Edition: A Manual of Practice*. AASHTO, July 2008.

Asphalt Institute. *Thickness Design, Asphalt Pavements for Highways and Streets*. Report MS-1, The Asphalt Institute, 1982.

Asphalt Pavement Alliance, "Perpetual Pavements: A Synthesis," APA 101, Asphalt Pavement Alliance, 2002.

Brown, E., L. Cooley, D. Hanson, C. Lynn, B. Powell, B. Prowell, and D. Watson. "NCAT Test Track Design, Construction, and Performance," NCAT Report 2002-12. National Center for Asphalt Technology, Auburn University, 2002.

Bushmeyer, B. "The Quest for Long-Life Asphalt Pavement," Better Roads, Februrary 2002.

Carpenter, S.H., K.A. Ghuzlan, and S.Shen. "Fatigue Endurance Limit for Highway and Airport Pavements," Journal of the Transportation Research Board, Transportation Research Record 1832, 2003.

Cheneviere, P. and V. Ramdas. "Cost benefit analysis aspects related to long-life pavements," International Journal of Pavement Engineering, Vol. 7, No. 2, June 2006, pp 125-152.

du Plesis, L., N.F. Coetzee, T.P. Hoover, J.T. Harvey, and C.L. Monismith. "Three decades of development and achievements: The Heavy Vehicle Simulator in accelerated pavement testing." *Proceedings of Sessions of GeoShangai*. American Society of Civil Engineers: 2006, pp. 45-54.

Epps, J.A. and C.L. Monismith. "Fatigue of Asphalt Concrete Mixtures – Summary of Existing Information," STP 508, American Society of Testing and Materials, Conshohocken, PA, 1972.

Estes, T. "Oregon Answers Perpetual Pavement Analysis with a Field Test," Better Roads, November 2005.

Fee, F. "Extended-Life Asphalt Pavement: new approaches to increase durability," TR News. No. 215, p 12, July/August 2001.

Ferne, B. "Long-life pavements – a European study by ELLPAG," International Journal of Pavement Engineering, Vol. 7, No. 2, pp 91-100.

Gierhart, D. "Analysis of Oklahoma Mix Designs for the National Center for Asphalt Technology Test Track using the Bailey Method," Transportation Research Board 2008 Annual Meeting, CD-ROM.

Harmelink, D., S. Shuler, and T. Aschenbrener. "Top-Down Cracking in Asphalt
Pavements: Causes, Effects, and Cures." Journal of Transportation Engineering,
Volume 134:1, pp 1-6, 2008.

Harm, E. "Illinois Extended-Life Hot-Mix Asphalt Pavements," Transportation
Research Circular, Number 503, 2001, pp 108-113.

Harvey, J.T., J.A. Deacon, B. Tsai, and C.L. Monismith. "Fatigue Performance of
Asphalt Concrete Mixes and Its Relationship to Asphalt Concrete Performance
in California," Report No. RTA-65W485-2, Berkley: California Department of
Transportation, 1995.

Harvey, J., Monismith, C., Horonjeff, R., Bejarano, M., Tsai, B.W. and V. Kannekanti,
"Long-Life AC Pavements: A Discussion of Design and Construction Criteria
Based on California Experience," International Symposium on Design and
Construction of Long Lasting Asphalt Pavements: Proceedings, National Center
for Asphalt Technology, 2004, pp 285-333.

Hornyak, N.J., J.A. Crovetti, D.E. Newman, and J.P. Schabelski. "Perpetual Pavement
Instrumentation for the Marquette Interchange Project – Phase 1," SPR #0092-
06-01, Wisconsin Highway Research Program, August 2007.

Huang, Yang H. *Pavement Design and Analysis*. New Jersey: Prentice Hall, 1993.

Hugo, F., and A.L. Epps. "NCHRP synthesis 325: Significant Findings from Full-Scale
Accelerated Pavement Testing." *National Cooperative Highway Research
Program*. Transportation Research Board, Washington, DC: 2004.

Kentucky Transportation Cabinet. *Pavement Design Guide (2007 Revision) for Projects
off the National Highway System less than 20,000,000 ESALs, less than 15,000*

AADT, and less than 20% trucks. Kentucky Transportation Cabinet Division of Highway Design, Lexington, KY, 2007.

Kuennen, T. "Perpetual pavement, two years later," Better Roads, March 2004.

Lu, L., D. Wang, and X. Than. "Predicted Model of Asphalt Pavement Non-Segregated Zone." International Conference on Transportation Engineering, Chengdu, China, 2007.

Mahoney, J.P. "Study of Long-Lasting Pavements in Washington State," Transportation Research Circular, Number 503, 2001, pp 88-95.

Marotta, T.W. *Basic Construction Materials*. Prentice-Hall: New Jersey, 2005.

Merrill, D., A. Van Dommelen, and L. Gaspar. "A review of practical experience throughout Europe on deterioration in fully-flexible and semi-rigid long-life pavements," International Journal of Pavement Engineering, Vol. 7, No. 2, pp 101-109.

Metcalf, J.B. "NCHRP Synthesis 235: Application of Full-Scale Accelerated Pavement Testing." *National Cooperative Highway Research Program*, Transportation Research Board. Washington, DC: 1996.

Miner, M.A. Estimation of Fatigue Life with Emphasis on Cumulative Damage. *Metal Fatigue*, edited by Sines and Wiseman, McGraw Hill, 1959, pp 278-89.

Monismith, C.L. J.A. Epps, and F.N. Finn. *Improved Asphalt Mix Design*. Proceedings, Association of Asphalt Paving Technologists Technical Sessions, San Antonio, Texas, 1985, pp 347-406.

Monismith, C.L. Analytically Based Asphalt Pavement Design and Rehabilitation: Theory in Practice, 1962-1992. *Transportation Research Record: Journal of the*

Transportation Research Board, No. 1354, TRB, National Research Council, Washington, D.C., 1992, pp. 5-26.

Muench, S.T., J.P. Mahoney, W. Wataru, L. Chong, and J. Romanowski. "Best Practices for Long-Lasting Low-Volume Pavements," Journal of Infrastructure Systems, Vol. 13, No. 4, pp 311-320, 2007.

Newcomb, D.E., Buncher, M., and I.J. Huddleston, "Concepts of Perpetual Pavements," Transportation Research Circular, Number 503, 2001, pp 4-11.

Nunn, M.E., A. Brown, D. Weston, and J.C. Nicholls. Design of Long-Life Flexible Pavements for Heavy Traffic, Report No. 250, Transportation Research Laboratory, Berkshire, U.K., 1997.

Nunn, M. and B.W. Ferne. "Design and Assessment of Long-Life Flexible Pavements," Transportation Research Circular, Number 503, 2001, pp 32-49.

Peterson, R.L., P. Turner, M. Anderson, and M. Buncher. "Determination of Threshold Strain Levels for Fatigue Endurance Limit in Asphalt Mixtures," International Symposium on Design and Construction of Long Lasting Asphalt Pavements: Proceedings, National Center for Asphalt Technology, 2004, pp 385-410.

Powell, R.B. *A History of Modern Accelerated Performance Testing of Pavement Structures*. NCAT Document (in-press), 2006.

Priest, A.L. "Methodology and Calibration of Fatigue Transfer Functions for Mechanistic-Empirical Flexible Pavement Design," NCAT Report 06-03, National Center for Asphalt Technology, Auburn University, 2006.

Prowell, B., E.R. Brown, J. Daniel, S. Bhattacharjee, H. Von Quintus, S. Carpenter, S. Shen, M. Anderson, A.K. Swamy, and S. Maghsoodloo. "Endurance Limits of

Hot Mix Asphalt Mixtures to Prevent Fatigue Cracking in Flexible Pavements." NCHRP Report 9-38, Updated Final Draft Report, National Center for Asphalt Technology, Auburn, AL. May 2008.

Rollings, R.S. and M.P. Rollings. "Pavement Failures: Oversights, Omissions and Wishful Thinking." *Journal of Performance of Constructed Facilities*, Volume 5:4, November 1991, pp. 271-286.

Rolt, J. "Long-Life Pavements," TRL Limited, United Kingdom, PA3736, 2001.

Romanoschi, S.A., A.J. Gisi, M. Portillo, and C. Dumitru. "The first findings from the Kansas Perpetual Pavements experiment" Transportation Research Board 2008 Annual Meeting, CD-ROM.

Saeed, A. and J.W. Hall. "NCHRP Report 512: Accelerated Pavement Testing Data Guidelines." *National Highway Cooperative Research Program*. Transportation Research Board, Washington, DC: 2003.

Scullion, T. "Perpetual pavements in Texas: state of the practice," Report 0-4822-1, Texas Department of Transportation, Texas Transportation Institute, May 2006.

Shook, J.F., F.N. Finn, M.W. Witczak, and C.L. Monismith. *Thickness Design of Asphalt Pavements – The Asphalt Institute Method*. Proceedings, 5th International Conference on Structural Design of Asphalt Pavements, Vol. 1, The Netherlands, 1982, pp. 17-44.

St. Martin, J., J.T. Harvey, F. Long, E. Lee, C.L. Monismith, and K. Herritt. "Long-Life Rehabilitation Design and Construction," Transportation Research Circular, Number 503, 2001, pp 50-65.

Tangella, R., J. Craus, J.A. Deacon, and C.L. Monismith. *Summary Report of Fatigue Response of Asphalt Mixtures*. TM-UCB-A-003A-89-3, SHRP Project A-003-A. University of California, Berkley: Institute of Transportation Studies, 1990.

Timm, D.H., D. E. Newcomb, and B. Birgisson. "Development of Mechanistic-Empirical Design for Minnesota," *Transportation Research Record: Journal of the Transportation Research Board, No. 1629*, TRB, National Research Council, Washington, D.C., 1998, pp.181-188.

Timm, D.H., A.L. Priest, and T.V. McEwen. Design and Instrumentation of the Structural Pavement Experiment at the NCAT Test Track. Report No 04-01, National Center for Asphalt Technology, Auburn University, 2004.

Timm, D.H. and A.L. Priest. Wheel Wander at the NCAT Test Track. Report No 05-02, National Center for Asphalt Technology, Auburn University, 2005.

Timm, D.H. and D.E. Newcomb. "Perpetual pavement design for flexible pavements in the US," International Journal of Pavement Engineering, Vol. 7, No. 2, 2006, pp 111-119.

Timm, D.H. and A.L. Priest. *Material Properties of the 2003 NCAT Test Track Structural Study*. Report No 06-01, National Center for Asphalt Technology, Auburn University, 2006.

Ursich, C. "Ohio takes perpetual pavement another step forward," Better Roads, November 2005.

Von Quintus, H.L. "Hot-Mix Asphalt Layer Thickness Designs for Longer-Life Bituminous Pavements," Transportation Research Circular, Number 503, 2001, pp 66-78.

Walubita, L. and T. Scullion. Perpetual Pavements in Texas: The Fort Worth SH 114
Project in Wise County, Report 0-4822, Texas Transportation Institute, Texas
Department of Transportation, January 2007.

Walubita, L.F., W. Liu, T. Scullion, and J. Leidy. "Modeling Perpetual Pavements
Using the Flexible Pavement System (FPS) Software," Transportation Research
Board 2008 Annual Meeting, CD-ROM.

Willis, J.R. and D.H. Timm. "A Forensic Investigation of Debonding in a Rich-Bottom
Pavement," *Transportation Research Record: Journal of the Transportation
Research Board, No. 2040*, TRB, National Research Council, Washington, D.C.,
2007, pp.107-114.

Willis, J.R. and D.H. Timm. "Repeatability of Asphalt Strain Measurements under Full
Scale Dynamic Loading," Journal of the Transportation Research Board,
Transportation Research Record, 2008 (in-print).

Willis, J.R. "A Synthesis of Practical and Appropriate Instrumentation Use for
Accelerated Pavement Testing," International Conference on Accelerated
Pavement Testing, 2008 (in-print).

Willis, J.R. and RB. Powell. "A Synthesis of Construction Practices for Accelerated
Loading Facilities in the United States." International Conference on Accelerated
Pavement testing, 2008 (in-print).

Wu, Z. and M. Hossain. "Lives of Mill-and-inlay Rehabilitation Stratetgies,"
International Journal of Pavement Engineering, Vol. 3, Number 3, pp 173-183,
2002.

Yang, Y., X. Gao, W. Lin, D.H. Timm, A.L. Priest, G.A. Huber, and D.A. Andrewski. "Perpetual Pavement Design in China," International Conference on Perpetual Pavement, Ohio Research Institute for Transportation and the Environment, 2005.